

Tetrahydropyrazolopyridinones as a Novel Class of Potent and Highly Selective LIMK Inhibitors

Alex G. Baldwin, David W. Foley, D. Heulyn Jones, Hyunah Lee, Ross Collins, Ben Wahab, Josephine H. Pedder, Loren Waters, Marie Paine, Lauramariú Schino, Gui Jie Feng, Benson M. Kariuki, Jonathan M. Elkins, John R. Atack, and Simon E. Ward*



Cite This: <https://doi.org/10.1021/acs.jmedchem.5c00974>



Read Online

ACCESS |



Metrics & More

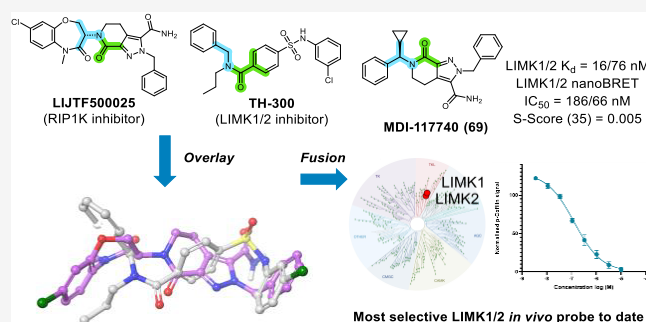


Article Recommendations



Supporting Information

ABSTRACT: LIMKs are serine/threonine and tyrosine kinases that play critical roles in regulating actin filament turnover, affecting key cellular processes such as cytoskeletal remodeling, proliferation and migration. Aberrant LIMK overactivation has been implicated in several diseases, including cancers and neurodegenerative disorders. Understanding the precise molecular mechanisms by which LIMKs modulate actin cytoskeletal dynamics necessitates highly potent and selective LIMK pharmacological inhibitors. We report the discovery of a novel class of allosteric dual-LIMK1/2 inhibitors based on the tetrahydropyrazolopyridinone scaffold. Using structure-based drug design, we identified MDI-117740 (**69**) as a highly potent dual-LIMK1/2 inhibitor with significantly improved DMPK properties compared to prior inhibitors, suitable for *in vivo* evaluation. Importantly, **69** has very low kinome promiscuity, including former off-target RIPK1, representing the most selective LIMK inhibitor reported to date. Such a chemical probe will enable researchers to selectively dissect LIMK activation under physiological or disease conditions and spur translation of new therapeutics targeting LIMK pathologies.



INTRODUCTION

The LIM domain kinases (LIMKs) are dual specificity, serine/threonine and tyrosine kinases that belong to the tyrosine-kinase family (TKL). They are a family of proteins comprised of two highly conserved members, LIMK1 and LIMK2, sharing 50% overall sequence similarity with 70% identity in the kinase domain. LIMKs have a unique structure of signaling domains composed of two N-terminal LIM domains and a PDZ domain, which are important in regulating kinase activity, a proline/serine-rich region and a C-terminal kinase domain.^{1–3} LIMK1/2 are a convergence point for at least four different signaling pathways: (i) the Rac-PAK (p21-activated kinase), (ii) Rho-ROCK (Rho kinase), (iii) Cdc42-MRCK α (myotonic dystrophy kinase-related Cdc42-binding kinase), and (iv) CaMKIV (Ca²⁺/calmodulin-dependent protein kinase) cascades. These upstream pathways all activate LIMKs by phosphorylating a conserved threonine residue, Thr508 in LIMK1 and Thr505 on LIMK2, on the activation loop.^{4–8} LIMK activation leads to phosphorylation at Ser3 of its substrates cofilin 1, cofilin 2, and destrin (actin depolymerizing factor) family of proteins, commonly referred to as “cofilin”.^{1,9} This phosphorylation event inactivates cofilin, causing actin polymerization and stabilization. Therefore, LIMKs are key regulators of actin motility, proliferation and migration, in addition to synapse

stability. There is also evidence that LIMKs regulate microtubule stability independently of their central role in modulating actin filament dynamics through interaction of its PDZ domain with tubulin.¹⁰

Inappropriate activation or overexpression of LIMK1 and LIMK2 has been associated with increased cellular invasion and tumor growth in several cancers, including breast,^{11–13} gastric,¹⁴ prostate^{15,16} and colorectal cancers.¹⁷ Fragile X Syndrome (FXS), the most common hereditary cause of intellectual disability and autism spectrum disorder (ASD), is caused by gene silencing of the fragile X mental retardation 1 protein (FMRP).¹⁸ This leads to LIMK1 activation due to increased levels of full length bone morphogenetic protein type II receptor (BMPRII) that directly binds LIMK1¹⁹ as well as increased activation through the Rac1-PAK1 pathway.^{20,21} Such inappropriate LIMK1 activity drives abnormal synaptic and dendritic spine morphology in the well-established *Fmr1* KO mouse model²⁰ and *Drosophila* model of FXS,²² which can also be

Received: April 7, 2025

Revised: July 21, 2025

Accepted: July 23, 2025

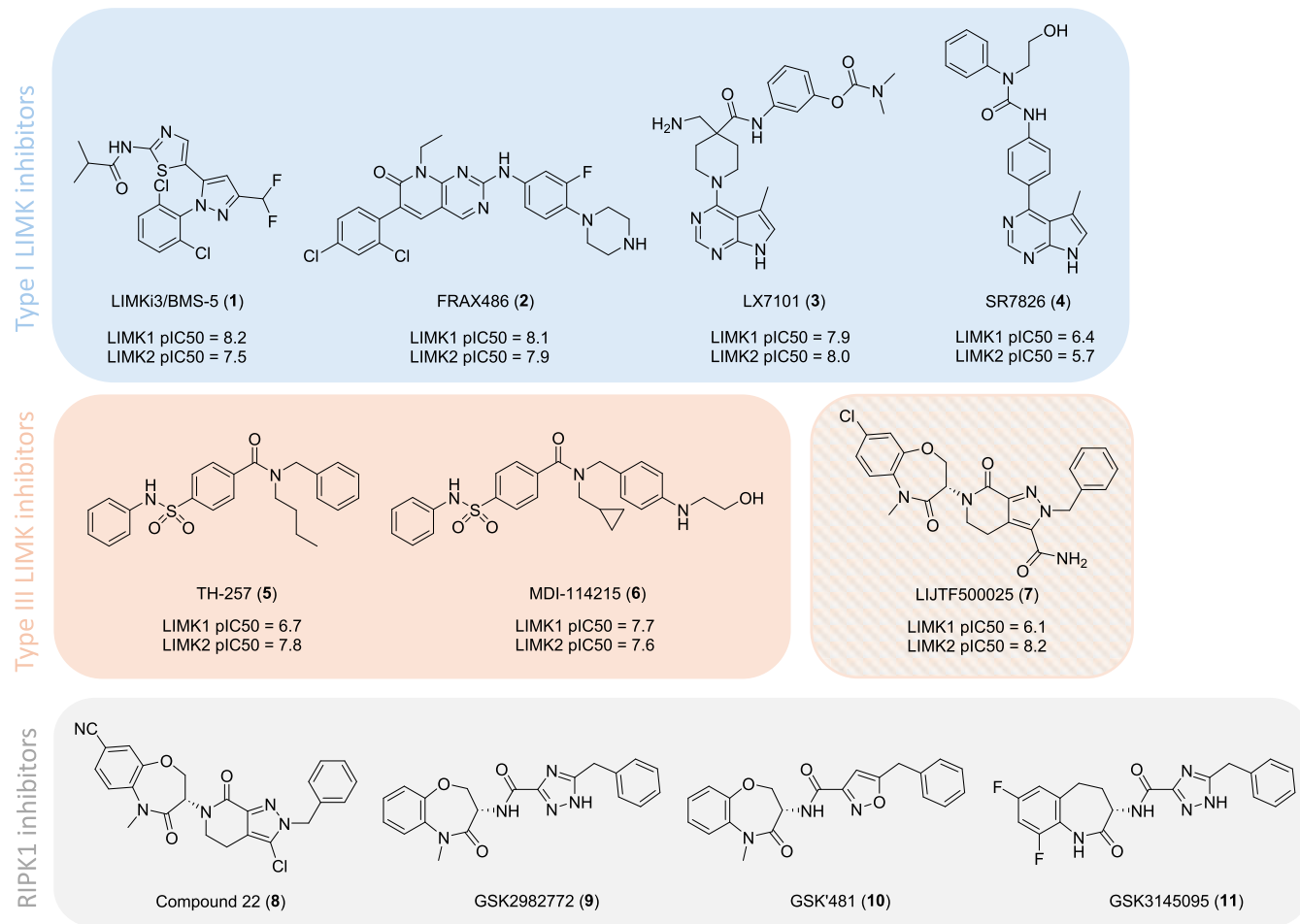


Figure 1. Chemical structures of reported LIMK1/2 inhibitors and structurally related RIPK1 inhibitors.

observed in FXS individuals.^{19,23,24} LIMK dysregulation has also been implicated in other CNS disorders, particularly Alzheimer's disease,²⁵ amyotrophic lateral sclerosis²⁶ and schizophrenia.^{27,28}

Given the pivotal role of LIMKs in disease and their therapeutic potential, there has been a growing number of reported LIMK inhibitors.^{9,29} The most characterized inhibitor is LIMKi3 (1, BMS-5, Figure 1), a highly potent, type I dual LIMK1/2 inhibitor originally developed by Bristol-Myers Squibb.³⁰ 1 inhibits cell proliferation and motility in several cancer cell lines,^{15,31,32} reverses abnormal dendritic spine morphology and normalizes anxiety-related behavior in the *Fmr1* KO mouse model.^{19,22} Nevertheless, it has promiscuous kinase selectivity³³ and has not been progressed further. FRAX486 (2, Figure 1) is a highly potent, CNS-penetrant group I PAK inhibitor that restores abnormal synaptic morphology and rescues seizures and behavioral abnormalities in *Fmr1* KO mice^{20,34} that was progressed as a clinical candidate for FXS. However, we have shown that 2 is unselective and strongly inhibits LIMK1/2,²⁹ therefore its efficacy in FXS models is likely to be attributed to dual PAK1/LIMK inhibition. The pyrrolopyrimidines LX7101 (3), developed by Lexicon Pharmaceuticals, and SR7826 (4, Figure 1) have also been disclosed as potent type I LIMK inhibitors.^{35–37} 3 is a dual LIMK/ROCK inhibitor that advanced to phase 1/2a clinical trials for primary open-angle glaucoma or ocular hypertension.³⁸ 4, an analogue devoid of ROCK inhibition, protects against A β -induced hippocampal thin spine loss, dendritic spine degener-

ation²⁵ and rescues impaired hippocampal long-term potentiation in neonatal *Fmr1* KO mice.³⁹ However, both 3 and 4 remain as unselective, type I LIMK1/2 inhibitors.^{29,40}

Consequently, there has been greater interest in developing allosteric type III LIMK1/2 inhibitors that are more selective and whose potencies are not appreciably different in PAK-phosphorylated LIMK variants.²⁹ TH-257 (5, Figure 1) reported by Knapp et al.³³ and closely related to a series first discovered by Lexicon Pharmaceuticals,⁴¹ is a highly selective, type III dual LIMK1/2 inhibitor that dose-dependently inhibits neurite outgrowth and reduces phospho-cofilin levels in human iPSC-derived cortical neurons from FXS patients.³⁹ We recently disclosed the very potent dual LIMK1/2 inhibitor MDI-114215 (6), which significantly reduces phospho-cofilin in hippocampal brain slices and rescues impaired long-term potentiation in the *Fmr1* KO mouse model. Unfortunately, compounds 5 and 6 could not be progressed further due to their suboptimal DMPK properties and poor CNS penetration, respectively.^{29,33,39} Therefore, alternative starting points to develop allosteric type III LIMK1/2 inhibitors with improved *in vitro* DMPK properties suitable for *in vivo* evaluation are highly desirable.

The X-ray crystal structure of the LIMK1 kinase domain bound to LIJTF500025 (7, Figure 1) was recently published (PDB: 7ATU).⁴² 7 was originally developed as a potent receptor interacting protein 1 (RIP1) kinase inhibitor by Takeda Pharmaceuticals as part of a CNS-penetrant, orally available RIPK1 inhibitor program leading to compound 22 (8, Figure 1).⁴³ This series features a tetrahydro-6*H*-pyrazolo[3,4-*c*]-

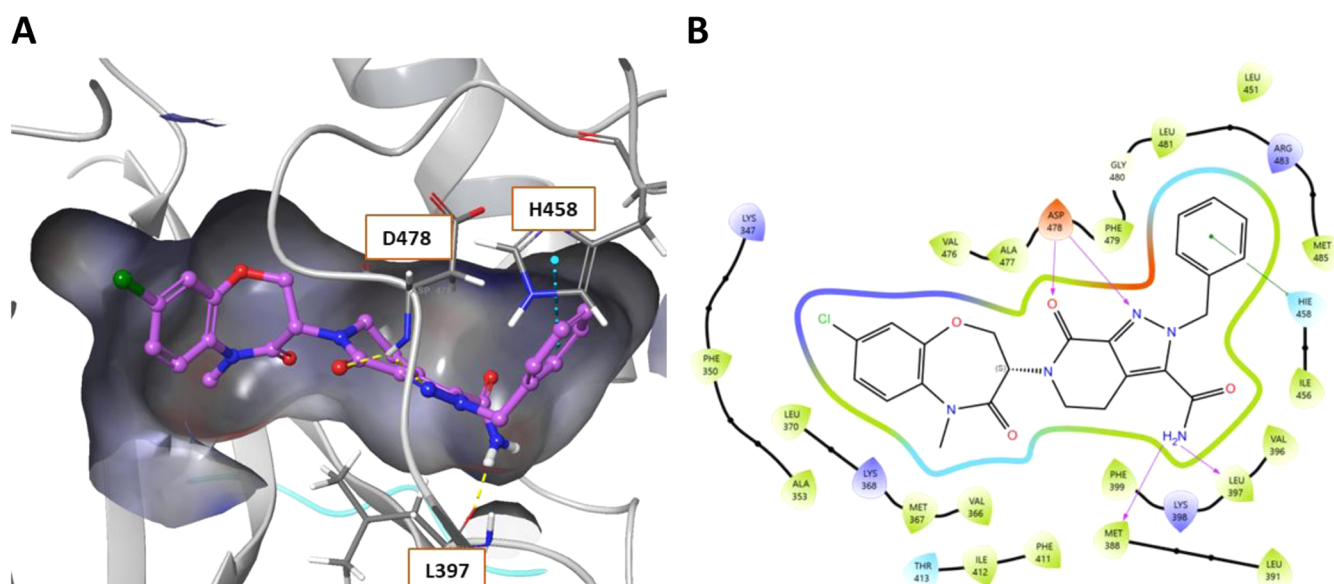


Figure 2. (A) Co-crystal structure of allosteric inhibitor 7 (LIJTF500025) bound to LIMK1 (PDB: 7ATU). (B) Ligand interaction diagram of 7. Shading represents the following: hydrophobic region (green), charged interaction (positive, blue; negative, red), polar (teal).

Table 1. Evaluation of Structurally Related RIPK1 Inhibitors 8–11 and Analogues 19–26 and 29 against LIMK1 and LIMK2 to Explore Early Structure-Activity Relationship (SAR) of LIJTF500025 (7)

				enzymatic pIC ₅₀ ^a	
compound	R ¹	R ²	series	LIMK1	LIMK2
7	CONH ₂	Cl	A	7.17 ^b	7.82 ^b
8	Cl	CN	A	<5	5.22 ^b
9	-	-	-	5.04 ^b	5.03 ^b
10	-	-	-	5.39 ^b	<5
11	-	-	-	5.13 ^b	5.12 ^b
19	Br	Cl	A	5.29 ± 0.57 ^c	5.91 ± 0.35 ^c
20	CONH ₂	Cl	B	5.24 ^b	5.53 ^b
21	CONH ₂	H	A	6.98 ± 0.03 ^c	7.95 ± 0.09 ^c
22	CONH ₂	H	B	<5	<5
23	CONHMe	H	A	5.76 ^b	5.82 ^b
24	CONHMe	H	B	<5	<5
25	CONMe ₂	H	A	<5	<5
26	CONMe ₂	H	B	<5	<5
29	-	-	-	<5	5.16 ^b

^aThe phosphorylation of cofilin was assessed by RapidFire mass spectrometry following an enzymatic assay. ^b*n* = 1. ^cMean of two independent experiments.

pyridin-7-one core designed from a merging strategy between an identified HTS hit and the previously reported RIPK1 inhibitor GSK2982772 (9, Figure 1).⁴⁴ 9 is a clinical candidate that has recently completed phase II clinical trials for psoriasis, ulcerative colitis and rheumatoid arthritis^{45–47} that constitutes an advanced RIPK1 inhibitor series developed by GlaxoSmithKline, exemplified by GSK'481 (10)⁴⁸ and GSK3145095 (11, Figure 1).⁴⁹

7 is a type III, allosteric dual LIMK1/2 and RIPK1 inhibitor whose binding to LIMK1 causes distortion of the P-loop and outward displacement of the αC helix, whereby the DFG motif adopts the DFG-out conformation.⁴² The central tetrahydropyrazolopyridinone core is supported in place with interactions of the carbonyl (and potentially pyrazolo N) with the catalytic D478 of the DFG loop. The ligand also makes an important diatomic interaction of the primary amide with M388/L397 and

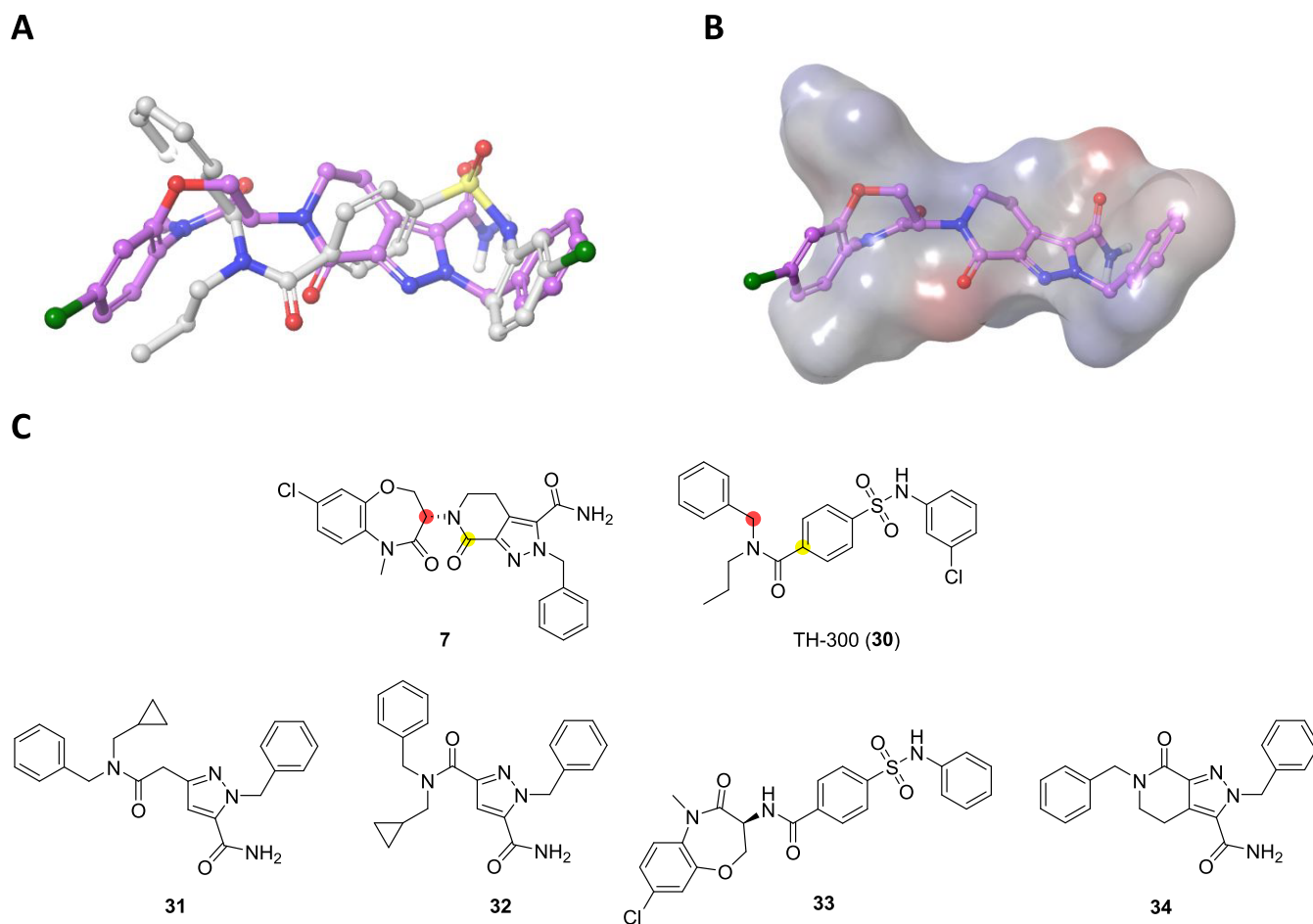


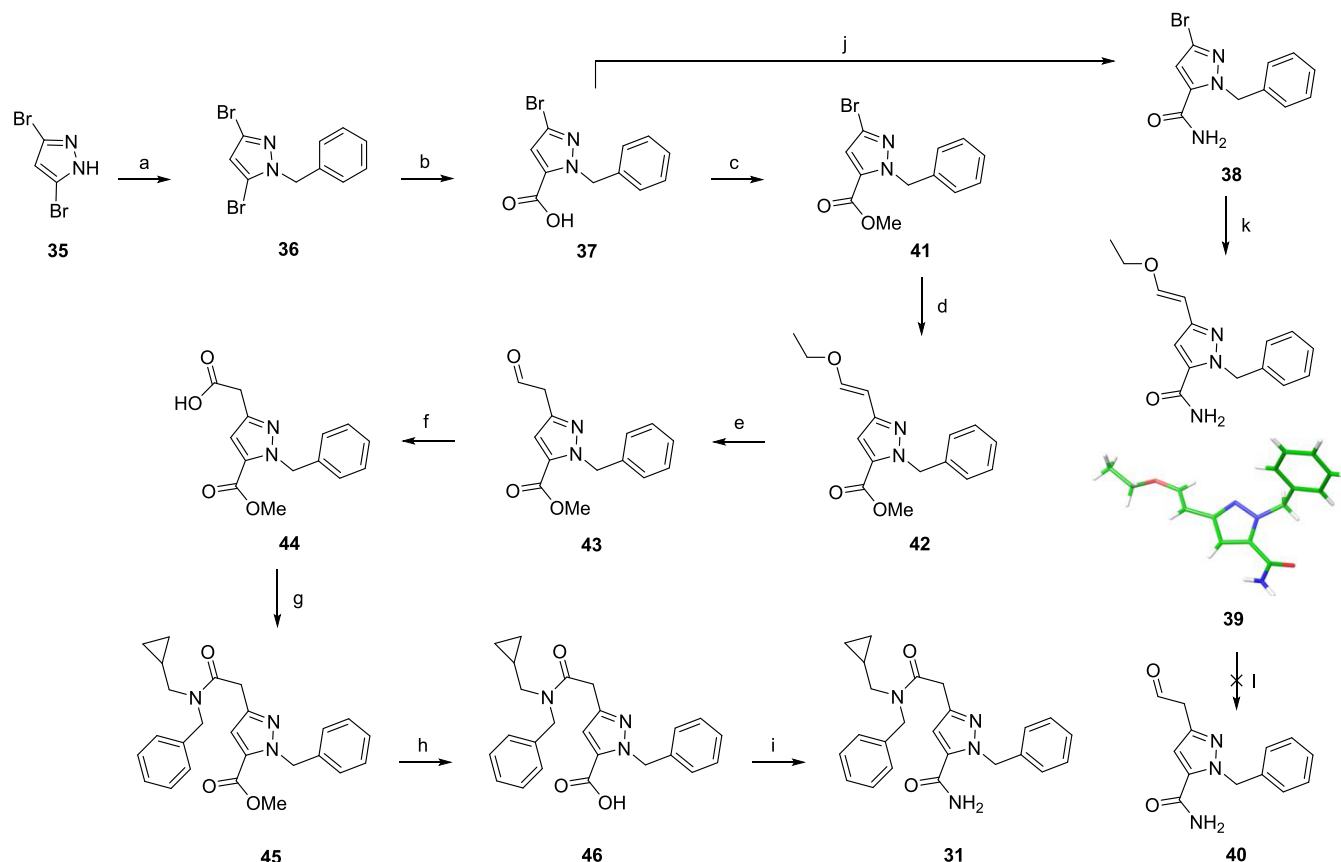
Figure 3. Overlay of RIPK1 inhibitor 7 (LJTF500025) and 30 (TH-300) and design of novel hybrids 31–34. (A) Binding mode images of 7 (from LIMK1, PDB: 7ATU, magenta) and 30 (from LIMK2, PDB: 5NXD, white). (B) The shape and electrostatic field of 30 (LIMK2, *loc cit.*) with 7 (LIMK1, *loc cit.*, magenta) overlaid. (C) Chemical structures of 7 and 30 highlighting key positions for hybrid generation (above) and designed hybrid molecules (below).

an edge π -cation interaction of the benzyl ring with H458 (Figure 2A). The narrow lipophilic back pocket is filled by the benzoxazepin-4-one motif which positions the haloaromatic into this hydrophobic region, encompassed by F350, A353, V366, and F479 (Figure 2B). Interestingly, comparable interactions were observed in the X-ray structure of TH-300 (30, Figure 3C), a close analogue of 5, in complex with LIMK2 (PDB: 5NXD) and the LIMK1 homology model of 6.³⁹ Given these similarities, we wished to develop a hybrid series between the RIPK1 inhibitor 7 and our potent dual LIMK1/2 inhibitor 6 that aimed to further improve the suboptimal *in vitro* DMPK properties of 6 while avoiding any related RIPK1 activity.

Here we report this merging strategy and successive SAR campaigns that led to the discovery of a novel class of highly potent, selective LIMK1/2 inhibitors devoid of RIPK1 binding. The most advanced molecule from this series, MDI-117740 (69), has similar LIMK1/2 binding and cellular potency and target engagement but significantly improved *in vitro* DMPK compared to our previously reported lead compound 6. Notably, 69 is the most selective LIMK inhibitor known to date. We also characterized structure-permeability relationships within this new series of allosteric inhibitors.

RESULTS AND DISCUSSION

To identify the chemical features necessary for potent dual LIMK1/2 activity, structurally related RIPK1 inhibitors 8–11 and an initial set of analogues of 7 were screened using our previously reported LIMK1/2 RapidFire mass spectrometry assay.²⁹ First, we attempted to access key intermediate 5-cyano-1H-pyrazole-3-carboxylate 12 (see Scheme S1) to enable a regioselective synthesis of amide analogues of 7 (Series A, Table 1) via nitrile hydrolysis and amide coupling. 5-Bromo-1H-pyrazole-3-carboxylate 14 was synthesized from ethyl 1-benzyl-5-hydroxy-1H-pyrazole-3-carboxylate 13 using POBr₃ and DMF prior to Wittig reaction with (methoxymethyl)-triphenylphosphonium chloride, HCl-mediated deprotection, reductive amination and ester hydrolysis/amide coupling (Scheme S1). Despite our more convergent synthetic route, late-stage Pd-catalyzed cyanation of 19 using Zn(CN)₂⁵⁰ failed to afford the nitrile derivative 12. As an alternative, derivatives 20–26 were synthesized similar to previously described by Yoshikawa et al.⁴³ using dimethyl 1-benzyl-4-(2-oxoethyl)-1H-pyrazole-3,5-dicarboxylate 27 and substituted benzoxazepine-4-one starting materials (Scheme S2). Typically, the reductive aminated intermediates 28a–b spontaneously cyclized overnight to afford a mixture of regioisomers. After separation by flash column chromatography and amide coupling, this led to two distinct series: 1-benzylpyrazolo-5-carboxamides (Series A)

Scheme 1. Synthesis of Hybrid 31^a

^aReagents and conditions: (a) (i) K_2CO_3 (1.3 equiv), DMF, 0 °C, (ii) BnBr (1.0 equiv), 0 °C \rightarrow rt, 40 min, 96%; (b) (i) $\text{iPrMgCl}\cdot\text{LiCl}$ (1.2 equiv), THF, -78 °C, 30 min, (ii) CO_2 , 20 min, 94%; (c) MeOH , SOCl_2 (3.0 equiv), rt, 18 h \rightarrow 50 °C, 18 h, 98%; (d) (*E*)-(2-ethoxyvinyl)boronic acid pinacol ester (1.3 equiv), $\text{Pd}(\text{dppf})_2\text{Cl}_2$ (0.1 equiv), Cs_2CO_3 (3.0 equiv), monoglyme/ H_2O , 80 °C, 18 h, 39%; (e) 4 M HCl in 1:1 dioxane/ DCM (8.0 equiv), rt, 1 h, quantitative; (f) oxone (1.0 equiv), DMF, rt, 1 h, 61%; (g) *N*-benzyl-1-cyclopropylmethanamine (1.0 equiv), HOBT (1.1 equiv), $\text{EDC}\cdot\text{HCl}$ (1.3 equiv), Et_3N (1.5 equiv), DCM , rt, 18 h, 22%; (h) $\text{LiOH}\cdot\text{H}_2\text{O}$ (1.3 equiv), 1:1:1 $\text{MeOH}/\text{THF}/\text{H}_2\text{O}$, rt, 2 h, 98%; (i) PyBOP (1.4 equiv), HOBT (1.4 equiv), DIPEA (3.9 equiv), NH_4Cl (1.9 equiv), DMF, rt, 1 h, 48%; (j) (i) SOCl_2 (19.6 equiv), 65 °C, 2 h, (ii) NH_4OH (5.9 equiv), DCM , rt, 5 min, 86% (over two steps); (k) (*E*)-(2-ethoxyvinyl)boronic acid pinacol ester (1.7 equiv), $\text{Pd}(\text{dppf})_2\text{Cl}_2$ (1.0 equiv), Cs_2CO_3 (1.2 equiv), monoglyme/ H_2O , 90 °C, 18 h, 89%; (l) 4 M HCl in 1:1 dioxane (5.0 equiv)/ DCM , rt, 1 h.

and 1-benzylpyrazolo-3-carboxamides (Series B, Table 1). Ring-opened analogue **29** was synthesized from **50** (see Scheme 2).

RIPK1 inhibitors **8–11** were not potent LIMK1 or LIMK2 inhibitors (Table 1). Given bromo analogue **19** also demonstrated poor potency, these data strongly suggest the C5-substituted amide moiety is indispensable for dual LIMK1/2 inhibitory activity. Indeed, mono- or dimethylation of the primary amide (**23** and **25**, respectively) led to significant weaker inhibitors (Table 1), consistent with its known HBD interactions with LIMK1 (Figure 2). Interestingly, comparison between the 1-benzylpyrazolo-5-carboxamide and 1-benzylpyrazolo-3-carboxamide regioisomers showed a clear preference for the 5-regioisomer, with the 3-regioisomer of **7** (**20**) displaying at least 100-fold potency drop against LIMK1 and LIMK2. Breaking the annulated 5,6-fused ring similarly led to weak inhibitory activity (**29**, Table 1), as did sulfonamide and secondary amine replacements of the amide in compound **29** (data not shown). Therefore, these initial SAR data indicate the tetrahydropyrazolo[3,4-*c*]pyridine-5-carboxamide moiety is a privileged scaffold to develop potent LIMK1/2 inhibitors. As the des-Cl analogue of **7** is also a highly potent RIPK1 inhibitor (compound **20**, $\text{pK}_i = 8.60^{43}$) and expectedly shows high RIPK1 binding in a kinase selectivity panel (27% of control @1 μM ,

data not shown), we sought to eliminate off-target RIPK1 activity through a hybridization approach with highly selective, allosteric LIMK inhibitors.

Using the X-ray crystal structures of LIMK2 bound to the allosteric inhibitor TH-300 (**30**, PDB: 5NXXD), **7** was overlaid in order to identify possible sites for hybrid generation. Although there is variance between the benzoxazepin-4-one and *N*-benzylpropyl motifs, the spatial and electrostatic fields between the 2-benzyl tetrahydropyrazolopyridine-3-carboxamide of **7** and *N*-phenylsulfamoylbenzamide of **30** share high similarity (Figure 3A). In particular, the electrostatic potentials are shared in two loci which demonstrate the common positioning of (i) the cyclic amide carbonyl of **7** and branched amide carbonyl in **30**, and (ii) the primary amide carbonyl of **7** and sulfonamide O in **30** (Figure 3B). Two instances where atoms from both series overlaid well were identified:

- (1) Carbonyl carbon of **7** with the quaternary carbon of **30** (highlighted in yellow).
- (2) sp^3 Hybridized carbon of **7** with the benzyl carbon of **30** (highlighted in red, Figure 3C).

For the yellow highlighted position, two hybrids were designed whereby the tetrahydropyrazolopyridone ring was opened and the tertiary amide was either extended by one CH_2

unit (hybrid 31) or directly attached (hybrid 32). In both instances, we targeted synthesis of the methylene cyclopropyl-containing amide as we previously observed a consistent 10-fold LIMK1/2 potency improvement compared to the propyl substituent.³⁹ A further two hybrids were proposed based on the second overlaid position highlighted in red; hybrid 33 that replaces the benzyl substituent of 30 with the benzoxazepin-4-one of 7, and the reversed hybrid 34, where the tertiary carbon of 7 was replaced with the benzyl group of 30.

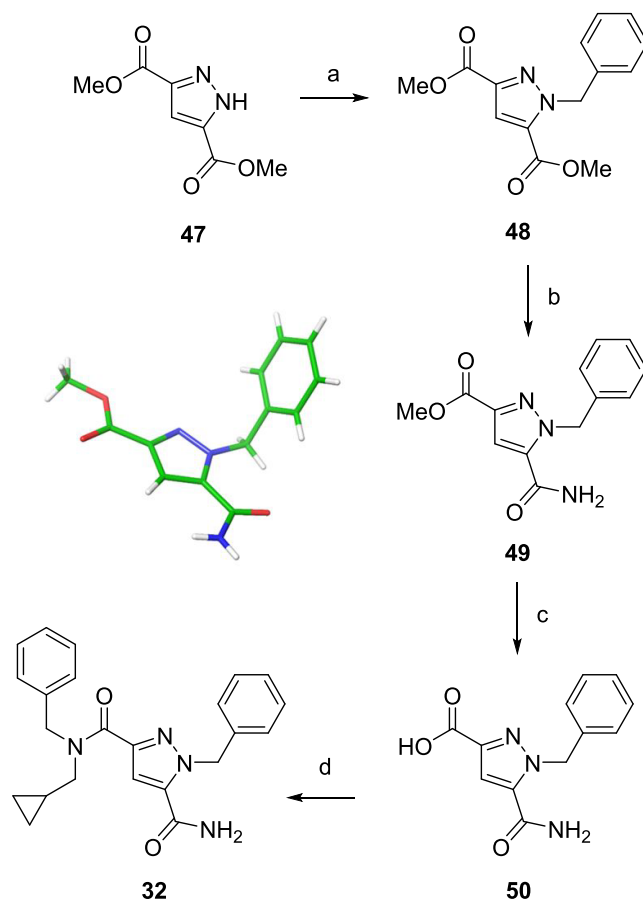
The synthesis of hybrid 31 proved challenging, with first attempts focused on installing the primary amide prior to formation of the tertiary amide bond (Scheme 1). Benzylation of 3,5-dibromopyrazole 35 proceeded cleanly, followed by a reported selective lithiation-quenching with carbon dioxide,⁵¹ which gave single regioisomer 37. Generation of the primary amide 38 via the acid chloride followed by a Suzuki reaction with (*E*)-(2-ethoxyvinyl)boronic acid pinacol ester gave 39, from which a single crystal was grown to confirm the regioselectivity of the lithiation step (Scheme 1). Unfortunately, acidic deprotection to give the aldehyde 40 was unsuccessful due to intermolecular attack of the primary amide on the aldehyde. Several different strategies to install the CH₂CO₂H via bromo intermediate 38 also failed. A change in strategy to unveil the primary amide at the end of the synthesis proved fruitful. Ester formation followed by Suzuki reaction gave intermediate 42 in satisfactory yield. This time, acidic deprotection to give the aldehyde was successful and following oxidation (44), *N*-benzyl-1-cyclopropylmethanamine was introduced via amide coupling to afford key intermediate 45. Finally, ester hydrolysis (46) and primary amide formation gave the target compound 31.

Hybrid 32 was synthesized according to Scheme 2. Benzylation of bis ester 47, followed by a partially selective monoester hydrolysis/primary amide formation sequence as previously reported⁵² gave intermediate 49, initially as a mixture of regioisomers (4:1 ratio). The major regioisomer was isolated and a single crystal grown for X-ray analysis, confirming the desired regiochemistry (Scheme 2). Subsequent ester hydrolysis to form 50 and primary amide formation yielded the target compound 32.

Hybrid 33 was easily accessible through a one-step amide coupling from the key amine intermediate 51 (Scheme 3), synthesized as previously described.²⁹ The final hybrid 34 was synthesized as shown in Scheme 4. Iodination in the presence of ceric ammonium nitrate followed by benzylation gave intermediate 53 in high yield. Suzuki reaction and successful enol ether deprotection gave the key aldehyde intermediate 27 in good yield. Reductive cyclization using 2-methylpyridine-2-borane complex proceeded cleanly, giving the expected two regioisomers 55 and 56 arising from cyclization onto either methyl ester. The mixture of regioisomers were hydrolyzed and amide coupled to afford primary amides 34 and 57 that were isolated in 17% and 9% yields, respectively. Initially, we relied upon the presence or absence of unique HMBC cross-peaks between the benzyl CH₂, amide NH₂ and lactam benzyl CH₂ for confirmation of the regiochemistry. However, we subsequently noted consistent patterns in the ¹H NMR, specifically differences in the peak position and splitting of the primary amide protons between the two regioisomers (Figure S4). Therefore, regiochemical assignment was possible in the absence of HMBC experiments.

All four hybrid targets 31–34 and regioisomer 57 were subsequently tested in a range of LIMK1/2 *in vitro* assays (Table 2). LIMK1/2 binding dissociation constants (*K*_d) were

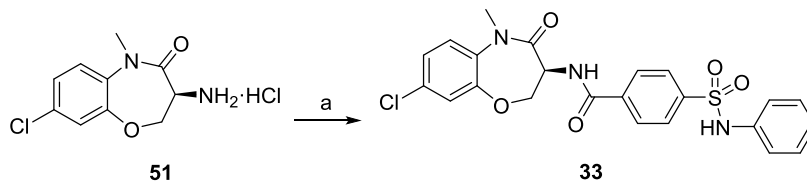
Scheme 2. Synthesis of Hybrid 32^a



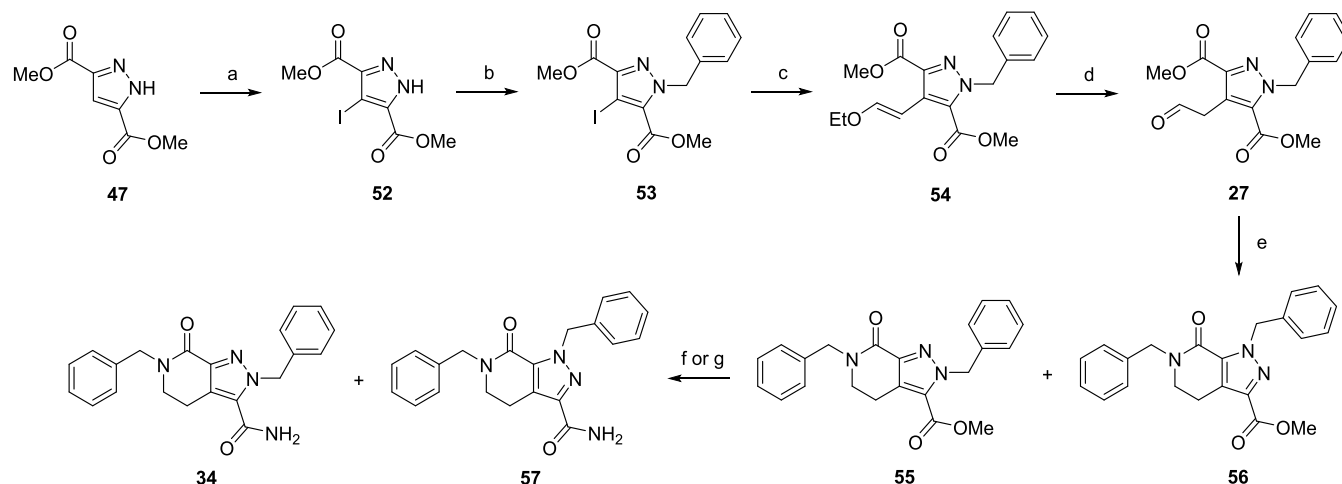
^aReagents and conditions: (a) (i) K₂CO₃ (1.3 equiv), DMF, 0 °C, (ii) BnBr (1.0 equiv), 0 °C → rt, 1 h, 93%; (b) (i) LiOH·H₂O (1.0 equiv), 1:1:1 MeOH/THF/H₂O, 0 °C, 2 h, (ii) SOCl₂ (21.0 equiv), 65 °C, 2 h, (iii) DCM, NH₄OH (4.0 equiv), rt, 5 min, 63%; (c) LiOH·H₂O (3 equiv), 1:1:1 MeOH/THF/H₂O, rt, 30 min, 80%; (d) (i) SOCl₂ (34.3 equiv), 65 °C, 2 h, (ii) DCM, Et₃N (2.5 equiv), *N*-benzyl-1-cyclopropylmethanamine (1.0 equiv), rt, 5 min, 21%.

measured using the *K*_dELECT platform (provided by Eurofins/DiscoverX) and inhibitory activity assessed using our previously reported RapidFire mass spectrometry assay.²⁹ Cellular target engagement and LIMK selectivity was measured using LIMK1 and LIMK2 NanoBRET assays in HEK293 cells, while cellular proof-of-mechanism was assessed by measuring p-cofilin levels in SH-SY5Y cells using the AlphaLISA platform. Since cofilin is a substrate of both LIMK1 and LIMK2, our assay is unable to assess selectivity against these enzymes in contrast to the NanoBRET assay. Hybrids 31 and 32 did not show any inhibition across the various assays and 33 showed only weak inhibition in the LIMK1/2 RapidFire assay (Table 2). We were excited to observe, however, that 1-benzylpyrazolo-5-carboxamide 34 showed potent LIMK1/2 binding and good inhibitory activity in both RapidFire and cellular assays, showing a pIC₅₀ value of 6.20 in the AlphaLISA p-cofilin assay. On the other hand, its 1-benzylpyrazolo-3-carboxamide regioisomer 57 was inactive in all *in vitro* assays (Table 2). This result was corroborated when we assessed all 1-benzylpyrazolo-3-carboxamides isomers that were isolated during the course of synthesizing the active 5-carboxamides (data not shown).

Based on novel analogue 34, a series of benzylic substituted analogues and replacements 58–72 were synthesized in an effort

Scheme 3. Synthesis of Hybrid 33^a

^aReagents and conditions: (a) 4-(phenylsulfamoyl)benzoic acid (1.0 equiv), HOBt (1.1 equiv), EDC·HCl (1.2 equiv), DIPEA (2.6 equiv), DCM, rt, 5 min, 94%.

Scheme 4. Synthesis of Hybrid 34 and Regioisomer 57^a

^aReagents and conditions: (a) I₂ (1.3 equiv), CAN (1.1 equiv), MeCN, rt, 48 h, 89%; (b) (i) K₂CO₃ (1.3 equiv), DMF, 0 °C, (ii) BnBr (1.0 equiv), 0 °C → rt, 1 h, 90%; (c) (*E*)-(2-ethoxyvinyl)boronic acid pinacol ester (1.7 equiv), Pd(dppf)₂Cl₂ (1.0 equiv), Cs₂CO₃ (2.1 equiv), monoglyme/water, 90 °C, 48 h, 77%; (d) 6 M HCl in 1:1 dioxane/THF (18.1 equiv), 0 °C → rt, 1 h, 66%; (e) benzylamine·HCl (1.3 equiv), 2-methylpyridine·BH₃ complex (1.5 equiv), AcOH (0.3 equiv), MeOH, 0 °C, 3 h, 42% (55), 22% (56); (f) (i) LiOH·H₂O (1.2 equiv), 1:1:1 MeOH/THF/H₂O, rt, 18 h, (ii) HOBt (1.1 equiv), EDC·HCl (1.3 equiv), DIPEA (2.4 equiv), NH₄Cl (3 equiv), DCM, rt, 18 h, 9% (for 34); (g) 7 M NH₃ in MeOH (87.5 equiv), 70 °C, 18 h, sealed tube, 17% (for 57).

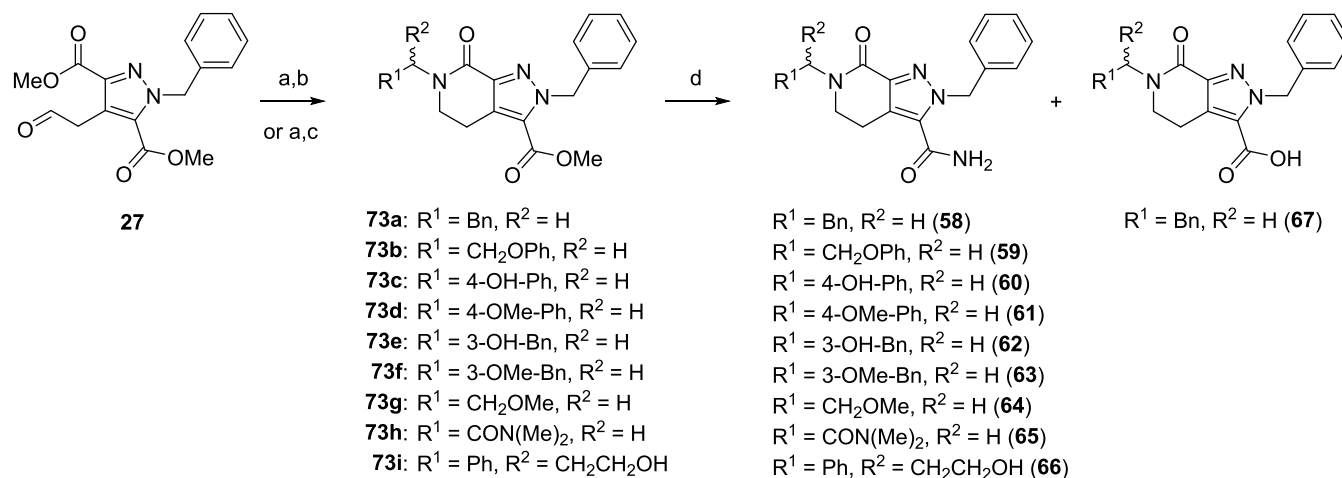
Table 2. Evaluation against LIMK1 and LIMK2 in Binding, Enzymatic and Cellular Target Engagement Assays Values to Explore Structure–Activity Relationship (SAR) of Hybrids 31–34 and Regioisomer 57^a

compound	binding affinity (pK _d) ^b		enzymatic pIC ₅₀		nanoBRET pIC ₅₀		alphaLISA pIC ₅₀
	LIMK1	LIMK2	LIMK1	LIMK2	LIMK1	LIMK2	
7	7.21 ^c	7.06 ^c	7.17 ^c	7.82 ^c	6.74 ± 0.15	7.02 ± 0.07	7.06 ± 0.04
21	7.73 ± 0.04 ^d	7.25 ± 0.04 ^d	6.98 ± 0.03 ^d	7.95 ± 0.09 ^d	6.15 ^c	6.29 ^c	6.58 ± 0.04
31	nd	nd	nd	nd	<5	<5	<5
32	nd	nd	<5	<5	<5	<5	<5
33	nd	nd	5.01 ^c	5.22 ^c	<5	<5	<5
34	6.80 ± 0.11	7.29 ± 0.05	6.16 ^c	7.03 ^c	5.77 ± 0.13	6.04 ± 0.01	6.20 ± 0.43 ^d
57	nd	nd	<5	<5	<5	<5	<5

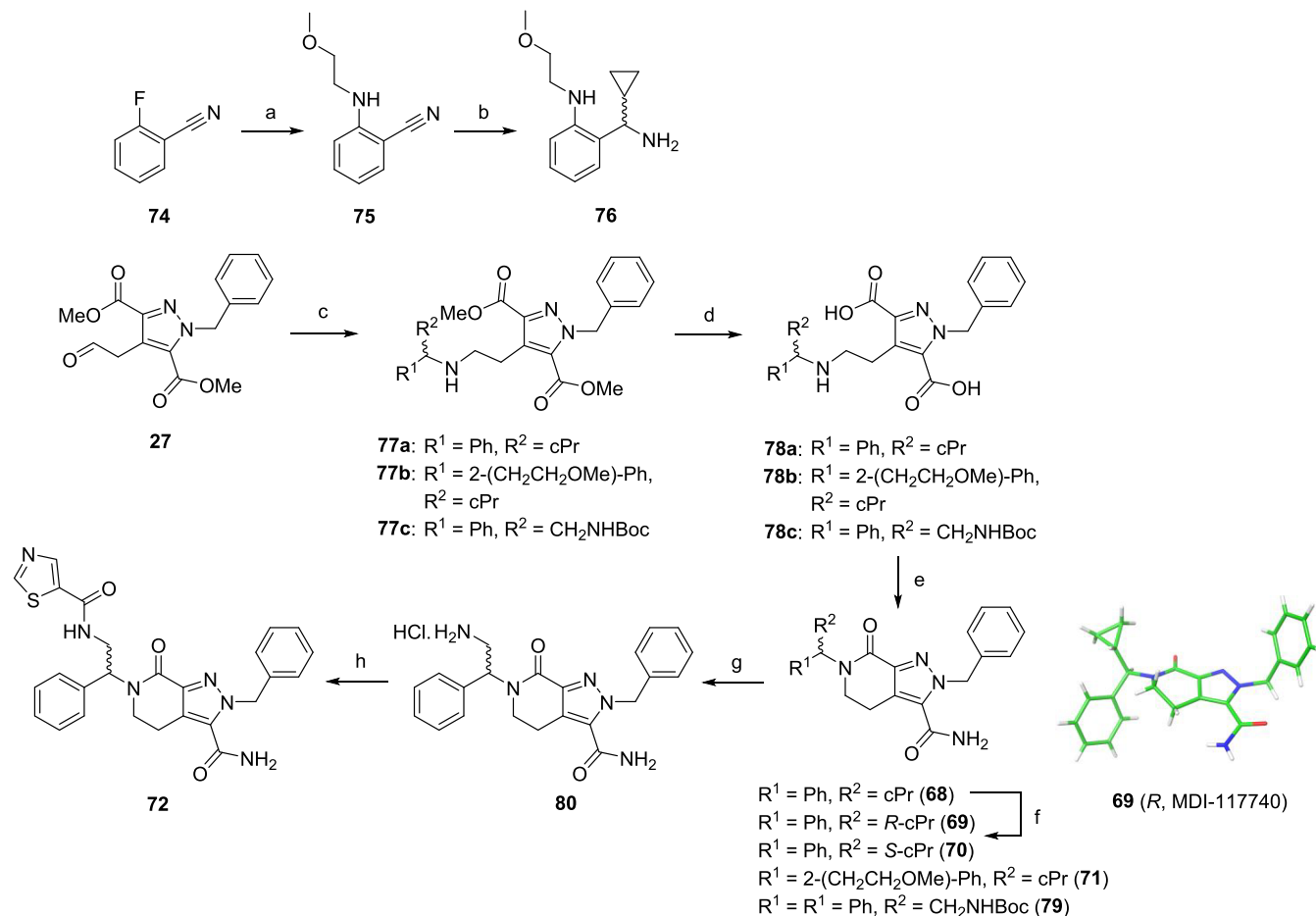
^aData are reported as mean ± SEM of at least three independent experiments, unless otherwise stated. ^bScreened at DiscoverX, Eurofins (San Diego). ^c*n* = 1. ^dMean of two independent experiments. nd, not determined.

to increase LIMK1 potency (Schemes 5 and 6). Again, we leveraged SAR knowledge gained from 6 where the cPr moiety increased LIMK1 inhibition by at least 10-fold³⁹ and molecular docking studies revealed that the benzylic position was the most suitable position to incorporate this group. Intermediates 73a–i were synthesized using a similar three-step reductive amination, ester hydrolysis and amide coupling route of a benzyl substituted or nonaromatic amine (Scheme 5), as previously discussed. However, we observed the majority of reductively aminated intermediates underwent spontaneous cyclization to form two regioisomers (in approximately 1:1 ratio) upon storage that negated the requirement for a conventional intramolecular

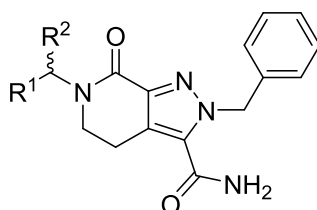
amide coupling. Primary amide formation was accomplished by refluxing in methanolic NH₃ to afford final compounds 58–66 (Scheme 5). Hydrolysis product 67 was also isolated as a side product from synthesis of 58. As expected, sterically hindered amines leading to 68–71 and 79 failed to undergo ring cyclization spontaneously, and instead were prepared according to Scheme 6 through a two-step, one-pot amide coupling of dicarboxylic acid 78a–c with the respective amine and NH₄Cl. Compound 71 was afforded from reductive amination of elaborated amine 76, itself synthesized through a two-step S_NAr and Grignard addition from 74 (Scheme 6). A putative hinge-binding hybrid 72 was also synthesized through Boc

Scheme 5. Synthesis of Substituted Tetrahydropyridinone Analogues 58–67^a

^aReagents and conditions: (a) $R^1R^2\text{NH}_2\cdot\text{HCl}$ (1.3–1.5 equiv), Pic-BH_3 (0.9 equiv), AcOH (0.7–2.1 equiv), MeOH , 0 °C, 3 h; 19–61%; (b) $R^1R^2\text{NH}_2$ (1.0–1.5 equiv), STAB (2.5 equiv), AcOH (0.8–2.4 equiv), DCE , rt, 18 h; 13–51% (for **73g** and **73h**); (c) 2 M AlMe_3 in toluene (3.4 equiv), 100 °C, 3 h, 53% (for **73i**); (d) 7 M NH_3 in MeOH (32.4–148.9 equiv), 70 °C, 18 h, sealed tube, 6–21%.

Scheme 6. Synthesis of Substituted Tetrahydropyridinone Analogues 68–72^a

^aReagents and conditions: (a) 2-methoxyethylamine (2.0 equiv), MeCN , 100 °C, 18 h, sealed tube, 34%; (b) cPrMgBr (3.0 equiv), THF , 100 °C, 15 min then NaBH_4 (5.0 equiv), MeOH , 0 °C, 30 min, 47%; (c) $R^1R^2\text{NH}_2\cdot\text{HCl}$ (1.0 equiv), Pic-BH_3 (1.0–1.5 equiv), AcOH (1.1–1.9 equiv), MeOH , 0 °C, 3 h, 22–45%; (d) $\text{LiOH}\cdot\text{H}_2\text{O}$ (3.0–5.0 equiv), $\text{THF/MeOH/H}_2\text{O}$, rt, 18 h, 78–91%; (e) NH_4Cl (5.0 equiv), HOBT (1.1 equiv), $\text{EDC}\cdot\text{HCl}$ (1.3 equiv), DIPEA (2.4 equiv), DCM , rt, 18 h, 5–48%; (f) chiral separation; (g) **79**, 4 M HCl in 1,4-dioxane (33.3 equiv), DCM , rt, 2 h, quantitative; (h) thiazole-5-carboxylic acid (1.0 equiv), HOBT (1.1 equiv), $\text{EDC}\cdot\text{HCl}$ (1.3 equiv), DIPEA (2.4 equiv), DCM , rt, 18 h, 42%.

Table 3. LIMK1 and LIMK2 K_d Values to Explore Structure–Activity Relationship (SAR) of Substituted Tetrahydropyridinone Analogues 58–72

compound	R^1	R^2	binding affinity (pK_d) ^a	
			LIMK1	LIMK2
34	Ph	H	6.80 ± 0.11	7.29 ± 0.05
58	Bn	H	5.31 ± 0.01	6.29 ± 0.03
59	PhOCH ₂	H	5.87 ± 0.09	7.02 ± 0.00
60	4-OH-Ph	H	6.08 ± 0.09	7.28 ± 0.05
61	4-OMe-Ph	H	5.95 ± 0.23	6.69 ± 0.21
62	3-OH-Bn	H	5.31 ± 0.04	5.92 ± 0.08
63	3-OMe-Bn	H	<5	6.24 ± 0.23
64	CH ₂ OMe	H	5.13 ± 0.14	5.90 ± 0.06
65	CON(Me) ₂	H	<5	5.28 ± 0.03
66 ^b	Ph	CH ₂ CH ₂ OH	6.73 ± 0.01	6.65 ± 0.07
67	see Scheme 5		<5	<5
68 ^b	Ph	cPr	7.37 ± 0.11	6.87 ± 0.02
69	Ph	R-cPr	7.80 ± 0.20	7.12 ± 0.00
70	Ph	S-cPr	6.87 ± 0.05	6.73 ± 0.12
71 ^b	2-((CH ₂) ₂ OMe)-Ph	cPr	<5	<5
72	see Scheme 6		6.27 ± 0.05	5.92 ± 0.08

^aData are reported as mean ± SEM of at least two independent experiments. ^bRacemic.

deprotection of intermediate **79** and subsequent amide coupling of **80** (Scheme 6), as we noted significant LIMK1 potency improvements when hybridized with our MDI-114215 series (data not shown) in line with previous reports with the Type II kinase inhibitor TH-470.^{29,33}

The synthesized analogues **58–72** were screened for binding dissociation constants (K_d). Although not a measure of inhibition, we previously observed that apparent K_d and RapidFire pIC₅₀ values were comparable across these *in vitro* assays (see Table 2 and previously described³⁹). The LIMK1/2 K_d binding data are shown in Table 3. The benzyl ring was found to be largely sensitive to substitutions with the most tolerated analogue **60** leading to an approximate 5-fold drop in LIMK1 potency with LIMK2 potency unchanged. Further attempts to extend the benzyl ring position (**62** and **63**) or replace with nonaromatic groups resulted in even greater loss of LIMK1/2 potency (Table 3). Based on a similar binding mode of **7** with LIMK1 compared to the TH-300 (**30**)-LIMK2 structure, we hypothesize that the benzyl ring forms a key π -cation interaction with the protonated K368, similar to other allosteric LIMK inhibitors. We and others have demonstrated the importance of benzyl positioning and aromaticity to maintain this interaction.^{33,39,41} Turning attention to the benzylic position, pleasingly our rationale to incorporate a racemic cPr group increased potency (**68**) and chiral resolution led to a significant potency gain against LIMK1 for the *R*-enantiomer (**69**, Table 3), whose absolute configuration was confirmed by X-ray crystallography (Scheme 6). Various alternative substituents previously reported that project past the gatekeeper residue T316 toward the hinge region did not lead to any noticeable potency gain (such as **66**), including the hinge-binding hybrid **72**.³⁹ Attempts to merge compound **69** with **6** conferred

nonbinding hybrids such as **71** (Table 3), which was consistent with our benzyl SAR. Therefore, through our SAR assessment, we identified **69** as a novel, highly potent dual LIMK1/2 binder that could be suitable as a tool inhibitor to explore LIMK biology.

Modeling of the binding mode of MDI-117740 (**69**) in LIMK1 (PDB: 7ATU) shows good alignment with LIJTF500025 (**7**, Figure 4), maintaining the key hydrogen bonding interactions with H458, D478 and L397 as described for **7** (Figure 5A). However, a difference in binding mode of the benzyl cyclopropylmethylene moiety is predicted which projects the amide substituents of **7** and **69** into different vectors (as shown by magenta and green arrows, respectively, Figure 4). The docked structure of **69** suggests that the *R*-cyclopropyl

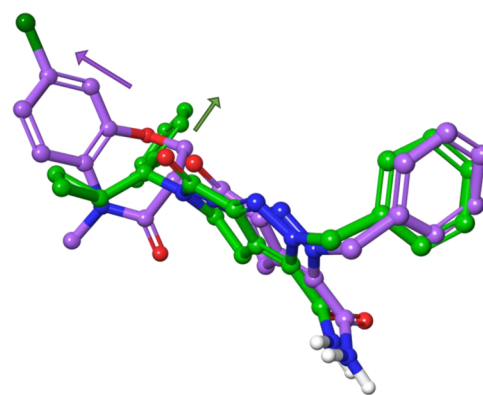


Figure 4. Overlay of modeled **69** (MDI-117740, green) superimposed with **7** (LIJTF500025, magenta) in LIMK1 (PDB: 7ATU, magenta). Ligands were extracted from LIMK1 for clarity.

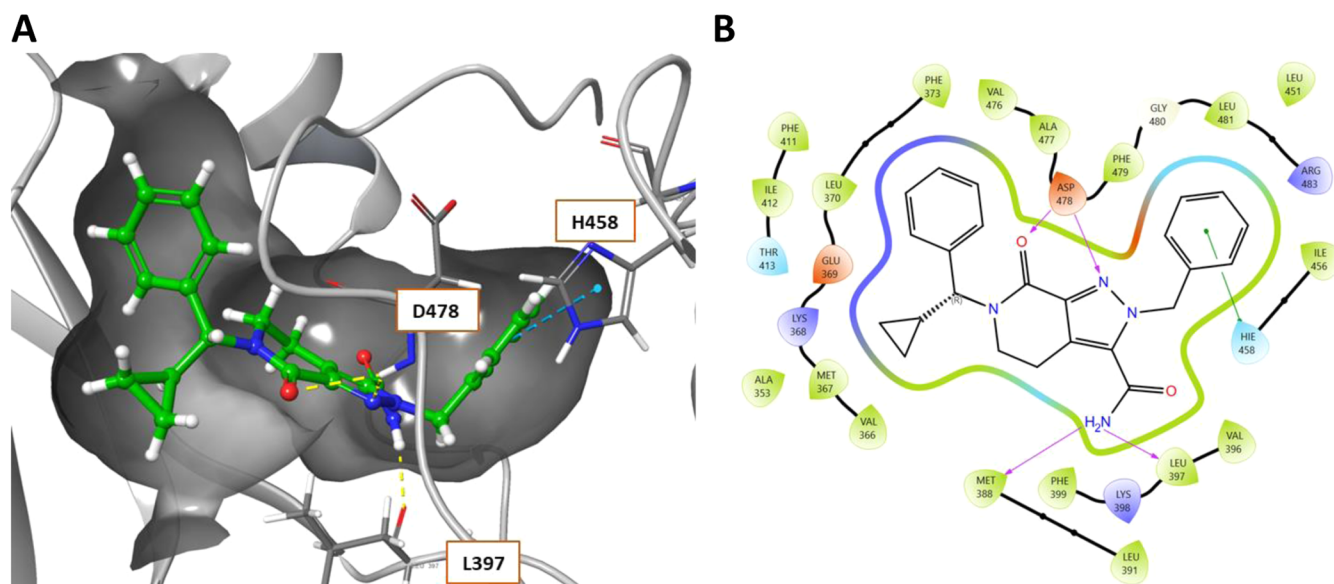
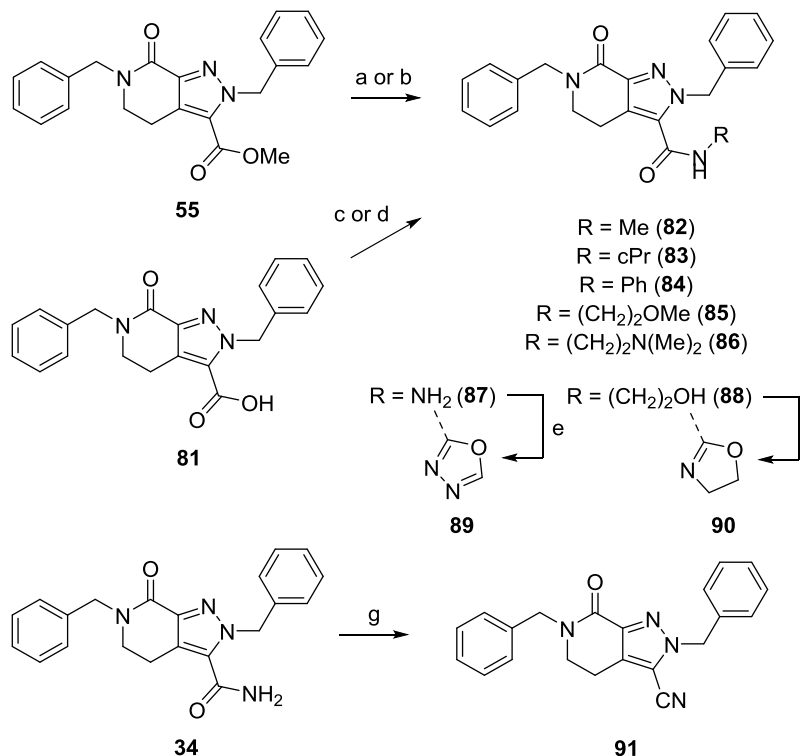


Figure 5. Novel LIMK1 binding mode revealed with **69** (MDI-117740). (A) **69** docked into the 7-LIMK1 cocrystal structure (PDB: 7ATU). The stereo configuration of the tetrahydropyrazolopyridinone core positions the benzyl cyclopropylmethylene moiety in a different subpocket compared to **7** (LIJTFS00025), as detailed in Figure 4. (B) Ligand interaction diagram of **69**. Shading represents the following: hydrophobic area (green), charged interaction (positive, blue; negative, red), polar (teal).

Scheme 7. Synthesis of Substituted Amides 82–88, Amide Isosteres 89–90 and Nitrile Analogue 91^a



^aReagents and conditions: (a) NH_2NH_2 (23.6 equiv), EtOH, 90 °C, 6 h, quantitative (when $\text{R} = \text{NH}_2$); (b) $\text{NH}_2(\text{CH}_2)_2\text{OH}$, DIPEA, MeOH, 130 °C, 16 h, 86% (when $\text{R} = (\text{CH}_2)_2\text{OH}$); (c) RNH_2 (1.5 equiv), T3P (3.0 equiv), DIPEA (2.6 equiv), THF, rt, 18 h, 5–35%; (d) RNH_2 (1.3–1.5 equiv), HOBt (1.1 equiv), EDC·HCl (1.3 equiv), DIPEA (2.5 equiv), DCM, rt, 18 h, 15–18%; (e) $\text{HC}(\text{OEt})_3$ (37.6 equiv), 100 °C, 18 h, 7%; (f) DEAD (1.5 equiv), PPh_3 (1.5 equiv), toluene, rt, 18 h, 4%; (g) TFAA (5.3 equiv), Et_3N (7.5 equiv), DCM, rt, 18 h, 40%.

group pushes into a small hydrophobic pocket enclosed by F479, the alkyl chain of K368, V366 and L367, which occupies the same hydrophobic niche of the *N*-Me group in **7**. Meanwhile, the phenyl ring is presented toward a hydrophobic tunnel comprising L370, L481, F411, and the alkyl chain of K368

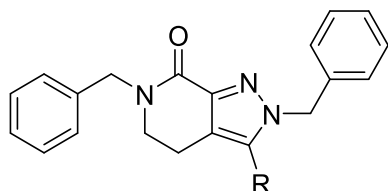
(Figure 5). This hydrophobic tunnel is the same as that exploited by MDI-114215 (**6**) with an ethanolamine-substituted aromatic pendant.³⁹

Using novel compound **34** as a template, we also further explored SAR around the primary amide through synthesis of

various amide replacements (**81–91**), substituted amides (**82–88**) and amide isosteres (**89–90**, Scheme 7). The cocrystal structure of **7** bound to LIMK1 (PDB: 7ATU) shows a bidentate H-bond interaction between the primary amide and L397/M388 (Figure 2) that we speculated was similarly important for LIMK1 potency on our new scaffold. To confirm this, a small set of secondary and tertiary amides **82–88** were synthesized through methyl ester **55** or carboxylic acid **81** that was amenable to various amide coupling conditions (Scheme 7). 1,3,4-Oxadiazole **89** was synthesized from hydrazide **87** and triethylorthoformate under reflux, while partially reduced oxazole **90** was generated from intramolecular cyclization of compound **88** under Mitsunobu conditions (Scheme 7). Attempts to oxidize the semireduced oxazole under various oxidation conditions (e.g., DDQ) unfortunately failed to furnish the desired oxazole product. Nitrile analogue **91** was synthesized by dehydrating primary amide **34** under the action of TFAA (Scheme 7).

The synthesized substituted amides and primary amide replacements were then screened against LIMK1 and LIMK2 in the K_d ELECT assay. The results unequivocally demonstrated that the primary amide was indispensable for LIMK1/2 binding (Table 4). The majority of compounds were found to be inactive with only weak binding affinities recorded for nitrile analogue **91** (Table 4). The strong requirement for an unsubstituted primary amide is consistent with both (i) 7-LIMK1 structure which forms key H-bond interactions with the protein through each

Table 4. LIMK1 and LIMK2 K_d Values to Explore Structure–Activity Relationship (SAR) of the Primary Amide of Lead Compound **34**



compound	R	binding affinity (pK_d) ^a	
		LIMK1	LIMK2
34	CONH ₂	6.80 ± 0.11	7.29 ± 0.05
55	CO ₂ Me	< 5	< 5
81	CO ₂ H	< 5	< 5
82	CONHMe	< 5	< 5
83	CONHcPr	< 5	< 5
84	CONHPh	< 5	< 5
85	CONH(CH ₂) ₂ OMe	< 5	< 5
86	CONH(CH ₂) ₂ N(Me) ₂	< 5	< 5
88	CONH(CH ₂) ₂ OH	< 5	< 5
89		< 5	< 5
90		< 5	< 5
91	CN	5.28 ± 0.05	5.12 ± 0.07

^aData are reported as mean ± SEM of at least two independent experiments.

amidic NH, and (ii) overlay of **7** with the TH-300 (**30**)-LIMK2 structure (PDB: 5NXX) that superposes the primary amide with the sulfonamide (Figure 3A), a group which also could not be substituted or replaced.³⁹ Indeed, similar to the primary amide-sulfonamide comparison, the benzyl ring of **7** superimposes very well with the aniline ring of **30** (Figure 3A), which we and others showed does not tolerate any modification.^{39,41} Therefore, we regard this region where type III allosteric inhibitors **6** and **7** bind deep into the protein pocket as inflexible and their unique space filling properties and H-bond interaction network as pivotal to LIMK1/2 binding or inhibition. As a result, we decided against further exploring modifications to the benzyl ring.

The most optimized molecule **69** was further evaluated for its suitability as an *in vitro* and *in vivo* tool by assessing cellular activity and DMPK properties (Table 5). **69** displayed excellent

Table 5. *In Vitro* and *In Vivo* DMPK Properties of **69**

	69 (MDI-117740)
nanoBRET LIMK1/2 pIC_{50} ^a	6.73 ± 0.09/7.18 ± 0.18
alphaLISA p-cofilin pIC_{50} ^a	6.89 ± 0.02
aq. solubility (μM, pH 7.0) ^b	85
R/H ^c microsomal CL (μL/min/mg)	96/48
i.v. dose (mg/kg)	0.2
AUC _{inf} (h·ng/mL)	262
CL _{int} (mL/min/kg)	13
V _D (L/kg)	0.5
T _{1/2} (h)	0.6
C _{max} (ng/mL) ^d	26.7
T _{max} (h) ^d	0.4
F% ^e	2
B/P ratio ^f	0.02

^aData are reported as mean ± SEM of at least three independent experiments. ^bAverage of at least two separate experiments. ^cRat and human microsomes. ^dDetermined after p.o. dosing at 3 mg/kg. ^eDetermined by comparison with 3 mg/kg dosing p.o. ^fDetermined internally after i.p. dosing at 10 mg/kg.

cellular target engagement and potently inhibits p-cofilin levels in SH-SY5Y cells. The *in vitro* DMPK properties of **69** were also significantly improved (Table 5) compared to **6** (aqueous solubility = 11 μM, rat/human microsomal CL_{int} = 289/98 μL/min/mg), a type III allosteric dual LIMK1/2 inhibitor that we recently disclosed where optimizing drug clearance was challenging.³⁹ Given its promising *in vitro* DMPK profile, we then assessed ADME properties of **69** through *in vivo* PK evaluation. The low *in vitro* microsomal clearance translated to low *in vivo* CL_{int} in male Sprague–Dawley rats and, again, was improved compared to **6** (CL_{int} = 33 mL/min/kg). This in turn led to enhanced drug exposure for **69** (654 nM), achieving >40-fold and >8-fold greater total drug concentration than LIMK1 and LIMK2 K_d , respectively. Other key parameters (V_D , $T_{1/2}$) were also acceptable after i.v. dosing (Table 5). Unfortunately, oral bioavailability of **69** was very low with maximal drug concentrations (C_{max}) in plasma reaching approximately 27 ng/mL after p.o. dosing (at 3 mg/kg) and no evidence of good CNS penetration was observed after i.p. dosing (at 10 mg/kg, Table 5). The limited CNS penetration of **69**, similar to other type III allosteric LIMK inhibitors, represents a limitation for studies exploring the role of LIMKs in neuronal function or synaptic regulation. Therefore, we suspected that **69** was a drug efflux

substrate given the effect of different routes of administration on the *in vivo* PK profile.

We carried out a structure-permeability relationship study to prove **69** was a drug efflux substrate and identify the chemical motifs responsible for poor permeability. Compounds were assessed in the Caco-2 permeability assay as it is widely used as a model of the intestinal epithelial barrier and thus predicts human intestinal permeability. The results are presented in Table 6. In

Table 6. Caco-2 Permeabilities and Efflux Ratios of Selected Compounds

compound	caco-2 permeability ^a		
	$P_{app(A-B)}$ ($\times 10^{-6}$ cm/s)	ER ^b	mean % recovery (A-B/B-A)
antipyrine ^c	44.1 \pm 1.59	0.95	86.6/92.7
atenolol ^d	0.28 \pm 0.02	1.94	87.8/93.8
talinalol ^e	0.31 \pm 0.07	37.9	79.1/92.0
estrone 3-sulfate ^f	0.45 \pm 0.06	52.3	61.4/84.4
7	5.11 \pm 0.51	13.9	85.9/74.2
19 ^g	6.84 \pm 0.16	1.20	36.5/25.9
21	3.06 \pm 0.08	14.6	91.2/85.3
32 ^h	18.8 \pm 1.89	2.00	40.5/66.2
34	7.00 \pm 0.74	6.79	85.4/85.6
55	40.6 \pm 0.95	0.85	72.3/63.2
57	28.3 \pm 1.22	0.96	63.2/66.5
59	10.0 \pm 0.52	5.54	82.9/81.5
64	1.93 \pm 0.30	11.0	87.1/96.1
66 ⁱ	0.38 \pm 0.17	86.9	84.2/84.3
68	8.29 \pm 0.44	6.32	77.2/65.2
69	10.1 \pm 0.07	5.52	81.5/82.2
82	12.8 \pm 0.53	4.29	76.1/85.7
89	44.5 \pm 1.86	1.09	84.4/85.6
90	38.5 \pm 2.84	1.04	69.8/71.0
91	35.0 \pm 0.22	0.97	72.3/64.3

^aData are reported as mean \pm SD of at least two independent experiments. ^bEfflux is calculated as $P_{app(A-B)}/P_{app(B-A)}$. ^cHuman absorption = 97%. ^dHuman absorption = 50%. ^eKnown P-gp substrate. ^fKnown BCRP substrate. ^gHigh C_0 value A-B direction and low recovery B-A direction. ^hLow C_0 value B-A direction was observed. ⁱCompound concentration from basolateral compartment below limit of quantification.

summary, we confirmed that **69** was a drug efflux substrate (ER = 5.5). Structure-permeability relationships also clearly showed that 1-benzylpyrazolo-5-carboxamides were exclusively subject to high efflux (ER > 2), whereas 1-benzylpyrazolo-3-carboxamides (e.g. **57**), primary amide isosteres/replacements (e.g., **89**) or ring-opened analogue **32** demonstrated low ER (Table 6). Thus, the privileged 1-benzylpyrazolo-5-carboxamide scaffold necessary for potent dual LIMK1/2 inhibition also leads to high drug efflux precluding oral dosing (and most likely low CNS penetration) that could not be separated, presenting significant challenges in developing a highly potent, selective, CNS-penetrant series with good oral bioavailability.

As exquisite kinome selectivity is an essential requirement for developing a LIMK selective tool compound, we assessed the wider kinome selectivity of **69** using the Eurofins/DiscoverX scanMAX panel of 468 kinases (which employs the KINOMEScan Technology, further details at <https://www.eurofinsdiscovery.com/solution/kinomescan-technology>, full kinome screening data are reported in Table S1). We chose to screen at a single concentration of 300 nM as approximately 10-

fold LIMK1 K_d (Table 3) and a selectivity score, S(35)-score, was calculated by dividing the number of kinases that bind by >35% with the total number of kinases tested in the panel. Smaller scores indicate higher selectivity and was used to facilitate comparison with reported literature LIMK inhibitors. The selectivity screen revealed an S(35)-score of 0.005 (Figure 6), making **69** the most selective dual LIMK1/2 inhibitor

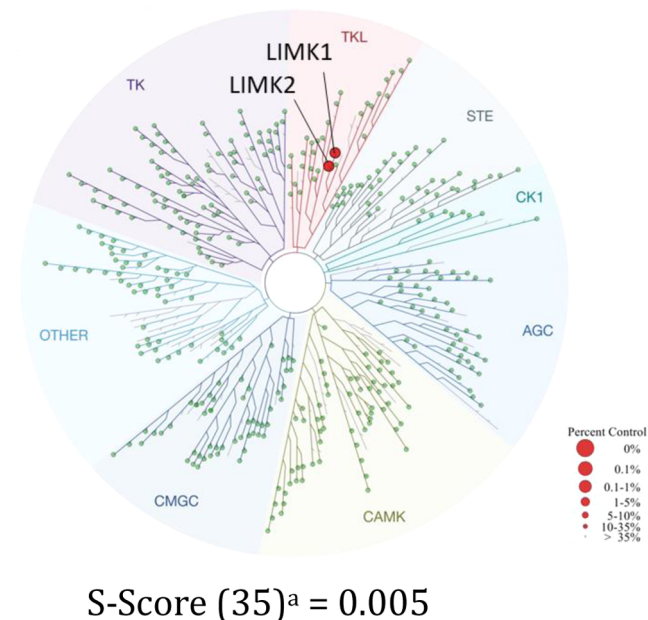


Figure 6. Kinome selectivity profiling of MDI-117740 (**69**). Selectivity profile using the scanMAX kinome wide selectivity assay (Eurofins), screened at 300 nM. Data are illustrated using the TREE_{spot} interaction map (DiscoverX). ^aNumber of nonmutant kinases that **69** binds to with %Ctrl <35 divided by the total number of distinct kinases tested.

reported to date.^{29,33} Importantly, no binding to RIPK1 was observed, a known off-target of **7**.^{42,43} In addition, **69** does not bind PAK1-2/4, ROCK1/2, MRCK α or CAMK4 that are known to activate LIMK1/2 through phosphorylation.^{4,6,8,53} Such a selective LIMK inhibitor is critical to prevent assay misinterpretation for researchers wanting to investigate LIMKs in health and disease, similar to previous observations with the now known dual LIMK/PAK inhibitor FRAX486.^{29,34}

To assess the functional impact of **69** on cell motility, an *in vitro* wound healing assay was performed in MDA-MB-231 cells for 48 h. A scratch was induced to confluent monolayers and cells were treated with **69**, FRAX486 (**2**) or a structurally related negative control (**57**, enzymatic LIMK1/2 pIC₅₀ < 5, Table 2) at three separate concentrations (0.25 μ M, 1 μ M, and 3 μ M) or untreated control. **2** was selected as the positive control as it was previously shown to significantly inhibit TNBC MDA-MB-231 cell migration in wound healing assays.⁵⁴ Wound closure was measured over 48 h and the percentage wound closure was quantified relative to the initial wound area. Treatment with compound **69** significantly inhibited wound closure compared to untreated control at 0.25 μ M and 1 μ M concentrations (p = 0.049 and p = 0.019, respectively) and had a more pronounced effect observed at 3 μ M (p = 0.006, Figure 7A). LIMK inhibitor **2** also induced significant effects on cell migration (0.25 μ M p = 0.015, 1 μ M p = 0.002 and 3 μ M p = 0.001, Figure 7B), consistent with previous literature.⁵⁴ No significant effect was observed for **57** (p = 0.46, Figure 7A/B). It should be noted that

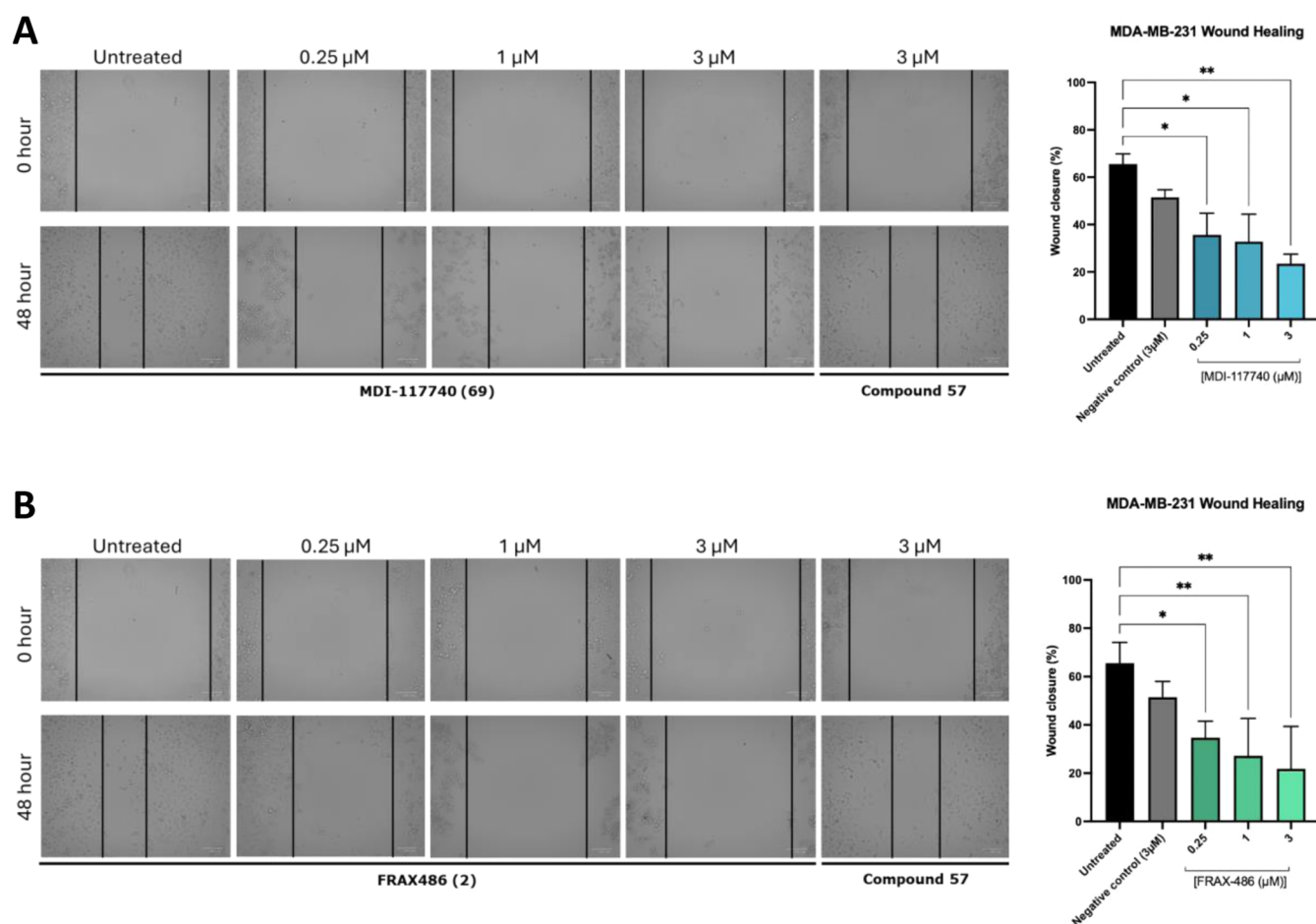


Figure 7. Effect of MDI-117740 (**69**) and FRAX486 (**2**) on cell migration in a wound healing assay in MDA-MB-231 cells. Confluent monolayers were scratched and treated with either compound **69** (A) or **2** (B) at 0.25, 1, or 3 μ M. Wound closure was assessed after 48 h. Representative images and quantification of wound area are shown. Scale bar: 100 μ m. Compound **69** inhibited wound closure at all tested concentrations in this experiment. Data are from four independent experiments.

cells treated at higher concentrations of compound **2** appear more rounded which may indicate mitotic arrest, a phenotype not observed upon treatment with compounds **57** or **69**. Given that **2** has broader kinome promiscuity than **69**,²⁹ this suggests that **2** might act on additional targets involved in cell division beyond LIMK1 or LIMK2. Further cell cycle analysis is warranted to confirm these observations. Taken together, these data strongly suggest that **69** is a potent and highly selective dual-LIMK1/2 inhibitor that demonstrates cellular target engagement, potent inhibition of cofilin phosphorylation, and positive LIMK-dependent downstream phenotypic effects on cell migration.

CONCLUSIONS

In summary, we have discovered and characterized tetrahydropyrazolopyridinones as a novel class of LIMK1/2 inhibitors. Structure-based drug design using the Takeda RIPK1 inhibitor 7-LIMK1 structure, together with our prior understanding of similar type III allosteric inhibitors, led to discovery of MDI-117740 (**69**) as a potent LIMK1/2 inhibitor that demonstrates good *in vivo* PK properties suitable as both an *in vitro* and *in vivo* probe when dosed intravenously. A structure-permeability relationships study confirmed that the indispensable 1-benzylpyrazolo-5-carboxamide scaffold is responsible for low oral bioavailability in this series due to high drug efflux.

Importantly, we show that **69** is the most selective LIMK1/2 inhibitor currently available in the literature, eliminating any pre-existing RIPK1 activity associated with **7**. The highly selective and potent dual LIMK1/2 inhibitor **69** described herein will facilitate understanding of the mechanistic roles of LIMK in disease and their application toward therapies targeting LIMK pathologies.

EXPERIMENTAL SECTION

General Methods. All commercial materials were used as received without further purification. Identity and purity checks were carried out prior to use in biological experiments using ¹H NMR spectroscopy and UPLC-MS analysis on the instruments as described below that are presented in the Supporting Information for reference. All final compounds were $\geq 95\%$ purity as determined by ¹H NMR and/or UPLC-MS analyses.

Materials. LIJTFS00125 (**7**), (3S)-3-amino-8-chloro-5-methyl-2,3-dihydro-1,5-benzoxazepin-4-one (as the hydrochloride or trifluoroacetate salt) and 4-(phenylsulfamoyl)benzoic acid were prepared as previously described.²⁹ N-benzyl-1-cyclopropylmethanamine was synthesized as previously described.³⁹

Synthetic Procedures and Compound Characterization. An example stacked ¹H NMR spectrum permitting regiochemical assignment of 1-benzylpyrazolo-carboxamides in the absence of HMBC experiments can be found in Figure S4. ¹H and ¹³C NMR spectra were recorded on a Bruker Avance III HD 500 or 400 MHz equipped with a Prodigy cryoprobe. Chemical shifts (δ) are defined in parts per million

(ppm). ^1H NMR spectra were referenced to tetramethylsilane (TMS, δ = 0.00 ppm) or residual undeuterated solvent (CDCl_3 , δ = 7.26 ppm; $\text{MeOH}-d_4$, δ = 3.31 ppm; $\text{DMSO}-d_6$, δ = 2.50 ppm). ^{13}C NMR spectra were referenced to undeuterated solvent (CDCl_3 , δ = 77.16 ppm; $\text{DMSO}-d_6$, δ = 39.52 ppm). Multiplicities are abbreviated as follows: s, singlet; d, doublet; t, triplet; q, quartet; dd, doublet of doublets; dt, doublet of triplets; m, multiplet; br, broad, or combinations thereof. Coupling constants were measured in Hertz (Hz). Liquid chromatography–mass spectrometry (LCMS) was primarily carried out on a Waters Acquity Hclass plus UPLC coupled to a Waters Acquity HPLC PDA detector and a Waters Acquity QDa API-ES mass detector. Samples were eluted through a BEH C_{18} 2.1 mm \times 50 mm, 1.7 μm column using H_2O and MeCN acidified by 0.1% formic acid. The gradient runs $\text{H}_2\text{O}/\text{MeCN}/\text{formic acid}$ at 90:10:0.1–10:90:0.1 for 3 min at 1.5 mL/min and detected at 254 nm. LCMS for key intermediates were also carried out on either a: (i) Waters HPLC equipped with XSelect CSH C_{18} 3.0 mm \times 50 mm \times 2.5 μm column with samples eluting using a gradient of 95:5–1:49 2.5 mM $(\text{NH}_4)\text{HCO}_3/\text{MeCN}$ for 5 min at 1 mL/min, or (ii) Waters HPLC equipped with XBridge CSH C_{18} 3.0 mm \times 50 mm \times 2.5 μm with sample eluting using a gradient of 95:5–1:49 $\text{H}_2\text{O}/\text{MeCN}$ acidified by 0.05% formic acid for 4 min at 1.2 mL/min, or (iii) LCMS EW21065–214-P1B1, or (iv) Shimadzu LC-20AB & MS 2020 with HALO C_{18} 3 mm \times 30 mm, 5 μm using 0.04% TFA in water and 0.02% TFA in MeCN at a flow rate of 2.0 mL/min. Accurate mass determination was performed on a Waters Synapt G2 SI with ESI probe. Molecular ion peaks are defined as mass/charge (m/z) ratios. Melting point analysis was carried out using an Electrothermal IA9100 digital melting point apparatus. Analytical thin-layer chromatography (TLC) was performed using VWR silica gel 60 on aluminum plates coated with F_{254} indicator. All spots were visualized with ultraviolet light using a VVP C-10 Chromato-Vue cabinet or stained using KMnO_4 . Normal-phase purifications were completed using a Teledyne ISCO CombiFlash NEXTGEN 300+ using silica gel with particle size 40–63 μm ; reverse-phase purifications were completed using a Teledyne ACCQPrep system equipped with a 20 mm \times 150 mm C_{18} column, or Waters system equipped with a 30 mm \times 250 mm C_{18} column, and eluted with a 10–100% $\text{MeOH}/\text{H}_2\text{O}$, 10–100% $\text{MeCN}/0.1\%$ formic acid in H_2O , or $\text{MeCN}/5$ mM $(\text{NH}_4)\text{HCO}_3$ gradient. Evaporation of solvents was conducted on a Buchi Rotavapor R-300.

General Procedure A—Reductive Amination. Unless otherwise stated, a suspension of a primary or secondary amine (1.1–1.5 equiv) and dimethyl 1-benzyl-4-(2-oxoethyl)-1H-pyrazole-3,5-dicarboxylate (**27**, 1 equiv) in MeOH (5–10 mL) was added acetic acid (0.1–0.3 mL, catalytic). The reaction mixture was cooled to 0 $^\circ\text{C}$ and stirred for 5 min until a solution resulted. 2-Methylpyridine borane complex (0.9–1.5 equiv) was then added and the resultant solution stirred at 0 $^\circ\text{C}$ for 3 h, allowing to warm to room temperature. Saturated NaHCO_3 (5–10 mL) was added and the mixture extracted with EtOAc (2 \times 10–20 mL). The organic layers were combined, dried over NaSO_4 , filtered and concentrated under reduced pressure. The crude mixture was purified by flash column chromatography and fractions containing product were combined and concentrated under reduced pressure to afford the reductive aminated product.

General Procedure B—Ester Hydrolysis. Unless otherwise stated, a solution of a methyl 7-oxo-4,5,6,7-tetrahydropyrazolo[3,4-*c*]pyridine carboxylate in either THF/water (1:1) or MeOH/THF/water (1:1:1) was added LiOH· H_2O (3–5 equiv). The reaction mixture was stirred at room temperature overnight. The reaction mixture was concentrated under reduced pressure. One M HCl (~5 mL) was added and a solid immediately precipitated. The precipitate was filtered, washed with water (10 mL) and dried thoroughly to afford the 7-oxo-4,5,6,7-tetrahydropyrazolo[3,4-*c*]pyridine carboxylic acid.

General Procedure C—Amide Coupling. Unless otherwise stated, DIPEA (1.5–2.4 equiv) was added to a solution of a 7-oxo-4,5,6,7-tetrahydropyrazolo[3,4-*c*]pyridine carboxylic acid (1 equiv), HOBT hydrate (1.1 equiv), EDC·HCl (1.2–1.3 equiv) in DCM (2–8 mL). The reaction mixture was stirred at room temperature for 30 min. A (un)substituted amine (1–5 equiv) was then added. The reaction mixture was further stirred at room temperature overnight. Saturated

NaHCO_3 (10 mL) was added and the reaction mixture stirred for 15 min at room temperature. The organic phase was separated using a phase separator and the filtrate concentrated under reduced pressure with silica. The crude mixture was purified by flash column chromatography and fractions containing product were combined and concentrated under reduced pressure to afford the substituted 7-oxo-4,5,6,7-tetrahydropyrazolo[3,4-*c*]pyridine carboxamide.

General Procedure D—Primary Amide Synthesis. Unless otherwise stated, a methyl 7-oxo-4,5,6,7-tetrahydro-2H-pyrazolo[3,4-*c*]pyridine carboxylate (1 equiv) was dissolved in 7 M NH_3 in MeOH (5–15 mL). The reaction mixture heated to 70 $^\circ\text{C}$ and stirred overnight in a sealed tube. The reaction mixture was concentrated under reduced pressure. The crude mixture was purified by reverse-phase column chromatography and fractions containing product were combined and concentrated under reduced pressure to afford the primary 7-oxo-4,5,6,7-tetrahydro-2H-pyrazolo[3,4-*c*]pyridine carboxamide.

Ethyl 1-Benzyl-5-bromo-4-formyl-1H-pyrazole-3-carboxylate (14). To the solution of ethyl 1-benzyl-5-hydroxy-1H-pyrazole-3-carboxylate (3.00 g, 12.1 mmol, 1.00 equiv) and POBr_3 (30.8 g, 107 mmol, 8.83 equiv) in DCE (45 mL) was added DMF (1.66 g, 22.7 mmol, 1.87 equiv) at room temperature under N_2 . Upon completion of addition, the mixture was heated to 90 $^\circ\text{C}$ and stirred for 72 h. The reaction mixture was poured carefully onto ice water (500 mL), then stirred at room temperature for 30 min. The mixture was extracted with EtOAc (500 mL), and the organic layer washed with brine (500 mL), dried over Na_2SO_4 , filtered and concentrated under reduced pressure to afford the crude product, which was purified by column chromatography (silica, 99:1 petrol/EtOAc to 9:1 petrol/EtOAc) to afford ethyl 1-benzyl-5-bromo-4-formyl-1H-pyrazole-3-carboxylate (**14**, 1.50 g, 4.44 mmol, 37% yield) as a yellow solid. ^1H NMR (400 MHz, $\text{DMSO}-d_6$) δ 10.24 (s, 1H), 7.48–7.15 (m, 5H), 5.57 (s, 2H), 4.36 (q, J = 7.1 Hz, 2H), 1.32 (t, J = 7.1 Hz, 3H). LCMS: EW21065–214-P1B1: Rt = 0.88 min; m/z 337.1 [$\text{M} + \text{H}$, ^{79}Br] $^+$.

Ethyl 1-Benzyl-5-bromo-4-(2-methoxyvinyl)-1H-pyrazole-3-carboxylate (15). To a solution of (methoxymethyl)-triphenylphosphonium chloride (10.9 g, 32.0 mmol, 2.00 equiv) in THF (50 mL) was added *t*-BuOK (3.59 g, 31.9 mmol, 2.00 equiv) at 0 $^\circ\text{C}$ under N_2 . The reaction mixture was stirred at 0 $^\circ\text{C}$ for 5 min, before a solution of ethyl 1-benzyl-5-bromo-4-formyl-1H-pyrazole-3-carboxylate (5.40 g, 16.0 mmol, 1.00 equiv) in THF (100 mL) was added. The mixture was stirred at room temperature for 12 h. The reaction mixture was poured onto ice water (200 mL), then extracted with EtOAc (100 mL). The organic layer was washed with brine (100 mL), dried over Na_2SO_4 , filtered and concentrated under reduced pressure to afford the crude product, which was purified by column chromatography (silica, 49:1 petrol/EtOAc to 9:1 petrol/EtOAc) to afford ethyl 1-benzyl-5-bromo-4-(2-methoxyvinyl)-1H-pyrazole-3-carboxylate (**15**, 5.02 g, 13.5 mmol, 61% yield) as a mixture of diastereomers (83% *trans* by coupling constant observed at 6.02 ppm compared to 6.16 ppm for minor *cis* isomer) as a light yellow solid. Major isomer (*trans*) reported: ^1H NMR (500 MHz, CDCl_3) δ 7.35–7.26 (m, 4H), 7.22–7.19 (m, 2H), 6.02 (d, J = 13.3 Hz, 1H), 5.47 (s, 2H), 4.42 (q, J = 7.1 Hz, 2H), 3.69 (s, 3H), 1.41 (t, J = 7.2 Hz, 3H). ACQUITY UPLC BEH C_{18} 1.7 μm : Rt = 1.85 min; m/z 387.0 [$\text{M} + \text{Na}$, ^{79}Br] $^+$, 389.0 [$\text{M} + \text{Na}$, ^{81}Br] $^+$.

Ethyl 1-Benzyl-5-bromo-4-(2-oxoethyl)-1H-pyrazole-3-carboxylate (16). Ethyl 1-benzyl-5-bromo-4-[(*E*)-2-methoxyvinyl]pyrazole-3-carboxylate (131 mg, 0.34 mmol) was dissolved in 4 M HCl in 1,4-dioxane (1.2 mL). UPLC analysis after 5 min indicated reaction was complete. The mixture was taken to pH 9 by addition of a saturated aqueous solution of NaHCO_3 (10 mL) and extracted with EtOAc (2 \times 30 mL). The organic phase was dried over MgSO_4 , filtered and concentrated under reduced pressure to give ethyl 1-benzyl-5-bromo-4-(2-oxoethyl)pyrazole-3-carboxylate (**16**, 106 mg, 0.287 mmol, 88% yield) as a colorless oil. ^1H NMR (500 MHz, CDCl_3) δ 9.67 (t, J = 1.4 Hz, 1H), 7.35–7.28 (m, 3H), 7.25–7.21 (m, 2H), 5.48 (s, 2H), 4.39 (q, J = 7.1 Hz, 2H), 3.80 (s, 2H), 1.37 (t, J = 7.1 Hz, 3H). ACQUITY UPLC BEH C_{18} 1.7 μm : Rt = 1.77 min; m/z 373.0 [$\text{M} + \text{Na}$, ^{79}Br] $^+$, 375.0 [$\text{M} + \text{Na}$, ^{81}Br] $^+$.

Ethyl 1-Benzyl-5-bromo-4-[2-[[[(3S)-8-chloro-5-methyl-4-oxo-2,3-dihydro-1,5-benzoxazepin-3-yl]amino]ethyl]pyrazole-3-carboxy-

late (17). Synthesized according to General Procedure A using ethyl 1-benzyl-5-bromo-4-(2-oxoethyl)pyrazole-3-carboxylate (100 mg, 0.27 mmol), [(3S)-8-chloro-5-methyl-4-oxo-2,3-dihydro-1,5-benzoxazepin-3-yl]ammonium trifluoroacetate (97 mg, 0.27 mmol), acetic acid (0.50 mL, 8.73 mmol) and borane-2-methylpyridine complex (38 mg, 0.35 mmol). Purified by flash column chromatography (silica, 12 g, 1:0 petrol/EtOAc to 0:1 petrol/EtOAc containing 1% Et₃N over 25 CV's) to give ethyl 1-benzyl-5-bromo-4-[2-[(3S)-8-chloro-5-methyl-4-oxo-2,3-dihydro-1,5-benzoxazepin-3-yl]amino]ethyl]pyrazole-3-carboxylate (17, 134 mg, 0.22 mmol, 88% yield) as a colorless solid. ¹H NMR (500 MHz, CDCl₃) δ 7.26–7.17 (m, 3H), 7.13–7.08 (m, 3H), 7.08–7.01 (m, 2H), 5.35 (s, 2H), 4.32–4.26 (m, 3H), 4.03–3.98 (m, 1H), 3.48 (dd, *J* = 11.6, 7.3 Hz, 1H), 3.28 (s, 3H), 2.81–2.61 (m, 3H), 2.38 (ddd, *J* = 10.3, 8.4, 5.9 Hz, 1H), 1.32–1.27 (m, 3H). NH not observed. ACQUITY UPLC BEH C₁₈ 1.7 μm: Rt = 1.67 min; *m/z* 563.1 [M + H, ⁸¹Br, ³⁵Cl]⁺.

1-Benzyl-5-bromo-4-[2-[(3S)-8-chloro-5-methyl-4-oxo-2,3-dihydro-1,5-benzoxazepin-3-yl]amino]ethyl]pyrazole-3-carboxylic Acid (18). Synthesized according to General Procedure B using ethyl 1-benzyl-5-bromo-4-[2-[(3S)-8-chloro-5-methyl-4-oxo-2,3-dihydro-1,5-benzoxazepin-3-yl]amino]ethyl]pyrazole-3-carboxylate (134 mg, 0.24 mmol) and LiOH·H₂O (60 mg, 1.43 mmol) to give 1-benzyl-5-bromo-4-[2-[(3S)-8-chloro-5-methyl-4-oxo-2,3-dihydro-1,5-benzoxazepin-3-yl]amino]ethyl]pyrazole-3-carboxylic acid (18, 127 mg, 0.22 mmol, quantitative yield) as a colorless solid. ACQUITY UPLC BEH C₁₈ 1.7 μm: Rt = 1.57 min; *m/z* 535.0 [M + H, ⁸¹Br, ³⁵Cl]⁺.

(S)-3-(2-Benzyl-3-bromo-7-oxo-2,4,5,7-tetrahydro-6H-pyrazolo[3,4-c]pyridin-6-yl)-8-chloro-5-methyl-2,3-dihydrobenzo[b][1,4]oxazepin-4(5H)-one (19). Synthesized according to General Procedure C using 1-benzyl-5-bromo-4-[2-[(3S)-8-chloro-5-methyl-4-oxo-2,3-dihydro-1,5-benzoxazepin-3-yl]amino]ethyl]pyrazole-3-carboxylic acid (127 mg, 0.24 mmol), HOBt hydrate (40 mg, 0.26 mmol), and EDC·HCl (55 mg, 0.29 mmol). Purified by flash column chromatography (silica, 12 g, 1:0 petrol/EtOAc to 0:1 petrol/EtOAc over 30 CV's) to afford (S)-3-(2-benzyl-3-bromo-7-oxo-2,4,5,7-tetrahydro-6H-pyrazolo[3,4-c]pyridin-6-yl)-8-chloro-5-methyl-2,3-dihydrobenzo[b][1,4]oxazepin-4(5H)-one (19, 84 mg, 0.16 mmol, 68% yield) as a colorless solid. ¹H NMR (500 MHz, CDCl₃) δ 7.34–7.27 (m, 3H), 7.27–7.22 (m, 3H), 7.19–7.15 (m, 2H), 5.90 (dd, *J* = 11.8, 8.1 Hz, 1H), 5.43 (s, 2H), 4.63 (dd, *J* = 11.8, 10.0 Hz, 1H), 4.41 (dd, *J* = 10.0, 8.1 Hz, 1H), 4.23 (dt, *J* = 12.0, 5.2 Hz, 1H), 3.55 (ddd, *J* = 12.0, 10.5, 4.4 Hz, 1H), 3.35 (s, 3H), 3.04 (ddd, *J* = 15.6, 10.4, 5.1 Hz, 1H), 2.64 (ddd, *J* = 15.6, 5.3, 4.4 Hz, 1H). ACQUITY UPLC BEH C₁₈ 1.7 μm: Rt = 1.85 min; *m/z* 539.0 [M + Na, ⁸¹Br, ³⁵Cl]⁺. ELSD/UV/¹H NMR purity: 100/94/90%.

(S)-1-Benzyl-6-(8-chloro-5-methyl-4-oxo-2,3,4,5-tetrahydrobenzo[b][1,4]oxazepin-3-yl)-7-oxo-4,5,6,7-tetrahydro-1H-pyrazolo[3,4-c]pyridine-3-carboxamide (20). Synthesized exactly as described for LIJTF500025 (7) in Collins et al.,²⁹ Step 5 through separation of the other regioisomer. The semipurified product collected after flash column chromatography (silica, 24 g, 1:0 petrol/EtOAc to 0:1 petrol/EtOAc over 25 CV's) was additionally purified by reverse-phase chromatography (9:1 H₂O/MeOH to 0:1 H₂O/MeOH over 25 min) to afford (S)-1-benzyl-6-(5-methyl-4-oxo-2,3,4,5-tetrahydrobenzo[b][1,4]oxazepin-3-yl)-7-oxo-4,5,6,7-tetrahydro-1H-pyrazolo[3,4-c]pyridine-3-carboxamide (20, 7 mg, 0.01 mmol, 9% yield) as a colorless solid. ¹H NMR (500 MHz, DMSO-*d*₆) δ 7.61 (s, 1H), 7.52 (d, *J* = 8.6 Hz, 1H), 7.42–7.37 (m, 3H), 7.35–7.22 (m, 3H), 7.19–7.15 (m, 2H), 5.67–5.58 (m, 2H), 5.48 (dd, *J* = 12.0, 7.7 Hz, 1H), 4.89 (dd, *J* = 12.0, 10.1 Hz, 1H), 4.41 (dd, *J* = 10.0, 7.7 Hz, 1H), 4.00 (ddd, *J* = 12.7, 7.4, 5.4 Hz, 1H), 3.69–3.60 (m, 1H), 3.28 (s, 3H), 3.11–2.93 (m, 2H). ACQUITY UPLC BEH C₁₈ 1.7 μm: Rt = 1.77 min; *m/z* 480.1 [M + H]⁺. ELSD/UV/¹H NMR purity: 100/89/97%.

Dimethyl 1-Benzyl-4-(2-oxoethyl)-1H-pyrazole-3,5-dicarboxylate (27). A solution of dimethyl (E)-1-benzyl-4-(2-ethoxyvinyl)-1H-pyrazole-3,5-dicarboxylate (0.57 g, 1.66 mmol) in THF (5 mL) at 0 °C was added slowly to an ice-cold solution of hydrochloric acid (6M, 5 mL, 30.0 mmol). The reaction mixture was stirred at 0 °C for 1 h, allowing to warm to room temperature. The reaction mixture was poured onto saturated NaHCO₃ solution (50 mL) and extracted with

EtOAc (3 × 25 mL). The organic phases were combined, dried over MgSO₄, filtered and concentrated under reduced pressure to afford dimethyl 1-benzyl-4-(2-oxoethyl)-1H-pyrazole-3,5-dicarboxylate (27, 0.49 g, 1.09 mmol, 66% yield, 70% purity) as a yellow oil. ¹H NMR (400 MHz, CDCl₃) δ 9.71 (s, 1H), 7.35–7.16 (m, 5H), 5.85 (s, 2H), 4.27 (s, 2H), 3.95 (s, 3H), 3.84 (s, 3H). ACQUITY UPLC BEH C₁₈ 1.7 μm: Rt = 1.66 min; *m/z* 317.0 [M + H]⁺.

Dimethyl (S)-1-Benzyl-4-(2-((5-methyl-4-oxo-2,3,4,5-tetrahydrobenzo[b][1,4]oxazepin-3-yl)amino)ethyl)-1H-pyrazole-3,5-dicarboxylate (28a). Synthesized according to General Procedure A using dimethyl 1-benzyl-4-(2-oxoethyl)-1H-pyrazole-3,5-dicarboxylate (235 mg, 0.74 mmol, 27), (3S)-3-amino-5-methyl-2,3,4,5-tetrahydro-1,5-benzoxazepin-4-one hydrochloride (180 mg, 0.79 mmol, 1.1 equiv), acetic acid (0.3 mL) and 2-methylpyridine borane complex (119 mg, 1.11 mmol, 1.5 equiv). Purified by flash column chromatography (silica, 24 g, 7:3 petrol/EtOAc to 0:1 petrol/EtOAc) to afford dimethyl (S)-1-benzyl-4-(2-((5-methyl-4-oxo-2,3,4,5-tetrahydrobenzo[b][1,4]oxazepin-3-yl)amino)ethyl)-1H-pyrazole-3,5-dicarboxylate (28a, 220 mg, 0.42 mmol, 52% yield) as a colorless glass. ¹H NMR (500 MHz, CDCl₃) δ 7.35–7.25 (m, 3H), 7.24–7.19 (m, 3H), 7.19–7.14 (m, 3H), 5.79 (s, 2H), 4.38 (dd, *J* = 10.1, 7.4 Hz, 1H), 4.09 (dd, *J* = 11.6, 10.1 Hz, 1H), 3.91 (s, 3H), 3.81 (s, 3H), 3.59 (dd, *J* = 11.6, 7.4 Hz, 1H), 3.41 (s, 3H), 3.18–3.03 (m, 2H), 2.87 (ddd, *J* = 11.2, 9.2, 5.4 Hz, 1H), 2.47 (ddd, *J* = 11.2, 9.0, 6.5 Hz, 1H). NH not observed. ACQUITY UPLC BEH C₁₈ 1.7 μm: Rt = 1.46 min; *m/z* 493.2 [M + H]⁺. ELSD/UV/¹H NMR purity: 100/87/95%.

(S)-2-Benzyl-6-(5-methyl-4-oxo-2,3,4,5-tetrahydrobenzo[b][1,4]oxazepin-3-yl)-7-oxo-4,5,6,7-tetrahydro-2H-pyrazolo[3,4-c]pyridine-3-carboxamide (21). Synthesized in a three-step telescope according to (i) General Procedure B using dimethyl (S)-1-benzyl-4-(2-((5-methyl-4-oxo-2,3,4,5-tetrahydrobenzo[b][1,4]oxazepin-3-yl)amino)ethyl)-1H-pyrazole-3,5-dicarboxylate (140 mg, 0.27 mmol) and LiOH·H₂O (57 mg, 1.35 mmol, 5 equiv). Product taken forward as crude to the next step. (ii) General Procedure C using (S)-1-benzyl-4-(2-((5-methyl-4-oxo-2,3,4,5-tetrahydrobenzo[b][1,4]oxazepin-3-yl)amino)ethyl)-1H-pyrazole-3,5-dicarboxylic acid (as crude), HOBt hydrate (45 mg, 0.29 mmol, 1.1 equiv), EDC·HCl (70 mg, 0.37 mmol, 1.3 equiv), DIPEA (0.11 mL, 0.64 mmol, 2.4 equiv). Formation of (S)-2-benzyl-6-(5-methyl-4-oxo-2,3,4,5-tetrahydrobenzo[b][1,4]oxazepin-3-yl)-7-oxo-4,5,6,7-tetrahydro-2H-pyrazolo[3,4-c]pyridine-3-carboxylic acid and its regioisomer were observed in approximately 1:1 ratio. Product taken forward as crude to the next step. (iii) General Procedure C using (S)-2-benzyl-6-(5-methyl-4-oxo-2,3,4,5-tetrahydrobenzo[b][1,4]oxazepin-3-yl)-7-oxo-4,5,6,7-tetrahydro-2H-pyrazolo[3,4-c]pyridine-3-carboxylic acid (as crude mixture of two regioisomers), HOBt hydrate (45 mg, 0.29 mmol, 1.1 equiv), EDC·HCl (70 mg, 0.37 mmol, 1.3 equiv), DIPEA (0.11 mL, 0.64 mmol, 2.4 equiv) and NH₄Cl (60 mg, 1.12 mmol). The reaction mixture was heated to 45 °C and stirred for 24 h. Purified by flash column chromatography (silica, 24 g, 1:0 petrol/EtOAc to 0:1 petrol/EtOAc over 25 CV's) to afford (S)-2-benzyl-6-(5-methyl-4-oxo-2,3,4,5-tetrahydrobenzo[b][1,4]oxazepin-3-yl)-7-oxo-4,5,6,7-tetrahydro-2H-pyrazolo[3,4-c]pyridine-3-carboxamide (21, 38 mg, 0.08 mmol, 28% yield) as a colorless solid. m.p.: 190 °C (dec). ¹H NMR (500 MHz, DMSO-*d*₆) δ 7.83 (br s, 1H), 7.73 (br s, 1H), 7.50 (dd, *J* = 7.9, 1.6 Hz, 1H), 7.35–7.23 (m, 6H), 7.19–7.15 (m, 2H), 5.63 (s, 2H), 5.55 (dd, *J* = 12.0, 7.9 Hz, 1H), 4.85 (dd, *J* = 12.0, 10.1 Hz, 1H), 4.34 (dd, *J* = 10.0, 7.9 Hz, 1H), 4.00 (ddd, *J* = 12.1, 6.9, 5.0 Hz, 1H), 3.59 (ddd, *J* = 12.4, 8.9, 4.6 Hz, 1H), 3.30 (s, 3H), 3.05 (ddd, *J* = 15.9, 8.9, 5.0 Hz, 1H), 2.84 (ddd, *J* = 15.9, 6.9, 4.6 Hz, 1H). ¹³C{¹H} NMR (125 MHz, DMSO-*d*₆) δ 168.9, 161.1, 160.2, 149.5, 141.0, 137.2, 136.7, 133.1, 128.6, 127.8, 127.6, 127.2, 125.9, 123.4, 122.6, 121.4, 74.4, 54.1, 50.7, 44.9, 34.8, 20.5. A HMBC cross peak is shared between the benzyl CH₂, amide NH₂ and lactam benzyl CH₂ which is only consistent with isomer as drawn. 97% purity by ¹H NMR despite residual MeOH present. ACQUITY UPLC BEH C₁₈ 1.7 μm: Rt = 1.54 min; *m/z* 468.1 [M + Na]⁺. HRMS calculated for C₂₄H₂₄N₅O₄: 446.1828; found 446.1817 [M + H]⁺. ELSD/UV/¹H NMR purity: 100/92/97%. Characterization data was consistent with previously published data.⁴³

(*S*)-1-Benzyl-6-(5-methyl-4-oxo-2,3,4,5-tetrahydrobenzo[*b*][1,4]-oxazepin-3-yl)-7-oxo-4,5,6,7-tetrahydro-1*H*-pyrazolo[3,4-*c*]pyridine-3-carboxamide (**22**). Synthesized according to the synthesis of **21**, Step iii through separation of the other regioisomer. The semipurified product collected after flash column chromatography (silica, 24 g, 1:0 petrol/EtOAc to 0:1 petrol/EtOAc over 25 CV's) was additionally purified by reverse-phase chromatography (9:1 H₂O/MeOH to 0:1 H₂O/MeOH over 25 min) to afford (*S*)-1-benzyl-6-(5-methyl-4-oxo-2,3,4,5-tetrahydrobenzo[*b*][1,4]-oxazepin-3-yl)-7-oxo-4,5,6,7-tetrahydro-1*H*-pyrazolo[3,4-*c*]pyridine-3-carboxamide (**22**, 18 mg, 0.04 mmol, 15% yield) as a colorless solid. m.p.: 212–213 °C. ¹H NMR (500 MHz, DMSO-*d*₆) δ 7.61 (s, 1H), 7.51–7.46 (m, 1H), 7.40 (d, *J* = 1.7 Hz, 1H), 7.36–7.21 (m, 6H), 7.19–7.13 (m, 2H), 5.67–5.57 (m, 2H), 5.49 (dd, *J* = 12.0, 7.8 Hz, 1H), 4.86 (dd, *J* = 12.0, 10.1 Hz, 1H), 4.35 (dd, *J* = 10.1, 7.8 Hz, 1H), 4.02 (ddd, *J* = 12.6, 7.3, 5.4 Hz, 1H), 3.65 (ddd, *J* = 12.6, 8.4, 5.3 Hz, 1H), 3.29 (s, 3H), 3.09–2.93 (m, 2H). ¹³C{¹H} NMR (125 MHz, DMSO-*d*₆) δ 168.6 (Cq), 163.1 (Cq), 158.2 (Cq), 149.4 (Cq), 140.8 (Cq), 136.9 (Cq), 136.6 (Cq), 131.7 (Cq), 128.6 (CH), 127.7 (CH), 127.4 (CH), 127.2 (CH), 125.9 (CH), 124.3 (CH), 123.4 (CH), 122.5 (Cq), 74.4 (CH₂), 53.9 (CH₂), 50.6 (CH), 45.3 (CH₂), 34.8 (CH₃), 20.7 (CH₂). ACQUITY UPLC BEH C₁₈ 1.7 μm: Rt = 1.66 min; *m/z* 468.1 [M + Na]⁺. HRMS calculated for C₂₄H₂₄N₅O₄: 446.1828, found: 446.1819 [M + H]⁺. ELSD/UV/¹H NMR purity: 98/91/98%.

(*S*)-2-Benzyl-*N*-methyl-6-(5-methyl-4-oxo-2,3,4,5-tetrahydrobenzo[*b*][1,4]-oxazepin-3-yl)-7-oxo-4,5,6,7-tetrahydro-2*H*-pyrazolo[3,4-*c*]pyridine-3-carboxamide (**23**). Synthesized according to the synthesis of **21** using MeNH₂·HCl in place of NH₄Cl in the last step. (*S*)-2-Benzyl-6-(5-methyl-4-oxo-2,3,4,5-tetrahydrobenzo[*b*][1,4]-oxazepin-3-yl)-7-oxo-4,5,6,7-tetrahydro-2*H*-pyrazolo[3,4-*c*]pyridine-3-carboxylic acid (177 mg, as crude mixture of two regioisomers), HOBt hydrate (60 mg, 0.39 mmol), EDC·HCl (95 mg, 0.50 mmol), DIPEA (1.45 mL, 0.85 mmol), MeNH₂·HCl (60 mg, 2.47 mmol). The semipurified product collected after flash column chromatography (silica, 24 g, 1:0 petrol/EtOAc to 0:1 petrol/EtOAc over 25 CV's) was additionally purified by reverse-phase chromatography (9:1 H₂O/MeOH to 0:1 H₂O/MeOH over 25 min) to afford (*S*)-2-benzyl-*N*-methyl-6-(5-methyl-4-oxo-2,3,4,5-tetrahydrobenzo[*b*][1,4]-oxazepin-3-yl)-7-oxo-4,5,6,7-tetrahydro-2*H*-pyrazolo[3,4-*c*]pyridine-3-carboxamide (**23**, 10 mg, 0.02 mmol, 6% yield) as a colorless glass. ¹H NMR (500 MHz, DMSO-*d*₆) δ 8.23 (q, *J* = 4.5 Hz, 1H), 7.50 (dd, *J* = 7.9, 1.6 Hz, 1H), 7.35–7.23 (m, 6H), 7.20–7.15 (m, 2H), 5.59 (s, 2H), 5.55 (dd, *J* = 12.0, 7.9 Hz, 1H), 4.84 (dd, *J* = 12.0, 10.1 Hz, 1H), 4.34 (dd, *J* = 10.1, 7.9 Hz, 1H), 4.00 (ddd, *J* = 12.1, 6.8, 5.0 Hz, 1H), 3.59 (ddd, *J* = 12.3, 9.0, 4.6 Hz, 1H), 3.30 (s, 3H), 3.03 (ddd, *J* = 15.8, 9.0, 5.0 Hz, 1H), 2.82 (ddd, *J* = 15.9, 6.8, 4.6 Hz, 1H), 2.76 (d, *J* = 4.6 Hz, 3H). ACQUITY UPLC BEH C₁₈ 1.7 μm: Rt = 1.71 min; *m/z* 460.2 [M + H]⁺. ELSD/UV/¹H NMR purity: 98/95/90%.

(*S*)-1-Benzyl-*N*-methyl-6-(5-methyl-4-oxo-2,3,4,5-tetrahydrobenzo[*b*][1,4]-oxazepin-3-yl)-7-oxo-4,5,6,7-tetrahydro-1*H*-pyrazolo[3,4-*c*]pyridine-3-carboxamide (**24**). Synthesized according to the synthesis of **23** through separation of the other regioisomer. Purified by flash column chromatography (silica, 24 g, 7:3 petrol/EtOAc to 0:1 petrol/EtOAc over 25 CV's) followed by reverse-phase chromatography (9:1 H₂O/MeOH to 0:1 H₂O/MeOH over 25 min) to afford (*S*)-1-benzyl-*N*-methyl-6-(5-methyl-4-oxo-2,3,4,5-tetrahydrobenzo[*b*][1,4]-oxazepin-3-yl)-7-oxo-4,5,6,7-tetrahydro-1*H*-pyrazolo[3,4-*c*]pyridine-3-carboxamide (**24**, 6 mg, 0.01 mmol, 3% yield) as a colorless solid. ¹H NMR (500 MHz, DMSO-*d*₆) δ 8.17 (q, *J* = 4.6 Hz, 1H), 7.51–7.45 (m, 1H), 7.34–7.22 (m, 6H), 7.17–7.14 (m, 2H), 5.68–5.57 (m, 2H), 5.49 (dd, *J* = 12.0, 7.8 Hz, 1H), 4.86 (dd, *J* = 12.0, 10.1 Hz, 1H), 4.36 (dd, *J* = 10.1, 7.8 Hz, 1H), 4.03 (ddd, *J* = 12.7, 7.4, 5.4 Hz, 1H), 3.70–3.61 (m, 1H), 3.29 (s, 3H), 3.10–2.94 (m, 2H), 2.72 (d, *J* = 4.7 Hz, 3H). ACQUITY UPLC BEH C₁₈ 1.7 μm: Rt = 1.83 min; *m/z* 460.2 [M + H]⁺. ELSD/UV/¹H NMR purity: 100/91/94%.

(*S*)-2-Benzyl-*N,N*-dimethyl-6-(5-methyl-4-oxo-2,3,4,5-tetrahydrobenzo[*b*][1,4]-oxazepin-3-yl)-7-oxo-4,5,6,7-tetrahydro-2*H*-pyrazolo[3,4-*c*]pyridine-3-carboxamide (**25**). Synthesized according to the synthesis of **21** using Me₂NH in place of NH₄Cl in the last step. (*S*)-2-Benzyl-6-(5-methyl-4-oxo-2,3,4,5-tetrahydrobenzo[*b*][1,4]-oxazepin-3-yl)-7-oxo-4,5,6,7-tetrahydro-2*H*-pyrazolo[3,4-*c*]

pyridine-3-carboxylic acid (177 mg, as crude mixture of two regioisomers), HOBt hydrate (60 mg, 0.39 mmol), EDC·HCl (95 mg, 0.50 mmol), DIPEA (1.45 mL, 0.85 mmol), Me₂NH (0.10 mL, 0.56 mmol). The semipurified product collected after flash column chromatography (silica, 24 g, 1:0 petrol/EtOAc to 0:1 petrol/EtOAc over 25 CV's) was additionally purified by reverse-phase chromatography (9:1 H₂O/MeOH to 0:1 H₂O/MeOH over 25 min) to afford (*S*)-2-benzyl-*N,N*-dimethyl-6-(5-methyl-4-oxo-2,3,4,5-tetrahydrobenzo[*b*][1,4]-oxazepin-3-yl)-7-oxo-4,5,6,7-tetrahydro-2*H*-pyrazolo[3,4-*c*]pyridine-3-carboxamide (**25**, 6 mg, 0.01 mmol, 3% yield) as a colorless glass. ¹H NMR (500 MHz, DMSO-*d*₆) δ 7.50 (dd, *J* = 7.7, 1.8 Hz, 1H), 7.36–7.22 (m, 6H), 7.19–7.12 (m, 2H), 5.57 (dd, *J* = 12.0, 7.9 Hz, 1H), 5.37 (s, 2H), 4.82 (dd, *J* = 12.0, 10.1 Hz, 1H), 4.33 (dd, *J* = 10.1, 7.9 Hz, 1H), 4.01 (ddd, *J* = 12.1, 6.9, 4.9 Hz, 1H), 3.60 (ddd, *J* = 12.8, 8.8, 4.6 Hz, 1H), 3.30 (s, 3H), 2.90 (s, 3H), 2.80 (ddd, *J* = 14.4, 8.9, 4.9 Hz, 1H), 2.71–2.65 (m, 4H). ACQUITY UPLC BEH C₁₈ 1.7 μm: Rt = 1.72 min; *m/z* 474.2 [M + H]⁺. ELSD/UV/¹H NMR purity: 99/94/94%.

(*S*)-1-Benzyl-*N,N*-dimethyl-6-(5-methyl-4-oxo-2,3,4,5-tetrahydrobenzo[*b*][1,4]-oxazepin-3-yl)-7-oxo-4,5,6,7-tetrahydro-1*H*-pyrazolo[3,4-*c*]pyridine-3-carboxamide (**26**). Synthesized according to the synthesis of **25** through separation of the other regioisomer. Purified by flash column chromatography (silica, 24 g, 7:3 petrol/EtOAc to 0:1 petrol/EtOAc over 25 CV's) followed by reverse-phase chromatography (9:1 H₂O/MeOH to 0:1 H₂O/MeOH over 25 min) to afford (*S*)-1-benzyl-*N,N*-dimethyl-6-(5-methyl-4-oxo-2,3,4,5-tetrahydrobenzo[*b*][1,4]-oxazepin-3-yl)-7-oxo-4,5,6,7-tetrahydro-1*H*-pyrazolo[3,4-*c*]pyridine-3-carboxamide (**26**, 7 mg, 0.01 mmol, 4% yield) as a colorless solid. ¹H NMR (500 MHz, DMSO-*d*₆) δ 7.49 (dd, *J* = 7.7, 1.8 Hz, 1H), 7.35–7.22 (m, 6H), 7.18–7.15 (m, 2H), 5.66–5.58 (m, 2H), 5.50 (dd, *J* = 12.0, 7.8 Hz, 1H), 4.86 (dd, *J* = 12.0, 10.1 Hz, 1H), 4.36 (dd, *J* = 10.1, 7.8 Hz, 1H), 4.02 (ddd, *J* = 12.7, 7.4, 5.3 Hz, 1H), 3.64 (ddd, *J* = 12.6, 8.5, 5.2 Hz, 1H), 3.30 (s, 3H), 3.20 (s, 3H), 3.00–2.80 (m, 5H). ACQUITY UPLC BEH C₁₈ 1.7 μm: Rt = 1.85 min; *m/z* 474.2 [M + H]⁺. ELSD/UV/¹H NMR purity: 100/92/90%.

(*S*)-1-Benzyl-*N*³-(5-methyl-4-oxo-2,3,4,5-tetrahydrobenzo[*b*][1,4]-oxazepin-3-yl)-1*H*-pyrazole-3,5-dicarboxamide (**29**). Synthesized according to General Procedure C using 1-benzyl-5-carbamoyl-1*H*-pyrazole-3-carboxylic acid (80 mg, 0.33 mmol), HOBt hydrate (55 mg, 0.36 mmol, 1.1 equiv), EDC·HCl (75 mg, 0.39 mmol, 1.2 equiv), DIPEA (84 μL, 0.49 mmol, 1.5 equiv) and (*S*)-3-amino-5-methyl-2,3-dihydrobenzo[*b*][1,4]-oxazepin-4(*SH*)-one hydrochloride (82 mg, 0.36 mmol, 1.1 equiv). Purified by flash column chromatography (silica, 4 g, 1:0 petrol/EtOAc to 0:1 petrol/EtOAc over 25 CV's) to afford (*S*)-1-benzyl-*N*³-(5-methyl-4-oxo-2,3,4,5-tetrahydrobenzo[*b*][1,4]-oxazepin-3-yl)-1*H*-pyrazole-3,5-dicarboxamide (**29**, 70 mg, 0.16 mmol, 49% yield) as a colorless solid. m.p.: 146–147 °C. ¹H NMR (500 MHz, CDCl₃) δ 7.86 (d, *J* = 7.1 Hz, 1H), 7.32–7.30 (m, 4H), 7.30–7.17 (m, 5H), 7.12 (s, 1H), 6.06 (s, 1H), 5.84 (d, *J* = 14.3 Hz, 1H), 5.77 (d, *J* = 14.3 Hz, 1H), 5.35 (s, 1H), 5.03 (dt, *J* = 11.2, 7.2 Hz, 1H), 4.72 (dd, *J* = 9.8, 7.4 Hz, 1H), 4.29 (dd, *J* = 11.2, 9.8 Hz, 1H), 3.45 (s, 3H). ¹³C{¹H} NMR (101 MHz, CDCl₃) δ 169.1 (Cq), 161.0 (Cq), 160.6 (Cq), 150.2 (Cq), 144.3 (Cq), 136.6 (Cq), 136.3 (Cq), 135.6 (Cq), 128.7 (CH), 128.1 (CH), 128.0 (CH), 126.0 (CH), 123.5 (CH), 123.0 (CH), 109.1 (CH), 77.3 (CH₂), 55.6 (CH₂), 49.3 (CH), 35.6 (CH₃). ACQUITY UPLC BEH C₁₈ 1.7 μm: Rt = 1.73 min; *m/z* 420.2 [M + H]⁺. HRMS calculated for C₂₂H₂₂N₅O₄: 420.1672, found: 420.1669 [M + H]⁺. ELSD/UV/¹H NMR purity: 99/91/96%.

1-Benzyl-3,5-dibromo-1*H*-pyrazole (**36**). A suspension of 3,5-dibromo-1*H*-pyrazole (2.50 g, 11.07 mmol) and K₂CO₃ (2.06 g, 14.68 mmol) in DMF (15 mL) was cooled in an ice-bath. Benzyl bromide (1.34 mL, 11.27 mmol) was added slowly over 5 min. The bath was removed and the mixture stirred at room temperature for 40 min, whereupon UPLC showed complete conversion to product. The reaction mixture was poured onto 350 mL ice-cold water, extracted with EtOAc (3 × 40 mL) and washed with brine (5 × 20 mL), dried over MgSO₄, filtered and concentrated under reduced pressure to give 1-benzyl-3,5-dibromo-1*H*-pyrazole (**36**, 3.34 g, 10.04 mmol, 96% yield) as a light-yellow thick oil. ¹H NMR (500 MHz, CDCl₃) δ 7.41–7.31

(m, 3H), 7.30–7.22 (m, 2H), 6.36 (s, 1H), 5.35 (s, 2H). ACQUITY UPLC BEH C₁₈ 1.7 μ m: Rt = 1.83 min; m/z 316.8 [M + H, ⁷⁹Br, ⁸¹Br]⁺.

1-Benzyl-3-bromo-1H-pyrazole-5-carboxylic Acid (37). To a cooled (–78 °C) solution of **36** (3.29 g, 10.4 mmol) in anhydrous THF (80 mL) was added dropwise iPrMgCl·LiCl (1.3 M in THF, 9.60 mL, 12.48 mmol). The solution took on a light-yellow color and was left to stir for 30 min. CO₂ was bubbled through the solution *via* cannula over a period of 20 min before removal of the cooling bath. The reaction mixture was concentrated under reduced pressure and redissolved in saturated aqueous solution of NaHCO₃ (50 mL) and extracted with DCM (20 mL). This extract was discarded and the aqueous brought to pH 3 and extracted with EtOAc (4 × 30 mL). The combined EtOAc extract was dried over MgSO₄, filtered and concentrated under reduced pressure to give 1-benzyl-3-bromo-1H-pyrazole-5-carboxylic acid (**37**, 2.61 g, 9.30 mmol, 94% yield) as a colorless solid. ¹H NMR (500 MHz, CD₃OD) δ 7.33–7.23 (m, 3H), 7.22 (ddd, J = 8.1, 1.4, 0.7 Hz, 2H), 6.89 (s, 1H), 5.72 (s, 2H). ACQUITY UPLC BEH C₁₈ 1.7 μ m: Rt = 1.54 min; m/z 282.9 [M + H, ⁸¹Br]⁺.

1-Benzyl-3-bromo-1H-pyrazole-5-carboxamide (38). A mixture of **37** (198 mg, 0.70 mmol) and SOCl₂ (1.0 mL, 13.71 mmol) was heated to 65 °C for 2 h. Once cooled, the mixture was concentrated under reduced pressure in a fumehood to give the acid chloride (colorless oil), which was used directly without further purification. The acid chloride was dissolved in DCM (5 mL) and cooled in an ice bath. Ammonia solution (0.20 mL, 35% by w/w aqueous solution) was added slowly dropwise. The cooling bath was removed and the reaction left to stir at room temperature overnight. The mixture was diluted with DCM (20 mL) and poured into a separating funnel containing a saturated aqueous solution of NaHCO₃ (20 mL). The layers were separated and the organic extract washed with additional NaHCO₃ solution (20 mL). The organic phase was dried over MgSO₄, filtered and concentrated under reduced pressure to give 1-benzyl-3-bromo-1H-pyrazole-5-carboxamide (**38**, 171 mg, 0.58 mmol, 86% yield) as a colorless viscous oil. ¹H NMR (500 MHz, CD₃OD) δ 7.29–7.19 (m, 5H), 6.86 (s, 1H), 5.72 (s, 2H), 4.93 (s, 2H). ACQUITY UPLC BEH C₁₈ 1.7 μ m: Rt = 1.42 min; m/z 281.9 [M + H, ⁸¹Br]⁺.

(E)-1-Benzyl-3-(2-ethoxyvinyl)-1H-pyrazole-5-carboxamide (39). A mixture of (E)-(2-ethoxyvinyl)boronic pinacol ester (0.22 mL, 1.04 mmol), **38** (171 mg, 0.61 mmol) and Cs₂CO₃ (0.42 g, 1.29 mmol) in monoglyme (4 mL) and water (0.4 mL) was degassed with N₂ for 15 min. [1,1'-Bis(diphenylphosphino)ferrocene]dichloropalladium(II) (0.04 g, 0.06 mmol) was added, the mixture degassed for a further 10 min before being heated to 90 °C overnight. The mixture was diluted with EtOAc (20 mL), washed with a saturated aqueous solution of NaHCO₃ (20 mL), the aqueous back-extracted with EtOAc (20 mL), the combined organics dried over MgSO₄, filtered and concentrated under reduced pressure to give the crude product, which was purified by automated column chromatography on silica (ISCO, 12 g, slow gradient from DCM to 20% MeOH in DCM with 1% Et₃N) to give (E)-1-benzyl-3-(2-ethoxyvinyl)-1H-pyrazole-5-carboxamide (**39**, 162 mg, 0.54 mmol, 89% yield) as a light brown solid. ¹H NMR (500 MHz, CDCl₃) δ 7.32–7.19 (m, 5H), 7.07 (d, J = 13.2 Hz, 1H), 6.44 (s, 1H), 5.86 (s, 1H), 5.77 (d, J = 13.2 Hz, 1H), 5.70 (s, 2H), 5.64 (s, 1H), 3.87 (q, J = 7.0 Hz, 2H), 1.33 (t, J = 7.0 Hz, 3H). ACQUITY UPLC BEH C₁₈ 1.7 μ m: Rt = 1.42 min; m/z 272.0 [M + H]⁺. Regiochemistry shown by small X-ray crystal structure analysis.

Methyl 1-Benzyl-3-bromo-1H-pyrazole-5-carboxylate Hydrochloride (41). To an ice-cold solution of **37** (2.00 g, 6.76 mmol) in MeOH (15 mL) was added dropwise SOCl₂ (1.48 mL, 20.28 mmol). Upon completion of addition, the cooling bath was removed and the mixture allowed to stir at room temperature for 1 h, overnight at room temperature, and finally at 50 °C for a further 12 h. The mixture was concentrated under reduced pressure in a fumehood to give methyl 1-benzyl-3-bromo-1H-pyrazole-5-carboxylate hydrochloride (**41**, 2.20 g, 6.30 mmol, 98% yield) as a brown solid. ¹H NMR (500 MHz, DMSO-*d*₆) δ 7.36–7.24 (m, 3H), 7.17 (d, J = 7.3 Hz, 2H), 7.06 (s, 1H), 5.67 (s, 2H), 3.81 (s, 3H). ACQUITY UPLC BEH C₁₈ 1.7 μ m: Rt = 1.80 min; m/z 297.1 [M-HCl + H, ⁸¹Br]⁺.

Methyl (E)-1-Benzyl-3-(2-ethoxyvinyl)-1H-pyrazole-5-carboxylate (42). A mixture of (E)-(2-ethoxyvinyl)boronic pinacol ester

(0.58 mL, 2.73 mmol) Cs₂CO₃ (2.03 g, 6.18 mmol) and **41** (683 mg, 2.06 mmol) in monoglyme (6.2 mL) and water (0.62 mL) was degassed with N₂ for 15 min. [1,1'-Bis(diphenylphosphino)ferrocene]dichloropalladium(II) (0.12 g, 0.16 mmol) was added, the mixture degassed again for 10 min before heating overnight at 80 °C. The reaction mixture was diluted with EtOAc (40 mL), washed with water (15 mL), the organic phase dried over MgSO₄, filtered and concentrated under reduced pressure to give the crude product, which was purified by automated column chromatography on silica (ISCO, 12 g, gradient from petroleum ether to EtOAc with 1% Et₃N) to give methyl (E)-1-benzyl-3-(2-ethoxyvinyl)-1H-pyrazole-5-carboxylate (**42**, 230 mg, 0.76 mmol, 39% yield) as a colorless solid. ¹H NMR (500 MHz, CDCl₃) δ 7.31–7.26 (m, 2H), 7.26–7.21 (m, 3H), 7.10 (d, J = 13.2 Hz, 1H), 6.74 (s, 1H), 5.80 (d, J = 13.2 Hz, 1H), 5.70 (s, 2H), 3.88 (q, J = 7.0 Hz, 2H), 3.81 (s, 3H), 1.33 (t, J = 7.0 Hz, 3H). ACQUITY UPLC BEH C₁₈ 1.7 μ m: Rt = 1.78 min; m/z 287.1 [M + H]⁺.

Methyl 1-Benzyl-3-(2-oxoethyl)-1H-pyrazole-5-carboxylate (43). **42** (230 mg, 0.8 mmol) was dissolved in DCM (2 mL) and 4 M HCl in dioxane (2 mL) was added. UPLC analysis after 1 h indicated reaction was complete. The mixture was taken to pH 9 by portion-wise addition of a saturated aqueous solution of NaHCO₃ (30 mL) and extracted with EtOAc (3 × 30 mL). The organic phase was dried over MgSO₄, filtered and concentrated under reduced pressure to give methyl 1-benzyl-3-(2-oxoethyl)-1H-pyrazole-5-carboxylate (**43**, 208 mg, 0.77 mmol, quantitative yield) as a colorless oil, which was used immediately in the next step due to stability concerns. ACQUITY UPLC BEH C₁₈ 1.7 μ m: Rt = 1.54 min; m/z 259.1 [M + H]⁺.

2-(1-Benzyl-5-(methoxycarbonyl)-1H-pyrazol-3-yl)acetic Acid (44). To a solution of **43** (222 mg, 0.86 mmol) in DMF (8 mL) was added oxone (528 mg, 0.86 mmol). UPLC analysis after stirring at room temperature for 1 h showed complete conversion to the acid. Aqueous 1 M HCl (15 mL) and EtOAc (50 mL) were added to the mixture. The layers were separated and the aqueous back-extracted with EtOAc (20 mL). The combined organic extracts were dried over MgSO₄, filtered and concentrated under reduced pressure to give the crude product, which was triturated with petroleum ether (3 × 35 mL) to give 2-(1-benzyl-5-(methoxycarbonyl)-1H-pyrazol-3-yl)acetic acid (**44**, 143 mg, 0.47 mmol, 61% yield) as a colorless solid. ¹H NMR (500 MHz, CDCl₃) δ 7.32–7.26 (m, 2H), 7.26–7.19 (m, 3H), 6.85 (s, 1H), 5.73 (s, 2H), 3.84 (s, 3H), 3.78 (s, 2H). CO₂H not observed. ACQUITY UPLC BEH C₁₈ 1.7 μ m: Rt = 1.52 min; m/z 275.1 [M + H]⁺.

Methyl 1-Benzyl-3-(2-(benzyl(cyclopropylmethyl)amino)-2-oxoethyl)-1H-pyrazole-5-carboxylate (45). To a mixture of HOBt (69.7 mg, 0.45 mmol), EDC·HCl (103 mg, 0.54 mmol), Et₃N (0.09 mL, 0.62 mmol) and **44** (126 mg, 0.41 mmol) in DCM (2 mL) was added a solution of N-benzyl-1-cyclopropylmethanamine (66.7 mg, 0.41 mmol) in DCM (2 mL). The mixture was left to stir overnight at room temperature. UPLC analysis showed the desired product, along with an unknown side-product. Saturated aqueous NaHCO₃ (5 mL) was added and the mixture stirred vigorously for 5 min before being passed through a phase separator. The filtrate was purified by normal phase automated column chromatography (12 g silica, ISCO, gradient from petroleum ether to EtOAc) to give methyl 1-benzyl-3-(2-(benzyl(cyclopropylmethyl)amino)-2-oxoethyl)-1H-pyrazole-5-carboxylate (**45**, 39 mg, 0.09 mmol, 22% yield) as a light-yellow oil. ¹H NMR (500 MHz, CDCl₃) δ 7.27–6.97 (m, 10H), 6.81 (s, 0.5H), 6.77 (s, 0.5H), 5.61 (s, 1H), 5.56 (s, 1H), 4.64 (s, 1H), 4.61 (s, 1H), 3.76 (s, 1H), 3.71 (s, 1.5H), 3.70 (s, 1.5H), 3.65 (s, 1H), 3.19 (d, J = 6.9 Hz, 1H), 3.07 (d, J = 6.6 Hz, 1H), 0.90–0.81 (m, 0.5H), 0.78–0.68 (m, 0.5H), 0.40–0.35 (m, 1H), 0.35–0.29 (m, 1H), 0.09–0.03 (m, 1H), 0.02 to –0.04 (m, 1H). Rotamers observed in approximately 1:1 ratio. ACQUITY UPLC BEH C₁₈ 1.7 μ m: Rt = 1.84 min; m/z 418.3 [M + H]⁺.

1-Benzyl-3-(2-(benzyl(cyclopropylmethyl)amino)-2-oxoethyl)-1H-pyrazole-5-carboxylic Acid (46). **45** (39 mg, 0.09 mmol) was dissolved in MeOH (0.25 mL), water (0.25 mL) and THF (0.25 mL). LiOH·H₂O (5.0 mg, 0.12 mmol) was added and the mixture stirred for 2 h at room temperature. The mixture was concentrated under reduced pressure and aqueous 1 M HCl (5.0 mL) was added. The product

precipitated out, the supernatant was removed by pipet and the solid washed twice with water (5 mL). The solid was dried in a vacuum oven overnight at 40 °C to give 1-benzyl-3-(2-(benzyl(cyclopropylmethyl)amino)-2-oxoethyl)-1H-pyrazole-5-carboxylic acid (**46**, 39 mg, 0.09 mmol, 98% yield) as a colorless solid. ¹H NMR (500 MHz, CDCl₃) δ 7.35–7.10 (m, 10H), 6.96 (s, 0.5H), 6.91 (s, 0.5H), 5.71 (s, 1H), 5.66 (s, 1H), 4.78 (s, 1H), 4.76 (s, 1H), 3.92 (s, 1H), 3.81 (s, 1H), 3.33 (d, *J* = 6.9 Hz, 1H), 3.21 (d, *J* = 6.6 Hz, 1H), 0.97 (dddd, *J* = 11.9, 7.0, 4.0, 1.6 Hz, 0.5H), 0.90–0.80 (m, 0.5H), 0.51–0.46 (m, 1H), 0.46–0.40 (m, 1H), 0.19–0.14 (m, 1H), 0.13–0.08 (m, 1H). CO₂H not observed. Rotamers observed in approximately 1:1 ratio. ACQUITY UPLC BEH C₁₈ 1.7 μm: Rt = 1.68 min; *m/z* 404.3 [M + H]⁺.

1-Benzyl-3-(2-(benzyl(cyclopropylmethyl)amino)-2-oxoethyl)-1H-pyrazole-5-carboxamide (31). To a solution of PyBOP (54 mg, 0.14 mmol), HOBt (22.2 mg, 0.14 mmol) and **46** (39 mg, 0.1 mmol) in DMF (0.4 mL) was added DIPEA (0.07 mL, 0.39 mmol) followed by NH₄Cl (10.3 mg, 0.19 mmol). The mixture was left to stir for 1 h, after which it was diluted in EtOAc (20 mL) and washed with a saturated solution of NaHCO₃ (3 × 30 mL). The organic fraction was dried over MgSO₄, filtered and concentrated under reduced pressure to give the crude product, which was purified by automated reverse-phase column chromatography (ACCQPrep, 30 min run from water to MeOH) to afford 1-benzyl-3-(2-(benzyl(cyclopropylmethyl)amino)-2-oxoethyl)-1H-pyrazole-5-carboxamide (**31**, 19 mg, 0.05 mmol, 48% yield) as a colorless viscous oil, which solidified upon standing. m.p.: 109–110 °C. ¹H NMR (500 MHz, CDCl₃) δ 7.32 (dd, *J* = 8.1, 6.5 Hz, 1H), 7.29–7.18 (m, 7H), 7.18–7.15 (m, 1H), 7.15–7.11 (m, 1H), 6.75 (s, 0.5H), 6.70 (s, 0.5H), 6.19 (s, 1H), 5.74 (s, 1H), 5.68 (s, 1H), 5.51 (s, 1H), 4.73 (s, 2H), 3.86 (s, 1H), 3.75 (s, 1H), 3.29 (d, *J* = 6.9 Hz, 1H), 3.20 (d, *J* = 6.6 Hz, 1H), 1.00–0.91 (m, 0.5H), 0.86 (dddd, *J* = 13.1, 9.7, 5.8, 1.5 Hz, 0.5H), 0.52–0.46 (m, 1H), 0.46–0.41 (m, 1H), 0.16 (dt, *J* = 6.1, 4.7 Hz, 1H), 0.11 (dt, *J* = 6.0, 4.8 Hz, 1H). ¹³C{¹H} NMR (101 MHz, CDCl₃) δ 170.6 (Cq), 170.1 (Cq), 161.2 (Cq), 145.7 (Cq), 145.6 (Cq), 137.5 (Cq), 137.5 (Cq), 136.9 (Cq), 135.1 (Cq), 135.0 (Cq), 129.0 (CH), 128.7 (CH), 128.6 (CH), 128.6 (CH), 127.8 (CH), 127.8 (CH), 127.7 (CH), 127.7 (CH), 127.4 (CH), 126.4 (CH), 108.1 (CH), 108.0 (CH), 54.6 (CH₂), 54.5 (CH₂), 51.9 (CH₂), 51.5 (CH₂), 50.4 (CH₂), 48.5 (CH₂), 47.8 (CH₂), 47.8 (CH₂), 34.0 (CH₂), 33.8 (CH₂), 10.2 (CH), 9.6 (CH), 3.9 (CH₂), 3.7 (CH₂). Rotamers observed in approximately 1:1 ratio. ACQUITY UPLC BEH C₁₈ 1.7 μm: Rt = 1.63 min; *m/z* 403.3 [M + H]⁺. HRMS calculated for C₂₄H₂₇N₄O₂, 403.2134, found 403.2136 [M + H]⁺. ELSD/UV/¹H NMR purity: nd/96/95%.

Dimethyl 1-Benzyl-1H-pyrazole-3,5-dicarboxylate (48). A suspension of dimethyl 1H-pyrazole-3,5-dicarboxylate (5.00 g, 27.15 mmol) and K₂CO₃ (5.05 g, 36 mmol) in DMF (50 mL) was cooled in an ice-bath. Benzyl bromide (3.28 mL, 27.64 mmol) was added slowly over 5 min. The bath was removed and the mixture stirred at room temperature for 1 h, whereupon UPLC showed complete conversion to product. The reaction mixture was poured onto 2 L ice-cold water, which precipitated the desired product. The solid was collected by filtration under vacuum and dried in a vacuum oven overnight to give dimethyl 1-benzylpyrazole-3,5-dicarboxylate (**48**, 6.954 g, 24.087 mmol, 93% yield) as a colorless solid. ¹H NMR (500 MHz, CDCl₃) δ 7.31 (s, 1H), 7.25–7.16 (m, 5H), 5.77 (s, 2H), 3.88 (s, 3H), 3.79 (s, 3H). ACQUITY UPLC BEH C₁₈ 1.7 μm: Rt = 1.65 min; *m/z* 275.0 [M + H]⁺.

Methyl 1-Benzyl-5-carbamoyl-1H-pyrazole-3-carboxylate (49). Synthesized according to method described in US 10,966,961 B2.⁵² To an ice-cold solution of dimethyl 1-benzylpyrazole-3,5-dicarboxylate (5.00 g, 17.32 mmol) in MeOH (40 mL), THF (40 mL) and water (16 mL) was added LiOH·H₂O (727 mg, 17.3 mmol). UPLC analysis after 2 h showed a mixture of starting material (30% by UV), monohydrolyzed material (66% by UV) and bis-hydrolyzed material (4%). The reaction mixture was concentrated under reduced pressure to give a basic aqueous mixture, which was diluted with water (40 mL) and extracted with DCM (2 × 40 mL). The aqueous phase was acidified and extracted with DCM (5 × 40 mL). The combined second extract was dried over MgSO₄, filtered, and concentrated under reduced pressure to give the crude products of monohydrolysis, which was used

directly in the next step. ACQUITY UPLC BEH C₁₈ 1.7 μm: Rt = 1.48 min; *m/z* 261.0 [M + H]⁺.

The monohydrolyzed material from above (3.25 g, 12.48 mmol) was heated in thionyl chloride (19.15 mL, 262.55 mmol) for 2 h. Excess thionyl chloride was removed under reduced pressure in a fumehood and the residue dissolved in DCM (10 mL) and added dropwise to a solution of ammonia solution (35% by weight solution in water, 0.32 mL, 49.92 mmol). UPLC analysis showed reaction completion with both regioisomers were present (80:20 ratio). Additional DCM (20 mL) was added and the mixture washed with aqueous saturated NaHCO₃ solution (2 × 30 mL). The organic phase was dried over MgSO₄, filtered and concentrated under reduced pressure to give the crude product, which was purified by flash column chromatography (silica, 12 g, 1:0 petrol/EtOAc to 0:1 petrol/EtOAc containing 5% Et₃N over 25 CV's) to afford methyl 1-benzyl-5-carbamoyl-pyrazole-3-carboxylate (**49**, 3.00 g, 10.99 mmol, 63% yield over two steps) as a colorless solid. ¹H NMR (500 MHz, CD₃OD) δ 7.34 (s, 1H), 7.31–7.22 (m, 5H), 5.83 (s, 2H), 3.90 (s, 3H). CONH₂ not observed. ACQUITY UPLC BEH C₁₈ 1.7 μm: Rt = 1.42 min; *m/z* 260.0 [M + H]⁺. Regioselectivity of monohydrolysis proven by single crystal analysis.

1-Benzyl-5-carbamoyl-1H-pyrazole-3-carboxylic Acid (50). Synthesized according to General Procedure B using methyl 1-benzyl-5-carbamoyl-pyrazole-3-carboxylate (600 mg, 2.31 mmol) and LiOH·H₂O (291 mg, 6.93 mmol) to give 1-benzyl-5-carbamoyl-1H-pyrazole-3-carboxylic acid (**50**, 454 mg, 1.75 mmol, 80% yield) as a colorless solid. ¹H NMR (500 MHz, DMSO-*d*₆) δ 12.96 (s, 1H), 8.11 (s, 1H), 7.66 (s, 1H), 7.40 (s, 1H), 7.36–7.24 (m, 3H), 7.20–7.14 (m, 2H), 5.82 (s, 2H). ACQUITY UPLC BEH C₁₈ 1.7 μm: Rt = 1.23 min; *m/z* 244.0 [M – H][–].

N³,1-Dibenzyl-N³-(cyclopropylmethyl)-1H-pyrazole-3,5-dicarboxamide (32). 1-Benzyl-5-carbamoyl-1H-pyrazole-3-carboxylic acid (**49** mg, 0.20 mmol, **50**) was heated in thionyl chloride (0.50 mL, 6.85 mmol) at 65 °C for 2 h. The mixture was concentrated under reduced pressure and dissolved in DCM (2 mL). Et₃N (0.07 mL, 0.50 mmol) was added followed by the dropwise addition of a solution of *N*-benzyl-1-cyclopropylmethanamine (35 mg, 0.20 mmol) in DCM (2 mL). UPLC analysis after 5 min indicated reaction completion. A saturated aqueous solution of NaHCO₃ was added and the mixture stirred vigorously for 5 min before being passed through a phase separator. The filtrate was concentrated under reduced pressure and purified by flash column chromatography (silica, 12 g, 1:0 petrol/EtOAc to 0:1 petrol/EtOAc containing 1% Et₃N over 20 CV's) to afford N³,1-dibenzyl-N³-(cyclopropylmethyl)pyrazole-3,5-dicarboxamide (**32**, 16 mg, 0.04 mmol, 21% yield) as a colorless solid. ¹H NMR (500 MHz, CD₃OD) δ 7.35–7.10 (m, 11H), 5.81 (s, 1H), 5.71 (s, 1H), 5.16 (s, 1H), 3.56 (d, *J* = 6.9 Hz, 1H), 3.37–3.32 (m, 1H), 1.14–1.04 (m, 1H), 0.51–0.45 (m, 1H), 0.44–0.39 (m, 1H), 0.25–0.19 (m, 1H), 0.09–0.03 (m, 1H). Rotamers observed in approximately 1:1 ratio. One benzyl proton is missing as underneath HDO peak. ACQUITY UPLC BEH C₁₈ 1.7 μm: Rt = 1.78 min; *m/z* 389.2 [M + H]⁺. ELSD/UV/¹H NMR purity: 100/94/90%.

(S)-N-(8-Chloro-5-methyl-4-oxo-2,3,4,5-tetrahydrobenzo[*b*][1,4]-oxazepin-3-yl)-4-(*N*-phenylsulfamoyl)benzamide (33). Synthesized according to General Procedure C using 4-(phenylsulfamoyl)benzoic acid (42 mg, 0.14 mmol), (3S)-3-amino-8-chloro-5-methyl-2,3-dihydro-1,5-benzoxazepin-4-one hydrochloride salt (40 mg, 0.14 mmol), HOBt hydrate (24 mg, 0.16 mmol), EDC·HCl (33 mg, 0.17 mmol) and DIPEA (0.06 mL, 0.36 mmol). Purified by flash column chromatography (silica, 12 g, 1:0 petrol/EtOAc to 0:1 petrol/EtOAc containing 1% Et₃N over 30 CV's) to afford (S)-N-(8-chloro-5-methyl-4-oxo-2,3,4,5-tetrahydrobenzo[*b*][1,4]-oxazepin-3-yl)-4-(*N*-phenylsulfamoyl)benzamide (**33**, 66 mg, 0.13 mmol, 94% yield) as a beige solid. ¹H NMR (500 MHz, CDCl₃) δ 7.78–7.73 (m, 4H), 7.41 (d, *J* = 6.9 Hz, 1H), 7.26–7.21 (m, 4H), 7.17 (dd, *J* = 8.4, 0.5 Hz, 1H), 7.12 (ddt, *J* = 8.0, 6.9, 1.2 Hz, 1H), 7.09–7.06 (m, 2H), 5.07 (dt, *J* = 11.3, 7.1 Hz, 1H), 4.73 (dd, *J* = 9.8, 7.4 Hz, 1H), 4.30 (dd, *J* = 11.3, 9.9 Hz, 1H), 3.42 (s, 3H). NH not observed. ¹³C{¹H} NMR (101 MHz, CDCl₃) δ 169.5 (Cq), 165.6 (Cq), 150.6 (Cq), 142.3 (Cq), 137.4 (Cq), 136.3 (Cq), 134.7 (Cq), 132.9 (Cq), 129.6 (CH), 128.1 (CH),

127.5 (CH), 126.2 (CH), 125.9 (CH), 124.3 (CH), 123.7 (CH), 121.9 (CH), 77.3 (CH₂), 49.8 (CH), 35.9 (CH₃). ACQUITY UPLC BEH C₁₈ 1.7 μ m: Rt = 1.76 min; *m/z* 486.2 [M + H]⁺. HRMS calculated for C₂₃H₂₁N₃O₃SCl: 486.0890, found: 486.0887 [M + H]⁺. ELSD/UV/¹H NMR purity: 100/97/88%.

Dimethyl 4-iodo-1H-pyrazole-3,5-dicarboxylate (52). To a solution of dimethyl 1H-pyrazole-3,5-dicarboxylate (10.0 g, 54.3 mmol) in MeCN (1 L) under inert atmosphere were added CAN (32.7 g, 59.8 mmol) and I₂ (17.9 g, 70.7 mmol). The reaction mixture was stirred at room temperature for 48 h. The reaction mixture was concentrated under reduced pressure, diluted with EtOAc (500 mL) and washed with 5% aq. Na₂S₂O₃ solution (200 mL). The organic layer was separated, dried over NaSO₄ and concentrated under *vacuo* to obtain the crude which was triturated with heptane (150 mL) and dried to afford dimethyl 4-iodo-1H-pyrazole-3,5-dicarboxylate (**52**, 15.0 g, 48.4 mmol, 89% yield) as an off-white solid. ¹H NMR (400 MHz, CDCl₃) δ 3.98 (s, 6H). NH not observed. ACQUITY UPLC BEH C₁₈ 1.7 μ m: Rt = 1.39 min; *m/z* 311.0 [M + H]⁺.

Dimethyl 1-Benzyl-4-iodo-pyrazole-3,5-dicarboxylate (53). K₂CO₃ (3.00 g, 21.4 mmol) was added to a solution of 4-iodo-1H-pyrazole-3,5-dicarboxylate (5.00 g, 16.1 mmol) in DMF (30 mL). The reaction mixture was cooled to 0 °C and benzyl bromide (1.95 mL, 16.4 mmol) was slowly added over 5 min. The reaction mixture was stirred at 0 °C for 1 h, allowing to warm to room temperature. The mixture was poured onto ice-cold water (350 mL) and the resultant precipitate filtered, washed with additional cold water (100 mL) and dried thoroughly to afford dimethyl 1-benzyl-4-iodo-pyrazole-3,5-dicarboxylate (**53**, 6.10 g, 14.5 mmol, 90% yield) as a colorless solid. ¹H NMR (500 MHz, CDCl₃) δ 7.37–7.27 (m, 3H), 7.25–7.18 (m, 2H), 5.84 (s, 2H), 3.99 (s, 3H), 3.89 (s, 3H). ACQUITY UPLC BEH C₁₈ 1.7 μ m: Rt = 1.78 min; *m/z* 401.1 [M + H]⁺.

Dimethyl (E)-1-Benzyl-4-(2-ethoxyvinyl)-1H-pyrazole-3,5-dicarboxylate (54). A 20 mL microwave vial was charged dimethyl 1-benzyl-4-iodo-pyrazole-3,5-dicarboxylate (2.00 g, 4.75 mmol), (E)-(2-ethoxyvinyl)boronic acid pinacol ester (1.71 mL, 8.08 mmol), CsCO₃ (3.30 g, 10.07 mmol), Pd(dppf)₂Cl₂ (0.33 g, 0.45 mmol), monoglyme (20 mL) and water (2 mL). The reaction mixture was degassed with N₂ for 10 min before heating to 90 °C and stirring overnight. The reaction mixture was diluted with EtOAc (60 mL) and filtered, separated and aqueous phase extracted with further EtOAc (20 mL). The organic phases were combined, dried over NaSO₄, filtered and concentrated under reduced pressure with Celite. The crude mixture was purified by flash column chromatography (silica, 40 g, 1:0 petrol/EtOAc to 7:3 petrol/EtOAc over 25 CV's). Fractions containing product were combined and concentrated under reduced pressure to afford dimethyl (E)-1-benzyl-4-(2-ethoxyvinyl)-1H-pyrazole-3,5-dicarboxylate (**54**, 1.40 g, 3.66 mmol, 77% yield) as a brown oil. ¹H NMR (500 MHz, CDCl₃) δ 7.40 (d, *J* = 12.9 Hz, 1H), 7.34–7.21 (m, 3H), 7.20–7.14 (m, 2H), 6.20 (d, *J* = 12.9 Hz, 1H), 5.77 (s, 2H), 3.97–3.92 (m, 5H), 3.83 (s, 3H), 1.35 (t, *J* = 7.0 Hz, 3H). ACQUITY UPLC BEH C₁₈ 1.7 μ m: Rt = 1.82 min; *m/z* 367.1 [M + Na]⁺.

Methyl 2,6-Dibenzyl-7-oxo-4,5,6,7-tetrahydro-2H-pyrazolo[3,4-c]pyridine-3-carboxylate (55). Synthesized according to General Procedure A using dimethyl 1-benzyl-4-(2-oxoethyl)-1H-pyrazole-3,5-dicarboxylate (5 g, 15.8 mmol, **27**), benzylamine hydrochloride (2.20 g, 20.6 mmol, 1.3 equiv), acetic acid (0.3 mL) and 2-methylpyridine borane complex (2.56 g, 23.7 mmol, 1.5 equiv), MeOH (50 mL). Purified by flash column chromatography (silica, 24 g, 1:0 heptane/EtOAc to 1:1 heptane/EtOAc over 25 CV's) to give methyl 2,6-dibenzyl-7-oxo-4,5,6,7-tetrahydro-2H-pyrazolo[3,4-c]pyridine-3-carboxylate (**55**, 2.50 g, 6.66 mmol, 42% yield) as a colorless solid. m.p.: 157–159 °C. ¹H NMR (500 MHz, CDCl₃) δ 7.40–7.23 (m, 10H), 5.83 (s, 2H), 4.78 (s, 2H), 3.85–3.81 (m, 3H), 3.48 (t, *J* = 6.7 Hz, 2H), 2.97 (t, *J* = 6.8 Hz, 2H). ¹³C{¹H} NMR (126 MHz, CDCl₃) δ 160.9 (Cq), 159.9 (Cq), 142.4 (Cq), 137.3 (Cq), 136.4 (Cq), 128.8 (CH), 128.6 (CH), 128.3 (CH), 128.14 (Cq), 128.12 (CH), 128.1 (CH), 127.7 (CH), 125.9 (Cq), 56.2 (CH₂), 52.1 (CH₃), 49.7 (CH₂), 46.6 (CH₂), 21.5 (CH₃). ACQUITY UPLC BEH C₁₈ 1.7 μ m: Rt = 1.78 min; *m/z* 376.3 [M + H]⁺. HRMS calculated for

C₂₂H₂₂N₃O₃: 376.1661, found: 376.1665 [M + H]⁺. ELSD/UV/¹H NMR purity: 100/93/99%.

Methyl 1,6-Dibenzyl-7-oxo-4,5,6,7-tetrahydro-1H-pyrazolo[3,4-c]pyridine-3-carboxylate (56). Synthesized according to the synthesis of **55** through separation of the other regioisomer to give methyl 1,6-dibenzyl-7-oxo-4,5,6,7-tetrahydro-1H-pyrazolo[3,4-c]pyridine-3-carboxylate (**56**, 1.30 g, 3.46 mmol, 22% yield) as a colorless solid. ¹H NMR (500 MHz, CDCl₃) δ 7.39–7.34 (m, 2H), 7.29–7.20 (m, 8H), 5.81 (s, 2H), 4.63 (s, 2H), 3.85 (s, 3H), 3.43 (t, *J* = 6.9 Hz, 2H), 2.97 (t, *J* = 6.9 Hz, 2H). ACQUITY UPLC BEH C₁₈ 1.7 μ m: Rt = 1.82 min; *m/z* 376.3 [M + H]⁺.

2,6-Dibenzyl-7-oxo-4,5,6,7-tetrahydro-2H-pyrazolo[3,4-c]pyridine-3-carboxamide (34). Synthesized according to General Procedure C using 2,6-dibenzyl-7-oxo-4,5,6,7-tetrahydro-2H-pyrazolo[3,4-c]pyridine-3-carboxylic acid (150 mg, 0.41 mmol, **80**), HOBt hydrate (61 mg, 0.45 mmol, 1.1 equiv), EDC·HCl (103 mg, 0.54 mmol, 1.3 equiv), DIPEA (0.18 mL, 1.03 mmol, 2.4 equiv) and NH₄Cl (66 mg, 1.24 mmol, 3 equiv). Purified by reverse-phase column chromatography (9:1 0.1% TFA in water/MeCN to 0:1 0.1% TFA in water/MeCN over 30 min) to afford 2,6-dibenzyl-7-oxo-4,5,6,7-tetrahydro-2H-pyrazolo[3,4-c]pyridine-3-carboxamide (**34**, 14 mg, 0.04 mmol, 9% yield) as an off-white solid. ¹H NMR (500 MHz, DMSO-*d*₆) δ 7.77 (br s, 1H), 7.62 (br s, 1H), 7.39–7.16 (m, 10H), 5.64 (s, 2H), 4.65 (s, 2H), 3.48 (t, *J* = 6.7 Hz, 2H), 2.89 (t, *J* = 6.7 Hz, 2H). ¹³C{¹H} NMR (101 MHz, DMSO-*d*₆) δ 161.0, 160.0, 141.3, 137.7, 137.1, 132.9, 128.48, 127.64, 127.61, 127.57, 127.1, 125.3, 120.6, 54.0, 48.7, 46.7, 19.9. A HMBC correlation (in DMSO-*d*₆) of amidic NH₂ (7.62 and 7.77 ppm) with C5 (132.9 ppm) and benzyl CH₂ (5.65 ppm) with C5 (132.9 ppm) was observed. Additionally, NOESY correlation was observed between amidic NH₂ (7.62 and 7.77 ppm) with benzyl CH₂ (5.65 ppm), which altogether is only consistent with isomer as drawn. ACQUITY UPLC BEH C₁₈ 1.7 μ m: Rt = 1.52 min; *m/z* 361.2 [M + H]⁺. HRMS calculated for C₂₁H₂₁N₄O₂: 361.1665, found 361.1675. ELSD/UV/¹H NMR purity: 100/100/94%.

1,6-Dibenzyl-7-oxo-4,5,6,7-tetrahydro-1H-pyrazolo[3,4-c]pyridine-3-carboxamide (57). Synthesized according to General Procedure D using methyl 1,6-dibenzyl-7-oxo-4,5,6,7-tetrahydro-1H-pyrazolo[3,4-c]pyridine-3-carboxylate (150 mg, 0.40 mmol, 1 equiv) and 7 M NH₃ in MeOH (5 mL). Purified by reverse-phase column chromatography (9:1 5 mM (NH₄)HCO₃ in water/MeCN to 0:1 5 mM (NH₄)HCO₃ in water/MeCN over 30 min) to 1,6-dibenzyl-7-oxo-4,5,6,7-tetrahydro-1H-pyrazolo[3,4-c]pyridine-3-carboxamide (**57**, 25 mg, 0.07 mmol, 17% yield) as an off-white solid. ¹H NMR (500 MHz, CDCl₃) δ 7.40–7.27 (m, 10H), 6.76 (s, 1H), 5.82 (s, 2H), 5.35 (s, 1H), 4.71 (s, 2H), 3.50 (t, *J* = 6.6 Hz, 2H), 3.10 (t, *J* = 6.9 Hz, 2H). ¹³C{¹H} NMR (100 MHz, DMSO-*d*₆) δ 163.1, 158.0, 140.6, 137.3, 137.0, 131.9, 130.0, 128.53, 128.47, 127.49, 127.45, 127.2, 123.5, 53.8, 48.6, 47.3, 20.1. A HMBC correlation (in DMSO-*d*₆) of benzyl CH₂ (5.77 ppm) and C5 (131.9 ppm) was identified only and no NOESY was observed between amidic NH₂ and benzyl CH₂, which is only consistent with isomer as drawn. ACQUITY UPLC BEH C₁₈ 1.7 μ m: Rt = 1.81 min; *m/z* 361.2 [M + H]⁺. ELSD/UV/¹H NMR purity: 100/89/98%.

Methyl 2-Benzyl-7-oxo-6-phenethyl-4,5,6,7-tetrahydro-2H-pyrazolo[3,4-c]pyridine-3-carboxylate (73a). Synthesized according to General Procedure A using dimethyl 1-benzyl-4-(2-oxoethyl)-1H-pyrazole-3,5-dicarboxylate (0.90 g, 2.84 mmol, **27**), phenethylamine hydrochloride (0.67 g, 4.27 mmol, 1.5 equiv), acetic acid (0.3 mL) and 2-methylpyridine borane complex (0.27 g, 2.56 mmol, 0.9 equiv). The crude uncyclized product after workup was kept at room temperature overnight, resulting in two cyclized regioisomers. Purified by flash column chromatography (silica, 12 g, 1:0 heptane/EtOAc to 1:1 heptane/EtOAc) to give methyl 2-benzyl-7-oxo-6-phenethyl-4,5,6,7-tetrahydro-2H-pyrazolo[3,4-c]pyridine-3-carboxylate (**73a**, 240 mg, 0.62 mmol, 22% yield) as a pale yellow oil. X-Select LCMS CSH C₁₈ 2.5 μ m: Rt = 2.08 min; *m/z* 390.0 [M + H]⁺.

2-Benzyl-7-oxo-6-phenethyl-4,5,6,7-tetrahydro-2H-pyrazolo[3,4-c]pyridine-3-carboxamide (58). Synthesized according to General Procedure D using methyl 2-benzyl-7-oxo-6-phenethyl-4,5,6,7-tetrahydro-2H-pyrazolo[3,4-c]pyridine-3-carboxylate (100 mg, 0.25 mmol) and 7 M NH₃ in MeOH (5 mL). Purified by reverse-phase column

chromatography (9:1 5 mM (NH₄)HCO₃ in water/MeCN to 0:1 5 mM (NH₄)HCO₃ in water/MeCN over 30 min) to give 2-benzyl-7-oxo-6-phenethyl-4,5,6,7-tetrahydro-2H-pyrazolo[3,4-c]pyridine-3-carboxamide (**58**, 20 mg, 0.05 mmol, 21% yield) as an off-white solid. m.p.: 169–171 °C. ¹H NMR (500 MHz, CDCl₃) δ 7.38–7.33 (m, 2H), 7.33–7.19 (m, 8H), 5.78 (s, 2H), 5.58 (br s, 2H), 3.78 (t, *J* = 6.6 Hz, 2H), 3.37 (t, *J* = 6.6 Hz, 2H), 2.95 (t, *J* = 7.1 Hz, 2H), 2.75 (t, *J* = 6.6 Hz, 2H). ¹³C{¹H} NMR (126 MHz, CDCl₃) δ 161.2 (Cq), 160.8 (Cq), 142.0 (Cq), 139.2 (Cq), 136.4 (Cq), 130.9 (CH), 129.0 (CH), 128.7 (CH), 128.3 (CH), 128.2 (CH), 126.7 (CH), 121.1 (Cq), 55.8 (CH₂), 49.2 (CH₂), 48.6 (CH₂), 34.5 (CH₂), 21.1 (CH₂). A HMBC correlation (in DMSO-*d*₆) of amidic NH₂ (7.71 and 7.82 ppm) with C5 (132.8 ppm) and benzyl CH₂ (5.69 ppm) with C5 (132.8 ppm) was observed, which is only consistent with isomer as drawn. ACQUITY UPLC BEH C₁₈ 1.7 μm: Rt = 1.57 min; *m/z* 375.3 [M + H]⁺. HRMS calculated for C₂₂H₂₃N₄O₂: 375.1821, found: 375.1817 [M + H]⁺. ELSD/UV/¹H NMR purity: 100/92/100%.

Methyl 2-Benzyl-7-oxo-6-(2-phenoxylethyl)-4,5,6,7-tetrahydro-2H-pyrazolo[3,4-c]pyridine-3-carboxylate (73b). Synthesized according to General Procedure A but reversed limiting reagent. Dimethyl 1-benzyl-4-(2-oxoethyl)-1H-pyrazole-3,5-dicarboxylate (0.80 g, 2.53 mmol, **27**), 2-phenoxylethylamine (0.50 mL, 3.79 mmol, 1.5 equiv), acetic acid (0.2 mL), 2-methylpyridine borane complex (243 mg, 2.27 mmol, 0.9 equiv). 4 M HCl in 1,4-dioxane (0.7 mL) was added to generate amine hydrochloride prior to reductive amination. The crude uncyclized product after workup was kept at room temperature overnight, resulting in two cyclized regioisomers. Purified by flash column chromatography (silica, 24 g, 7:3 heptane/EtOAc to 0:1 heptane/EtOAc) to give methyl 2-benzyl-7-oxo-6-(2-phenoxylethyl)-4,5,6,7-tetrahydro-2H-pyrazolo[3,4-c]pyridine-3-carboxylate (**73b**, 200 mg, 0.49 mmol, 20% yield) as an off-white solid. X-Select LCMS CSH C₁₈ 1.5 μm: Rt = 2.17 min; *m/z* 406.2 [M + H]⁺.

2-Benzyl-7-oxo-6-(2-phenoxylethyl)-4,5,6,7-tetrahydro-2H-pyrazolo[3,4-c]pyridine-3-carboxamide (59). Synthesized according to General Procedure D using methyl 2-benzyl-7-oxo-6-(2-phenoxylethyl)-4,5,6,7-tetrahydro-2H-pyrazolo[3,4-c]pyridine-3-carboxylate (150 mg, 0.37 mmol) and 7 M NH₃ in MeOH (5 mL). Purified by reverse-phase column chromatography (9:1 0.1% TFA in water/MeCN to 1:9 0.1% TFA in water/MeCN over 30 min) to give 2-benzyl-7-oxo-6-(2-phenoxylethyl)-4,5,6,7-tetrahydro-2H-pyrazolo[3,4-c]pyridine-3-carboxamide (**59**, 20 mg, 0.05 mmol, 14% yield) as an off-white solid. m.p.: 95–97 °C. ¹H NMR (500 MHz, DMSO-*d*₆) δ 7.77 (s, 1H), 7.65 (s, 1H), 7.35–7.24 (m, 5H), 7.21–7.17 (m, 2H), 6.97–6.91 (m, 3H), 5.63 (s, 2H), 4.14 (t, *J* = 5.7 Hz, 2H), 3.80 (t, *J* = 5.7 Hz, 2H), 3.69 (t, *J* = 6.6 Hz, 2H), 2.91 (t, *J* = 6.6 Hz, 2H). ¹³C{¹H} NMR (126 MHz, CDCl₃) δ 161.0 (Cq), 158.6 (Cq), 142.1 (Cq), 136.5 (Cq), 130.9 (Cq), 129.7 (CH), 128.7 (CH), 128.2 (CH), 128.1 (CH), 121.4 (Cq), 121.2 (CH), 114.5 (CH), 67.3 (CH₂), 55.8 (CH₂), 49.8 (CH₂), 47.0 (CH₂), 21.4 (CH₂). A HMBC correlation of amidic NH₂ (7.65 and 7.77 ppm) with C5 (132.9 ppm) and benzyl CH₂ (5.63 ppm) with C5 (132.9 ppm) was observed, which is only consistent with isomer as drawn. ACQUITY UPLC BEH C₁₈ 1.7 μm: Rt = 1.57 min; *m/z* 389.2 [M – H][–]. HRMS calculated for C₂₂H₂₁N₄O₃: 389.1616, found: 389.1598 [M – H][–]. ELSD/UV/¹H NMR purity: 100/93/100%.

Methyl 2-Benzyl-6-(4-hydroxybenzyl)-7-oxo-4,5,6,7-tetrahydro-2H-pyrazolo[3,4-c]pyridine-3-carboxylate and Methyl 1-Benzyl-6-(4-hydroxybenzyl)-7-oxo-4,5,6,7-tetrahydro-1H-pyrazolo[3,4-c]pyridine-3-carboxylate (73c). Synthesized according to General Procedure A using dimethyl 1-benzyl-4-(2-oxoethyl)-1H-pyrazole-3,5-dicarboxylate (0.80 g, 2.53 mmol, **27**), 4-hydroxybenzylamine (0.47 g, 3.79 mmol, 1.5 equiv), acetic acid (0.3 mL) and 2-methylpyridine borane complex (243 mg, 2.27 mmol, 0.9 equiv). 4 M HCl in 1,4-dioxane (0.7 mL) was added to generate amine hydrochloride prior to reductive amination. The crude uncyclized product after workup was kept at room temperature overnight, resulting in two cyclized regioisomers. Purified by flash column chromatography (silica, 24 g, 1:0 heptane/EtOAc to 1:1 heptane/EtOAc) to afford a mixture of two regioisomers methyl 2-benzyl-6-(4-hydroxybenzyl)-7-oxo-4,5,6,7-tetrahydro-2H-pyrazolo[3,4-c]pyridine-3-carboxylate and methyl 1-benzyl-6-(4-hydroxybenzyl)-7-oxo-4,5,6,7-tetrahydro-1H-

pyrazolo[3,4-c]pyridine-3-carboxylate (**73c**, 0.60 g, 1.53 mmol, 61% yield) as a pale yellow solid. X-Select LCMS CSH C₁₈ 2.5 μm: Rt = 2.32 min; *m/z* 392.1 [M + H]⁺, Rt = 2.43; *m/z* 392.1 [M + H]⁺.

2-Benzyl-6-(4-hydroxybenzyl)-7-oxo-4,5,6,7-tetrahydro-2H-pyrazolo[3,4-c]pyridine-3-carboxamide (60). Synthesized according to General Procedure D using methyl 2-benzyl-6-(4-hydroxybenzyl)-7-oxo-4,5,6,7-tetrahydro-2H-pyrazolo[3,4-c]pyridine-3-carboxylate (0.50 g, 1.27 mmol, as mixture of two regioisomers) and 7 M NH₃ in MeOH (15 mL). Purified by reverse-phase column chromatography (9:1 10 mM (NH₄)HCO₃ in water/MeCN to 0:1 10 mM (NH₄)HCO₃ in water/MeCN over 30 min) to give 2-benzyl-6-(4-hydroxybenzyl)-7-oxo-4,5,6,7-tetrahydro-2H-pyrazolo[3,4-c]pyridine-3-carboxamide (**60**, 28 mg, 0.07 mmol, 6% yield) as an off-white solid. m.p.: 148–149 °C. ¹H NMR (500 MHz, DMSO-*d*₆) δ 9.33 (s, 1H), 7.76 (s, 1H), 7.61 (s, 1H), 7.36–7.25 (m, 3H), 7.23–7.18 (m, 2H), 7.13–7.07 (m, 2H), 6.73–6.69 (m, 2H), 5.64 (s, 2H), 4.52 (s, 2H), 3.43 (t, *J* = 6.7 Hz, 2H), 2.85 (t, *J* = 6.7 Hz, 2H). ¹³C{¹H} NMR (126 MHz, DMSO-*d*₆) δ 161.1 (Cq), 159.8 (Cq), 156.6 (Cq), 141.5 (Cq), 137.2 (Cq), 132.9 (Cq), 129.1 (CH), 128.5 (CH), 127.8 (Cq), 127.7 (CH), 127.6 (CH), 120.6 (Cq), 115.2 (CH), 54.0 (CH₂), 48.1 (CH₂), 46.4 (CH₂), 19.9 (CH₂). A HMBC correlation of amidic NH (7.76 ppm) with C5 (132.9 ppm) and benzyl CH₂ (5.64 ppm) with C5 (132.9 ppm) was observed, which is only consistent with isomer as drawn. ACQUITY UPLC BEH C₁₈ 1.7 μm: Rt = 1.39 min; *m/z* 377.2 [M + H]⁺. HRMS calculated for C₂₁H₂₁N₄O₃: 377.1614, found: 377.1599 [M + H]⁺. ELSD/UV/¹H NMR purity: 100/100/100%.

Methyl 2-Benzyl-6-(4-methoxybenzyl)-7-oxo-4,5,6,7-tetrahydro-2H-pyrazolo[3,4-c]pyridine-3-carboxylate (73d). Synthesized according to General Procedure A using dimethyl 1-benzyl-4-(2-oxoethyl)-1H-pyrazole-3,5-dicarboxylate (0.80 g, 2.53 mmol, **27**), 4-methoxybenzylamine (0.50 g, 3.79 mmol, 1.5 equiv), acetic acid (0.3 mL) and 2-methylpyridine borane complex (0.24 g, 2.27 mmol, 0.9 equiv). 4 M HCl in 1,4-dioxane (0.8 mL) was added to generate amine hydrochloride prior to reductive amination. The crude uncyclized product after workup was kept at room temperature overnight, resulting in two cyclized regioisomers. Purified by flash column chromatography (silica, 24 g, 1:0 heptane/EtOAc to 1:1 heptane/EtOAc) to give methyl 2-benzyl-6-(4-methoxybenzyl)-7-oxo-4,5,6,7-tetrahydro-2H-pyrazolo[3,4-c]pyridine-3-carboxylate (**73d**, 0.20 g, 0.49 mmol, 20% yield) as a pale yellow solid. X-Select LCMS CSH C₁₈ 2.5 μm: Rt = 1.87 min; *m/z* 406.2 [M + H]⁺.

2-Benzyl-6-(4-methoxybenzyl)-7-oxo-4,5,6,7-tetrahydro-2H-pyrazolo[3,4-c]pyridine-3-carboxamide (61). Synthesized according to General Procedure D using methyl 2-benzyl-6-(4-methoxybenzyl)-7-oxo-4,5,6,7-tetrahydro-2H-pyrazolo[3,4-c]pyridine-3-carboxylate (200 mg, 0.49 mmol) and 7 M NH₃ in MeOH (10 mL). Purified by reverse-phase column chromatography (9:1 0.1% TFA in water/MeCN to 0:1 0.1% TFA in water/MeCN over 30 min) to give 2-benzyl-6-(4-methoxybenzyl)-7-oxo-4,5,6,7-tetrahydro-2H-pyrazolo[3,4-c]pyridine-3-carboxamide (**61**, 14 mg, 0.04 mmol, 7% yield) as an off-white solid. m.p.: 195–196 °C. ¹H NMR (500 MHz, DMSO-*d*₆) δ 7.76 (s, 1H), 7.61 (s, 1H), 7.36–7.25 (m, 3H), 7.24–7.19 (m, 4H), 6.92–6.86 (m, 2H), 5.64 (s, 2H), 4.57 (s, 2H), 3.73 (s, 3H), 3.44 (t, *J* = 6.7 Hz, 2H), 2.86 (t, *J* = 6.7 Hz, 2H). ¹³C{¹H} NMR (126 MHz, CDCl₃) δ 160.9 (Cq), 160.8 (Cq), 159.3 (Cq), 142.1 (Cq), 136.6 (Cq), 130.9 (Cq), 129.7 (CH), 129.3 (Cq), 128.7 (CH), 128.3 (CH), 128.1 (CH), 120.9 (Cq), 114.2 (CH), 55.8 (CH₂), 55.4 (CH₃), 49.0 (CH₂), 46.3 (CH₂), 21.2 (CH₂). ACQUITY UPLC BEH C₁₈ 1.7 μm: Rt = 1.54 min; *m/z* 391.3 [M + H]⁺. HRMS calculated for C₂₂H₂₃N₄O₃: 391.1770, found: 391.1765 [M + H]⁺. ELSD/UV/¹H NMR purity: 100/95/100%.

Methyl 2-Benzyl-6-(3-hydroxyphenethyl)-7-oxo-4,5,6,7-tetrahydro-2H-pyrazolo[3,4-c]pyridine-3-carboxylate and Methyl 1-Benzyl-6-(3-hydroxyphenethyl)-7-oxo-4,5,6,7-tetrahydro-1H-pyrazolo[3,4-c]pyridine-3-carboxylate (73e). Synthesized according to General Procedure A using dimethyl 1-benzyl-4-(2-oxoethyl)-1H-pyrazole-3,5-dicarboxylate (0.80 g, 2.53 mmol, **27**), 3-(2-aminoethyl)phenol (0.52 mL, 3.79 mmol, 1.5 equiv), acetic acid (0.3 mL) and 2-methylpyridine borane complex (0.24 g, 2.27 mmol, 0.9 equiv). 4 M HCl in 1,4-dioxane (0.7 mL) was added to generate amine hydrochloride prior to reductive amination. The crude uncyclized

product after workup was kept at room temperature overnight, resulting in two cyclized regioisomers. Purified by flash column chromatography (silica, 24 g, 1:0 heptane/EtOAc to 3:7 heptane/EtOAc) to give methyl 2-benzyl-6-(3-hydroxyphenethyl)-7-oxo-4,5,6,7-tetrahydro-2H-pyrazolo[3,4-c]pyridine-3-carboxylate and methyl 1-benzyl-6-(3-hydroxyphenethyl)-7-oxo-4,5,6,7-tetrahydro-1H-pyrazolo[3,4-c]pyridine-3-carboxylate (**73e**, 0.40 g, 0.98 mmol, 39% yield) as a pale yellow solid. X-Select LCMS CSH C₁₈ 2.5 μ m: Rt = 1.13 min; m/z 406.3 [M + H]⁺, Rt = 1.16 min, m/z 406.3 [M + H]⁺.

2-Benzyl-6-(3-hydroxyphenethyl)-7-oxo-4,5,6,7-tetrahydro-2H-pyrazolo[3,4-c]pyridine-3-carboxamide (62). Synthesized according to General Procedure D using methyl 2-benzyl-6-(3-hydroxyphenethyl)-7-oxo-4,5,6,7-tetrahydro-2H-pyrazolo[3,4-c]pyridine-3-carboxylate (400 mg, 0.98 mmol, as mixture of two regioisomers) and 7 M NH₃ in MeOH (15 mL). Purified by reverse-phase column chromatography (9:1 5 mM (NH₄)HCO₃ in water/MeCN to 0:1 5 mM (NH₄)HCO₃ in water/MeCN over 30 min) to give 2-benzyl-6-(3-hydroxyphenethyl)-7-oxo-4,5,6,7-tetrahydro-2H-pyrazolo[3,4-c]pyridine-3-carboxamide (**62**, 30 mg, 0.08 mmol, 8% yield) as an off-white solid. m.p.: 184–186 °C. ¹H NMR (500 MHz, DMSO-*d*₆) δ 9.27 (s, 1H), 7.76 (s, 1H), 7.65 (s, 1H), 7.35–7.25 (m, 3H), 7.21–7.17 (m, 2H), 7.07 (t, J = 7.7 Hz, 1H), 6.67–6.63 (m, 2H), 6.59 (ddd, J = 8.0, 2.5, 1.0 Hz, 1H), 5.63 (s, 2H), 3.64–3.57 (m, 2H), 3.48 (t, J = 6.6 Hz, 2H), 2.84 (t, J = 6.6 Hz, 2H), 2.73 (t, J = 7.5 Hz, 2H). ¹³C{¹H} NMR (101 MHz, DMSO-*d*₆) δ 161.1 (Cq), 159.6 (Cq), 157.3 (Cq), 141.6 (Cq), 140.5 (Cq), 137.2 (Cq), 132.8 (Cq), 129.3 (CH), 128.5 (CH), 127.61 (CH), 127.57 (CH), 120.6 (Cq), 119.3 (CH), 115.5 (CH), 113.2 (CH), 54.0 (CH₂), 47.6 (CH₂), 47.3 (CH₂), 33.5 (CH₂), 20.0 (CH₂). A HMBC correlation of amidic NH₂ (7.65 and 7.76 ppm) with C5 (132.8 ppm) was observed, similarly benzyl CH₂ (5.63 ppm) with C5 (132.8 ppm) and lactam CH₂ (2.84 ppm) with C5 (132.8 ppm) was observed, which is only consistent with isomer as drawn. ACQUITY UPLC BEH C₁₈ 1.7 μ m: Rt = 1.44 min; m/z 391.3 [M + H]⁺. HRMS calculated for C₂₂H₂₃N₄O₃: 391.1770, found: 391.1770 [M + H]⁺. ELSD/UV/¹H NMR purity: 100/87/97%.

Methyl 2-Benzyl-6-(3-methoxyphenethyl)-7-oxo-4,5,6,7-tetrahydro-2H-pyrazolo[3,4-c]pyridine-3-carboxylate (73f). Synthesized according to General Procedure A using dimethyl 1-benzyl-4-(2-oxoethyl)-1H-pyrazole-3,5-dicarboxylate (0.80 g, 2.53 mmol, **27**), 3-methoxyphenethylamine (0.55 mL, 3.79 mmol, 1.5 equiv), acetic acid (0.3 mL) and 2-methylpyridine borane complex (0.24 g, 2.27 mmol, 0.9 equiv). 4 M HCl in 1,4-dioxane (0.7 mL) was added to generate amine hydrochloride prior to reductive amination. The crude uncyclized product after workup was kept at room temperature overnight, resulting in two cyclized regioisomers. Purified by flash column chromatography (silica, 24 g, 7:3 heptane/EtOAc to 1:4 heptane/EtOAc) to give methyl 2-benzyl-6-(3-methoxyphenethyl)-7-oxo-4,5,6,7-tetrahydro-2H-pyrazolo[3,4-c]pyridine-3-carboxylate (**73f**, 0.20 g, 0.48 mmol, 19% yield) as a brown oil. X-Select LCMS CSH C₁₈ 2.5 μ m: Rt = 2.65 min; m/z 420.2 [M + H]⁺.

2-Benzyl-6-(3-methoxyphenethyl)-7-oxo-4,5,6,7-tetrahydro-2H-pyrazolo[3,4-c]pyridine-3-carboxamide (63). Synthesized according to General Procedure D using methyl 2-benzyl-6-(3-methoxyphenethyl)-7-oxo-4,5,6,7-tetrahydro-2H-pyrazolo[3,4-c]pyridine-3-carboxylate (200 mg, 0.47 mmol) and 7 M NH₃ in MeOH (10 mL). Purified by reverse-phase column chromatography (9:1 10 mM (NH₄)HCO₃ in water/MeCN to 0:1 10 mM (NH₄)HCO₃ in water/MeCN over 30 min) to give 2-benzyl-6-(3-methoxyphenethyl)-7-oxo-4,5,6,7-tetrahydro-2H-pyrazolo[3,4-c]pyridine-3-carboxamide (**63**, 21 mg, 0.05 mmol, 11% yield) as an off-white solid. m.p.: 162–163 °C. ¹H NMR (500 MHz, DMSO-*d*₆) δ 7.76 (s, 1H), 7.65 (s, 1H), 7.36–7.24 (m, 3H), 7.23–7.17 (m, 3H), 6.85–6.80 (m, 2H), 6.78–6.74 (m, 1H), 5.63 (s, 2H), 3.72 (s, 3H), 3.67–3.62 (m, 2H), 3.49 (t, J = 6.6 Hz, 2H), 2.88–2.78 (m, 4H). ¹³C{¹H} NMR (126 MHz, CDCl₃) δ 160.9 (Cq), 160.6 (Cq), 159.9 (Cq), 142.2 (Cq), 140.9 (Cq), 136.6 (Cq), 130.9 (Cq), 129.7 (CH), 128.7 (CH), 128.3 (CH), 128.1 (CH), 121.4 (CH), 121.0 (Cq), 114.6 (CH), 112.1 (CH), 55.8 (CH₂), 55.4 (CH₃), 49.0 (CH₂), 48.5 (CH₂), 34.6 (CH₂), 21.2 (CH₂). ACQUITY UPLC BEH C₁₈ 1.7 μ m: Rt = 1.57 min; m/z 405.3 [M + H]⁺. HRMS calculated for

C₂₃H₂₅N₄O₃: 405.1927, found: 405.1912 [M + H]⁺. ELSD/UV/¹H NMR purity: 100/100/98%.

Methyl 2-Benzyl-6-(2-methoxyethyl)-7-oxo-4,5,6,7-tetrahydro-2H-pyrazolo[3,4-c]pyridine-3-carboxylate (73g). To a solution of dimethyl 1-benzyl-4-(2-oxoethyl)-1H-pyrazole-3,5-dicarboxylate (0.70 g, 2.21 mmol) in DCE (10 mL) were added 2-methoxyethylamine (0.29 mL, 3.32 mmol), Na(OAc)₃BH (1.17 g, 5.53 mmol) and AcOH (0.3 mL). The reaction mixture was stirred at room temperature overnight. The reaction mixture was diluted with DCM (50 mL) and washed with saturated NaHCO₃ solution (30 mL). The organic layer was dried over NaSO₄, filtered and concentrated under reduced pressure to obtain the crude uncyclized product which was kept at room temperature overnight, resulting in formation of two cyclized regioisomers. The crude mixture was purified by flash column chromatography (silica, 24 g, 1:0 heptane/EtOAc to 0:1 heptane/EtOAc over 25 CV's). Fractions containing product were combined and concentrated under reduced pressure to afford methyl 2-benzyl-6-(2-methoxyethyl)-7-oxo-4,5,6,7-tetrahydro-2H-pyrazolo[3,4-c]pyridine-3-carboxylate (**73g**, 100 mg, 0.29 mmol, 13% yield) as a pale yellow solid. X-Select LCMS CSH C₁₈ 2.5 μ m: Rt = 2.80 min; m/z 344.2 [M + H]⁺.

2-Benzyl-6-(2-methoxyethyl)-7-oxo-4,5,6,7-tetrahydro-2H-pyrazolo[3,4-c]pyridine-3-carboxamide (64). Synthesized according to General Procedure D using methyl 2-benzyl-6-(2-methoxyethyl)-7-oxo-4,5,6,7-tetrahydro-2H-pyrazolo[3,4-c]pyridine-3-carboxylate (100 mg, 0.29 mmol) and 7 M NH₃ in MeOH (5 mL). Purified by reverse-phase column chromatography (9:1 10 mM (NH₄)HCO₃ in water/MeCN to 0:1 10 mM (NH₄)HCO₃ in water/MeCN over 30 min) to give 2-benzyl-6-(2-methoxyethyl)-7-oxo-4,5,6,7-tetrahydro-2H-pyrazolo[3,4-c]pyridine-3-carboxamide (**64**, 15 mg, 0.05 mmol, 16% yield) as an off-white solid. m.p.: 143–145 °C. ¹H NMR (500 MHz, DMSO-*d*₆) δ 7.77 (s, 1H), 7.64 (s, 1H), 7.35–7.24 (m, 3H), 7.22–7.17 (m, 2H), 5.63 (s, 2H), 3.61–3.55 (m, 4H), 3.48 (t, J = 5.6 Hz, 2H), 3.25 (s, 3H), 2.89 (t, J = 6.6 Hz, 2H). ¹³C{¹H} NMR (126 MHz, CDCl₃) δ 161.1 (Cq), 160.8 (Cq), 142.2 (Cq), 136.6 (Cq), 131.0 (Cq), 128.7 (CH), 128.3 (CH), 128.1 (CH), 121.2 (Cq), 71.8 (CH₂), 59.0 (CH₃), 55.7 (CH₂), 49.3 (CH₂), 46.9 (CH₂), 21.3 (CH₃). ACQUITY UPLC BEH C₁₈ 1.7 μ m: Rt = 1.32 min; m/z 329.2 [M + H]⁺. HRMS calculated for C₁₇H₂₁N₄O₃: 329.1614, found: 329.1621 [M + H]⁺. ELSD/UV/¹H NMR purity: 100/93/100%.

Methyl 2-Benzyl-6-(2-(dimethylamino)-2-oxoethyl)-7-oxo-4,5,6,7-tetrahydro-2H-pyrazolo[3,4-c]pyridine-3-carboxylate (73h). To a solution of dimethyl 1-benzyl-4-(2-oxoethyl)-1H-pyrazole-3,5-dicarboxylate (0.70 g, 2.21 mmol) in DCE (7 mL) were added 2-amino-N,N-dimethylacetamide (0.31 mL, 2.21 mmol), Na(OAc)₃BH (1.17 g, 5.53 mmol) and AcOH (0.1 mL). The reaction mixture was stirred at room temperature overnight. The reaction mixture was diluted with DCM (50 mL) and washed with saturated NaHCO₃ solution (30 mL). The organic layer was dried over NaSO₄, filtered and concentrated under reduced pressure to obtain the crude uncyclized product which was kept at room temperature overnight, resulting in formation of two cyclized regioisomers. The crude mixture was purified by flash column chromatography (silica, 24 g, 1:0 DCM/MeOH to 49:1 DCM/MeOH over 25 CV's). Fractions containing product were combined and concentrated under reduced pressure to afford methyl 2-benzyl-6-(2-(dimethylamino)-2-oxoethyl)-7-oxo-4,5,6,7-tetrahydro-2H-pyrazolo[3,4-c]pyridine-3-carboxylate (**73h**, 0.42 g, 1.13 mmol, 51% yield) as an off-white solid. X-Bridge LCMS BEH C₁₈ 2.5 μ m: Rt = 1.17 min; m/z 371.1 [M + H]⁺.

2-Benzyl-6-(2-(dimethylamino)-2-oxoethyl)-7-oxo-4,5,6,7-tetrahydro-2H-pyrazolo[3,4-c]pyridine-3-carboxamide (65). Synthesized according to General Procedure D using methyl 2-benzyl-6-(2-(dimethylamino)-2-oxoethyl)-7-oxo-4,5,6,7-tetrahydro-2H-pyrazolo[3,4-c]pyridine-3-carboxylate (0.40 g, 1.08 mmol) and 7 M NH₃ in MeOH (5 mL). Purified by reverse-phase column chromatography (9:1 5 mM (NH₄)HCO₃ in water/MeCN to 0:1 5 mM (NH₄)HCO₃ in water/MeCN over 30 min) to give 2-benzyl-6-(2-(dimethylamino)-2-oxoethyl)-7-oxo-4,5,6,7-tetrahydro-2H-pyrazolo[3,4-c]pyridine-3-carboxamide (**65**, 15 mg, 0.04 mmol, 6% yield) as an off-white solid. m.p.: 160–161 °C. ¹H NMR (500 MHz, DMSO-*d*₆) δ 7.78 (s, 1H), 7.67 (s,

1H), 7.35–7.25 (m, 3H), 7.22–7.18 (m, 2H), 5.64 (s, 2H), 4.31 (s, 2H), 3.56 (t, $J = 6.7$ Hz, 2H), 2.98 (s, 3H), 2.92 (t, $J = 6.7$ Hz, 2H), 2.83 (s, 3H). $^{13}\text{C}\{^1\text{H}\}$ NMR (126 MHz, CDCl_3) δ 167.9 (Cq), 161.0 (Cq), 141.7 (Cq), 136.6 (Cq), 131.1 (Cq), 128.7 (CH), 128.2 (CH), 128.1 (CH), 121.7 (Cq), 55.8 (CH_2), 48.5 (CH_2), 47.6 (CH_2), 36.7 (CH_3), 35.8 (CH_3), 21.1 (CH_2). ACQUITY UPLC BEH C_{18} 1.7 μm : Rt = 1.24 min; m/z 354.1 $[\text{M}-\text{H}]^-$. HRMS calculated for $\text{C}_{18}\text{H}_{20}\text{N}_3\text{O}_3$: 354.1566, found: 354.1561 $[\text{M}-\text{H}]^-$. ELSD/UV/ ^1H NMR purity: 100/92/100%.

Methyl 2-Benzyl-6-(3-hydroxy-1-phenylpropyl)-7-oxo-4,5,6,7-tetrahydro-2H-pyrazolo[3,4-*c*]pyridine-3-carboxylate (73i). Synthesized in two steps according to (i) General Procedure A using dimethyl 1-benzyl-4-(2-oxoethyl)-1H-pyrazole-3,5-dicarboxylate (1.50 g, 4.74 mmol, 27), 3-amino-3-phenyl-1-propanol (0.93 g, 6.17 mmol, 1.3 equiv), acetic acid (0.2 mL) and 2-methylpyridine borane complex (0.46 g, 4.27 mmol, 0.9 equiv). Purified by flash column chromatography (silica, 24 g, 1:0 DCM/MeOH to 9:1 DCM/MeOH) to afford dimethyl 1-benzyl-4-(2-((3-hydroxy-1-phenylpropyl)amino)ethyl)-1H-pyrazole-3,5-dicarboxylate (0.90 g, 1.99 mmol, 42% yield) as a yellow liquid. Product taken forward as crude to the next step. (ii) To a solution of dimethyl 1-benzyl-4-(2-((3-hydroxy-1-phenylpropyl)amino)ethyl)-1H-pyrazole-3,5-dicarboxylate (0.30 g, 0.66 mmol) in toluene (5 mL) was added AlMe_3 (2 M in toluene, 1.10 mL, 2.25 mmol). The reaction mixture was heated to 100 °C and stirred for 3 h. The reaction mixture was cooled to room temperature, quenched with saturated Rochelle salt solution (60 mL) and extracted with EtOAc (2 \times 70 mL). The organic layers were combined, dried over NaSO_4 , filtered and concentrated under reduced pressure. The crude mixture was purified by flash column chromatography (silica, 12 g, 1:0 heptane/EtOAc to 3:7 heptane/EtOAc over 25 CV's). Fractions containing product were combined and concentrated under reduced pressure to afford methyl 2-benzyl-6-(3-hydroxy-1-phenylpropyl)-7-oxo-4,5,6,7-tetrahydro-2H-pyrazolo[3,4-*c*]pyridine-3-carboxylate (73i, 0.15 g, 0.35 mmol, 53% yield) as a brown liquid. XSelect LCMS CSH C_{18} 2.5 μm : 2.15 min; m/z 420.3 $[\text{M} + \text{H}]^+$.

2-Benzyl-6-(3-hydroxy-1-phenylpropyl)-7-oxo-4,5,6,7-tetrahydro-2H-pyrazolo[3,4-*c*]pyridine-3-carboxamide (66). Synthesized according to General Procedure D using methyl 2-benzyl-6-(3-hydroxy-1-phenylpropyl)-7-oxo-4,5,6,7-tetrahydro-2H-pyrazolo[3,4-*c*]pyridine-3-carboxylate (150 mg, 0.35 mmol) and 7 M NH_3 in MeOH (5 mL). Purified by flash column chromatography (silica, 12 g, 1:0 DCM/MeOH to 19:1 DCM/MeOH over 25 CV's) to give 2-benzyl-6-(3-hydroxy-1-phenylpropyl)-7-oxo-4,5,6,7-tetrahydro-2H-pyrazolo[3,4-*c*]pyridine-3-carboxamide (66, 29 mg, 0.07 mmol, 20% yield) as an off-white solid. m.p.: 182–184 °C. ^1H NMR (500 MHz, $\text{DMSO}-d_6$) δ 7.74 (s, 1H), 7.59 (s, 1H), 7.39–7.31 (m, 6H), 7.30–7.25 (m, 2H), 7.23–7.20 (m, 2H), 5.91 (dd, $J = 9.6, 6.0$ Hz, 1H), 5.67–5.58 (m, 2H), 4.50 (t, $J = 5.1$ Hz, 1H), 3.50–3.39 (m, 3H), 3.09–3.02 (m, 1H), 2.86–2.78 (m, 1H), 2.74–2.66 (m, 1H), 2.19–2.07 (m, 2H). $^{13}\text{C}\{^1\text{H}\}$ NMR (100 MHz, $\text{DMSO}-d_6$) δ 161.5 (Cq), 160.5 (Cq), 142.1 (Cq), 140.6 (Cq), 137.6 (Cq), 133.3 (Cq), 129.0 (CH), 128.9 (CH), 128.2 (CH), 128.0 (CH), 127.8 (CH), 120.9 (Cq), 58.6 (CH_2), 54.5 (CH_2), 51.5 (CH), 42.1 (CH_2), 33.2 (CH_2), 20.6 (CH_2). A HMBc correlation of amidic NH_2 (7.59 and 7.74 ppm) with C5 (133.3 ppm) and benzyl CH_2 (5.58–5.67 ppm) with C5 (133.3 ppm) was observed, which is only consistent with isomer as drawn. ACQUITY UPLC BEH C_{18} 1.7 μm : Rt = 1.49 min; m/z 405.3 $[\text{M} + \text{H}]^+$. HRMS calculated for $\text{C}_{23}\text{H}_{25}\text{N}_4\text{O}_3$: 405.1927, found 405.1929 $[\text{M} + \text{H}]^+$. ELSD/UV/ ^1H NMR purity: 95/95/95%.

2-Benzyl-7-oxo-6-phenethyl-4,5,6,7-tetrahydro-2H-pyrazolo[3,4-*c*]pyridine-3-carboxylic acid (67). Synthesized according to synthesis of 58 and isolated as a major side-product. Purified by reverse-phase column chromatography (9:1 5 mM $(\text{NH}_4)\text{HCO}_3$ in water/MeCN to 0:1 5 mM $(\text{NH}_4)\text{HCO}_3$ in water/MeCN over 30 min). Fractions containing product were combined and concentrated under reduced pressure to give 2-benzyl-7-oxo-6-phenethyl-4,5,6,7-tetrahydro-2H-pyrazolo[3,4-*c*]pyridine-3-carboxylic acid (67, 28 mg, 0.07 mmol, 30% yield) as an off-white solid. m.p.: 80 °C. ^1H NMR (500 MHz, CDCl_3) δ 7.36–7.19 (m, 10H), 5.78 (s, 2H), 3.84–3.77 (m, 2H), 3.39 (t, $J = 6.8$ Hz, 2H), 2.96 (t, $J = 7.2$ Hz, 2H), 2.91 (t, $J = 6.8$ Hz, 2H). OH

not observed. $^{13}\text{C}\{^1\text{H}\}$ NMR (126 MHz, CDCl_3) δ 162.3 (Cq), 161.3 (Cq), 142.0 (Cq), 138.9 (Cq), 136.1 (Cq), 129.0 (CH), 128.8 (CH), 128.7 (CH), 128.2 (CH), 128.2 (CH), 127.9 (Cq), 127.1 (Cq), 126.8 (CH), 56.2 (CH_2), 49.6 (CH_2), 48.8 (CH_2), 34.4 (CH_2), 21.2 (CH_2). The structure was assigned based on structural confirmation by HMBC of 58. ACQUITY UPLC BEH C_{18} 1.7 μm : Rt = 1.63 min; m/z 376.3 $[\text{M} + \text{H}]^+$. HRMS calculated for $\text{C}_{22}\text{H}_{22}\text{N}_3\text{O}_3$: 376.1661, found: 376.1653 $[\text{M} + \text{H}]^+$. ELSD/UV/ ^1H NMR purity: 100/91/98%.

2-((2-Methoxyethyl)amino)benzonitrile (75). To a stirred solution of 2-fluorobenzonitrile (5.00 g, 41.3 mmol) in MeCN (50 mL) was added 2-methoxyethylamine (7.18 mL, 82.6 mmol). The reaction mixture was heated to 100 °C and stirred overnight in a sealed tube. The reaction mixture was cooled to room temperature and concentrated under reduced pressure. The crude mixture was purified by flash column chromatography (silica, 24 g, 1:0 heptane/EtOAc to 9:1 heptane/EtOAc over 25 CV's). Fractions containing product were combined and concentrated under reduced pressure to afford 2-((2-methoxyethyl)amino)benzonitrile (75, 2.50 g, 14.19 mmol, 34% yield) as a colorless liquid. ^1H NMR (400 MHz, CDCl_3) δ 7.42–7.35 (m, 2H), 6.72–6.64 (m, 2H), 4.86 (br s, 1H), 3.62 (t, $J = 5.3$ Hz, 2H), 3.41 (s, 3H), 3.39–3.34 (m, 2H). X-Select LCMS CSH C_{18} 2.5 μm : Rt = 1.43 min; m/z 177.0 $[\text{M} + \text{H}]^+$.

2-(Amino(cyclopropyl)methyl)-N-(2-methoxyethyl)aniline (76). To a stirred solution of 2-((2-methoxyethyl)amino)benzonitrile (0.30 g, 1.70 mmol) in THF (3 mL) was added cyclopropylmagnesium bromide (0.5 M in THF, 10 mL, 5.11 mmol). The reaction mixture was irradiated in a microwave at 100 °C for 15 min. After completion of the reaction, NaBH_4 (0.32 g, 8.52 mmol) in MeOH (6 mL) was added at 0 °C. The reaction mixture was stirred at 0 °C for 30 min, allowing to warm to room temperature. The reaction mixture was diluted with water (5 mL) and extracted with EtOAc (2 \times 5 mL). The organic layers were combined, dried over NaSO_4 , filtered and concentrated under reduced pressure. The crude mixture was purified by flash column chromatography (silica, 12 g, 1:0 heptane/EtOAc to 3:2 heptane/EtOAc over 25 CV's). Fractions containing product were combined and concentrated under reduced pressure to afford 2-(amino(cyclopropyl)methyl)-N-(2-methoxyethyl)aniline (76, 0.70 g, 3.18 mmol, 47% yield) as a yellow liquid. ^1H NMR (400 MHz, CDCl_3) δ 7.23–7.13 (m, 2H), 6.71–6.61 (m, 2H), 3.66 (t, $J = 5.4$ Hz, 3H), 3.40 (s, 4H), 3.36–3.28 (m, 3H), 3.07 (br d, $J = 9.3$ Hz, 1H), 1.47–1.41 (m, 1H), 0.66–0.52 (m, 2H), 0.30–0.20 (m, 2H).

Dimethyl 1-Benzyl-4-(2-((cyclopropyl(phenyl)methyl)amino)ethyl)-1H-pyrazole-3,5-dicarboxylate (77a). Synthesized according to General Procedure A but reversed limiting reagent. Dimethyl 1-benzyl-4-(2-oxoethyl)-1H-pyrazole-3,5-dicarboxylate (1.11 g, 3.53 mmol, 1.3 eq, 27), cyclopropyl(phenyl)methanamine hydrochloride (0.40 g, 2.72 mmol), AcOH (0.3 mL), 2-methylpyridine borane complex (0.44 g, 4.08 mmol, 1.5 equiv). Purified by flash column chromatography (silica, 24 g, 1:0 heptane/EtOAc to 0:1 heptane/EtOAc over 25 CV's) to give dimethyl 1-benzyl-4-(2-((cyclopropyl(phenyl)methyl)amino)ethyl)-1H-pyrazole-3,5-dicarboxylate (77a, 0.55 g, 1.23 mmol, 45% yield) as a yellow gum. ^1H NMR (400 MHz, CDCl_3) δ 7.32–7.16 (m, 10H), 5.77 (s, 2H), 3.92 (s, 3H), 3.76–3.70 (m, 3H), 3.28–3.14 (m, 2H), 2.91 (d, $J = 8.8$ Hz, 1H), 2.73–2.61 (m, 2H), 2.06 (s, 1H), 1.11–1.02 (m, 1H), 0.62–0.55 (m, 1H), 0.43–0.35 (m, 1H), 0.32–0.27 (m, 1H), 0.24–0.15 (m, 1H).

1-Benzyl-4-(2-((cyclopropyl(phenyl)methyl)amino)ethyl)-1H-pyrazole-3,5-dicarboxylic Acid (78a). Synthesized according to General Procedure B using dimethyl 1-benzyl-4-(2-((cyclopropyl(phenyl)methyl)amino)ethyl)-1H-pyrazole-3,5-dicarboxylate (0.55 g, 1.23 mmol) and $\text{LiOH}\cdot\text{H}_2\text{O}$ (0.26 g, 6.15 mmol, 5 equiv) to give 1-benzyl-4-(2-((cyclopropyl(phenyl)methyl)amino)ethyl)-1H-pyrazole-3,5-dicarboxylic acid (78a, 0.40 g, 0.95 mmol, 78% yield) as an off-white solid. ^1H NMR (400 MHz, $\text{DMSO}-d_6$) δ 12.92 (br s, 1H), 9.94 (br s, 1H), 7.46–7.17 (m, 10H), 5.83–5.63 (m, 2H), 3.56–3.46 (m, 1H), 3.23–3.20 (m, 2H), 3.12–3.00 (m, 1H), 2.96–2.81 (m, 1H), 1.30–1.15 (m, 1H), 0.70–0.50 (m, 1H), 0.45–0.34 (m, 1H), 0.19–0.09 (m, 1H), 0.01 to –0.18 (m, 1H). CH not observed as overlapping with HDO peak. X-Select LCMS BEH C_{18} 2.5 μm : Rt = 0.74 min; m/z 420.0 $[\text{M} + \text{H}]^+$.

2-Benzyl-6-(cyclopropyl(phenyl)methyl)-7-oxo-4,5,6,7-tetrahydro-2H-pyrazolo[3,4-c]pyridine-3-carboxamide (68). Synthesized according to General Procedure C using 1-benzyl-4-((cyclopropyl(phenyl)methyl)amino)ethyl)-1H-pyrazole-3,5-dicarboxylic acid (400 mg, 0.95 mmol), HOBt hydrate (142 mg, 1.04 mmol, 1.1 equiv), EDC·HCl (237 mg, 1.23 mmol, 1.3 equiv), DIPEA (0.40 mL, 2.38 mmol, 2.5 equiv) and NH₄Cl (254 mg, 4.75 mmol, 5 equiv). Purified by reverse-phase column chromatography (9:1 5 mM (NH₄)HCO₃ in water/MeCN to 0:1 5 mM (NH₄)HCO₃ in water/MeCN over 30 min) to afford *rac*-2-benzyl-6-(cyclopropyl(phenyl)methyl)-7-oxo-4,5,6,7-tetrahydro-2H-pyrazolo[3,4-c]pyridine-3-carboxamide (**68**) as a colorless solid. ¹H NMR (500 MHz, DMSO-*d*₆) δ 7.78 (s, 1H), 7.63 (s, 1H), 7.49–7.19 (m, 10H), 5.68–5.58 (m, 2H), 5.00–4.90 (m, 1H), 3.65–3.54 (m, 1H), 2.94–2.72 (m, 2H), 1.58–1.44 (m, 1H), 1.30–1.18 (m, 1H), 0.90–0.74 (m, 1H), 0.60–0.42 (m, 1H), 0.37–0.27 (m, 1H). 1H for CH₂ for one enantiomer not observed as overlapping with HDO peak. ACQUITY UPLC BEH C₁₈ 1.7 μm: Rt = 1.64 min, *m/z* 401.3 [M + H]⁺. HRMS calculated for C₂₄H₂₅N₄O₂: 401.1978, found: 401.1970 [M + H]⁺. ELSD/UV/¹H NMR purity: 100/96/98%.

(R)-2-Benzyl-6-(cyclopropyl(phenyl)methyl)-7-oxo-4,5,6,7-tetrahydro-2H-pyrazolo[3,4-c]pyridine-3-carboxamide (MDI-117740, 69). Racemate **68** was resolved by chiral separation (Daicel CHIRALPAK IG 250 mm × 4.6 mm, 5 μm, 7:3 0.1% DEA in *n*-hexane/1:1 DCM/MeOH, flow rate: 1 mL/min) to afford (R)-2-benzyl-6-(cyclopropyl(phenyl)methyl)-7-oxo-4,5,6,7-tetrahydro-2H-pyrazolo[3,4-c]pyridine-3-carboxamide (**69**, 130 mg, 0.32 mmol, 34% yield) as a colorless solid. m.p.: 203–205 °C. ¹H NMR (500 MHz, CDCl₃) δ 7.46–7.43 (m, 2H, H26,30), 7.33–7.30 (m, 2H, H16,20), 7.29–7.20 (m, 6H, H17–19, H27–29), 5.79–5.72 (m, 2H, H24), 5.43 (s, 2H, NH₂), 5.19 (d, *J* = 10.3 Hz, 1H, H14), 3.63–3.55 (m, 1H, HS'), 3.30–3.22 (m, 1H, HS), 2.82–2.70 (m, 2H, H4,4'), 1.32–1.23 (m, 1H, H21), 0.84–0.78 (m, 1H, H22'/23'), 0.65–0.58 (m, 1H, H22'/23'), 0.54–0.47 (m, 2H, H22',H23'). ¹³C{¹H} NMR (126 MHz, CDCl₃) δ 160.86 (C1/C10), 160.80 (C1/C10), 142.4 (C2), 140.3 (C15), 136.6 (C25), 130.7 (C9), 128.7 (C27,29), 128.6 (C17,19), 128.4 (C16,20), 128.2 (C18), 127.7 (C26,30), 127.5 (C28), 120.9 (C3), 59.8 (C14), 55.9 (C24), 42.5 (C5), 21.6 (C4), 12.4 (C21), 6.3 (C22/23), 3.5 (C22/23). Absolute stereochemistry confirmed by small X-ray crystal structure analysis. ACQUITY UPLC BEH C₁₈ 1.7 μm: Rt = 1.67 min; *m/z* 401.3 [M + H]⁺. HRMS calculated for C₂₄H₂₅N₄O₂: 401.1978, found: 401.1981 [M + H]⁺. ELSD/UV/¹H NMR purity: 100/94/96%.

(S)-2-Benzyl-6-(cyclopropyl(phenyl)methyl)-7-oxo-4,5,6,7-tetrahydro-2H-pyrazolo[3,4-c]pyridine-3-carboxamide (70). Synthesized according to the synthesis of **68** through separation of the other enantiomer to afford (S)-2-benzyl-6-(cyclopropyl(phenyl)methyl)-7-oxo-4,5,6,7-tetrahydro-2H-pyrazolo[3,4-c]pyridine-3-carboxamide (**70**, 20 mg, 0.05 mmol, 5% yield) as a colorless solid. m.p.: 204–205 °C; ¹H NMR (500 MHz, CDCl₃) δ 7.54–7.49 (m, 2H), 7.41–7.27 (m, 8H), 5.88–5.77 (m, 2H), 5.46 (s, 2H), 5.27 (d, *J* = 10.3 Hz, 1H), 3.70–3.61 (m, 1H), 3.38–3.29 (m, 1H), 2.91–2.76 (m, 2H), 1.38–1.29 (m, 1H), 0.93–0.84 (m, 1H), 0.73–0.64 (m, 1H), 0.63–0.52 (m, 2H). ¹³C{¹H} NMR (126 MHz, CDCl₃) δ 160.86 (Cq), 160.79 (Cq) 142.4 (Cq), 140.3 (Cq), 136.6 (Cq), 130.7 (Cq), 128.7 (CH), 128.6 (CH), 128.4 (CH), 128.2 (CH), 127.7 (CH), 127.5 (CH), 120.9 (Cq), 59.8 (CH), 55.9 (CH₂), 42.5 (CH₂), 21.5 (CH₂), 12.4 (CH), 6.3 (CH₂), 3.5 (CH₂). Absolute stereochemistry confirmed based on single X-ray structure analysis of **69**. ACQUITY UPLC BEH C₁₈ 1.7 μm: Rt = 1.66 min; *m/z* 401.3 [M + H]⁺. HRMS calculated for C₂₄H₂₅N₄O₂: 401.1978, found: 401.1982 [M + H]⁺. ELSD/UV/¹H NMR purity: 100/92/93%.

Dimethyl 1-Benzyl-4-(2-((cyclopropyl(2-((2-methoxyethyl)amino)phenyl)methyl)amino)ethyl)-1H-pyrazole-3,5-dicarboxylate (77b). Synthesized according to General Procedure A but reversed limiting reagent. Dimethyl 1-benzyl-4-(2-oxoethyl)-1H-pyrazole-3,5-dicarboxylate (0.55 g, 1.74 mmol, 1.1 equiv, **27**), 2-(amino(cyclopropyl)methyl)-*N*-(2-methoxyethyl)aniline (0.35 g, 1.59 mmol, **76**), AcOH (0.1 mL), 2-methylpyridine borane complex (0.19 g, 1.79 mmol, 1.2 equiv). Purified by flash column chromatography (silica, 12 g, 1:0 heptane/EtOAc to 7:3 heptane/EtOAc over 25 CV's) to give dimethyl 1-benzyl-4-(2-((cyclopropyl(2-((2-methoxyethyl)amino)-

phenyl)methyl)amino)ethyl)-1H-pyrazole-3,5-dicarboxylate (**77b**, 0.30 g, 0.58 mmol, 36% yield) as a yellow gum. X-Select LCMS BEH C₁₈ 2.5 μm: Rt = 1.95 min; *m/z* 521.5 [M + H]⁺.

1-Benzyl-4-(2-((cyclopropyl(2-((2-methoxyethyl)amino)phenyl)methyl)amino)ethyl)-1H-pyrazole-3,5-dicarboxylic acid (78b). Synthesized according to General Procedure B using dimethyl 1-benzyl-4-(2-((cyclopropyl(2-((2-methoxyethyl)amino)phenyl)methyl)amino)ethyl)-1H-pyrazole-3,5-dicarboxylate (300 mg, 0.58 mmol) and LiOH·H₂O (121 mg, 2.88 mmol, 5 equiv) to give 1-benzyl-4-(2-((cyclopropyl(2-((2-methoxyethyl)amino)phenyl)methyl)amino)ethyl)-1H-pyrazole-3,5-dicarboxylic acid (**78b**, 250 mg, 0.50 mmol, 88% yield) as an off-white solid. X-Select LCMS BEH C₁₈ 2.5 μm: Rt = 0.88 min; *m/z* 533.6 [M + MeCN]⁺.

2-Benzyl-6-(cyclopropyl(2-((2-methoxyethyl)amino)phenyl)methyl)-7-oxo-4,5,6,7-tetrahydro-2H-pyrazolo[3,4-c]pyridine-3-carboxamide (71). Synthesized through two-step telescope according to General Procedure C (for both steps) using 1-benzyl-4-(2-((cyclopropyl(2-((2-methoxyethyl)amino)phenyl)methyl)amino)ethyl)-1H-pyrazole-3,5-dicarboxylic acid (250 mg, 0.50 mmol), HOBt hydrate (75 mg, 0.55 mmol, 1.1 equiv), EDC·HCl (126 mg, 0.66 mmol, 1.3 equiv) and DIPEA (0.22 mL, 1.27 mmol, 2.4 equiv).

After cyclization in the first step, NH₄Cl (27 mg, 0.50 mmol, 5 equiv), HOBt hydrate (75 mg, 0.55 mmol, 1.1 equiv), EDC·HCl (126 mg, 0.66 mmol, 1.3 equiv) and DIPEA (0.22 mL, 1.27 mmol, 2.4 equiv) were added to the crude mixture. Purified by reverse-phase column chromatography (9:1 5 mM (NH₄)HCO₃ in water/MeCN to 0:1 5 mM (NH₄)HCO₃ in water/MeCN over 30 min) to give 2-benzyl-6-(cyclopropyl(2-((2-methoxyethyl)amino)phenyl)methyl)-7-oxo-4,5,6,7-tetrahydro-2H-pyrazolo[3,4-c]pyridine-3-carboxamide (**71**, 46 mg, 0.10 mmol, 19% yield) as a colorless solid. m.p.: 97–99 °C. ¹H NMR (500 MHz, CDCl₃) δ 7.80 (d, *J* = 7.9 Hz, 0.26H), 7.67 (d, *J* = 2.3 Hz, 0.80H), 7.53 (d, *J* = 8.0 Hz, 0.24H), 7.49 (d, *J* = 2.3 Hz, 0.85H), 7.47–7.44 (m, 0.21H), 7.39–7.35 (m, 2.48H), 7.31–7.22 (m, 5H), 5.79–5.63 (m, 2H), 5.28–5.22 (m, 1H), 4.06–3.98 (m, 0.40H), 3.94–3.85 (m, 1.87H), 3.78–3.68 (m, 0.74H), 3.62–3.52 (m, 0.93H), 3.42–3.28 (m, 2.49H), 3.24 (s, 2.33H), 3.20 (s, 0.73H), 2.86 (d, *J* = 12.6 Hz, 1.27H), 1.49–1.38 (m, 1H), 0.92–0.81 (m, 2H), 0.79–0.73 (m, 1H), 0.48–0.40 (m, 1H). Atropisomers observed in approximately 3:1 ratio. ¹³C{¹H} NMR (126 MHz, CDCl₃) δ 160.9 (Cq), 142.3 (Cq), 136.6 (Cq), 130.6 (Cq), 129.1 (CH), 128.7 (CH), 128.49 (CH), 128.47 (CH), 128.2 (CH), 121.0 (Cq), 70.9 (CH₂), 58.9 (CH₃), 56.3 (CH), 55.8 (CH₂), 42.1 (CH₂), 21.4 (CH₂), 12.6 (CH), 5.0 (CH₂), 4.8 (CH₂). CH₂ and 2 x Cq not observed. ACQUITY UPLC BEH C₁₈ 1.7 μm: Rt = 1.69 min; *m/z* 474.3 [M + H]⁺. HRMS calculated for C₂₇H₃₂N₅O₃: 474.2505, found: 474.2505 [M + H]⁺. ELSD/UV/¹H NMR purity: 100/93/92%.

Dimethyl 1-Benzyl-4-(2-((2-((tert-butoxycarbonyl)amino)-1-phenylethyl)amino)ethyl)-1H-pyrazole-3,5-dicarboxylate (77c). Synthesized according to General Procedure A using dimethyl 1-benzyl-4-(2-oxoethyl)-1H-pyrazole-3,5-dicarboxylate (0.40 g, 1.26 mmol, **27**), *tert*-butyl (2-amino-2-phenylethyl)carbamate (0.30 g, 1.26 mmol, 1 equiv), AcOH (0.1 mL) and 2-methylpyridine borane complex (0.14 g, 1.26 mmol, 1 equiv). Purified by flash column chromatography (silica, 12 g, 1:0 heptane/EtOAc to 6:4 heptane/EtOAc over 25 CV's) to give dimethyl 1-benzyl-4-(2-((2-((tert-butoxycarbonyl)amino)-1-phenylethyl)amino)ethyl)-1H-pyrazole-3,5-dicarboxylate (**77c**, 0.15 g, 0.27 mmol, 22% yield) as a pale-yellow gum. X-Select LCMS BEH C₁₈ 2.5 μm: Rt = 1.56 min; *m/z* 537.2 [M + H]⁺.

1-Benzyl-4-(2-((2-((tert-butoxycarbonyl)amino)-1-phenylethyl)amino)ethyl)-1H-pyrazole-3,5-dicarboxylic Acid (78c). Synthesized according to General Procedure B using dimethyl 1-benzyl-4-(2-((2-((tert-butoxycarbonyl)amino)-1-phenylethyl)amino)ethyl)-1H-pyrazole-3,5-dicarboxylate (150 mg, 0.27 mmol) and LiOH·H₂O (35 mg, 0.83 mmol, 3 equiv) to give 1-benzyl-4-(2-((2-((tert-butoxycarbonyl)amino)-1-phenylethyl)amino)ethyl)-1H-pyrazole-3,5-dicarboxylic acid (**78c**, 130 mg, 0.26 mmol, 91% yield) as an off-white solid. X-Select LCMS BEH C₁₈ 2.5 μm: Rt = 0.70 min; *m/z* 509.6 [M + H]⁺.

***tert*-Butyl (2-(2-Benzyl-3-carbamoyl-7-oxo-2,4,5,7-tetrahydro-6H-pyrazolo[3,4-c]pyridin-6-yl)-2-phenylethyl)carbamate (79).** Syn-

thesized through two-step telescope according to General Procedure C (for both steps) using 1-benzyl-4-(2-((*tert*-butoxycarbonyl)-amino)-1-phenylethyl)aminoethyl)-1*H*-pyrazole-3,5-dicarboxylic acid (130 mg, 0.25 mmol), HOBt hydrate (37 mg, 0.28 mmol, 1.1 equiv), EDC·HCl (63 mg, 0.33 mmol, 1.3 equiv) and DIPEA (0.11 mL, 0.61 mmol, 2.4 equiv).

After cyclization in the first step, NH₄Cl (68 mg, 1.27 mmol, 5 equiv), HOBt hydrate (37 mg, 0.28 mmol, 1.1 equiv), EDC·HCl (63 mg, 0.33 mmol, 1.3 equiv) and DIPEA (0.11 mL, 0.61 mmol, 2.4 equiv) were added to the crude mixture. Purified by reverse-phase column chromatography (9:1 5 mM (NH₄)HCO₃ in water/MeCN to 0:1 5 mM (NH₄)HCO₃ in water/MeCN over 30 min) to give *tert*-butyl (2-(2-benzyl-3-carbamoyl-7-oxo-2,4,5,7-tetrahydro-6*H*-pyrazolo[3,4-*c*]pyridin-6-yl)-2-phenylethyl)carbamate (**79**, 60 mg, 0.12 mmol, 48% yield) as a colorless solid. X-Select LCMS BEH C₁₈ 2.5 μm: Rt = 1.33 min; *m/z* 488.0 [M – H][–].

6-(2-Amino-1-phenylethyl)-2-benzyl-7-oxo-4,5,6,7-tetrahydro-2*H*-pyrazolo[3,4-*c*]pyridine-3-carboxamide Hydrochloride (80**).** To a stirred solution of *tert*-butyl (2-(2-benzyl-3-carbamoyl-7-oxo-2,4,5,7-tetrahydro-6*H*-pyrazolo[3,4-*c*]pyridin-6-yl)-2-phenylethyl)carbamate (50 mg, 0.12 mmol) in DCM (1 mL) was added 4 M HCl in 1,4 dioxane (1 mL). The reaction mixture was stirred at room temperature for 2 h. The reaction mixture was concentrated under reduced pressure to afford 6-(2-amino-1-phenylethyl)-2-benzyl-7-oxo-4,5,6,7-tetrahydro-2*H*-pyrazolo[3,4-*c*]pyridine-3-carboxamide (**80**, 50 mg, 0.12 mmol) as a crude off-white solid, which was taken forward to the next step.

***N*-(2-(2-Benzyl-3-carbamoyl-7-oxo-2,4,5,7-tetrahydro-6*H*-pyrazolo[3,4-*c*]pyridin-6-yl)-2-phenylethyl)thiazole-5-carboxamide (**72**).** Synthesized according to General Procedure C using 6-(2-amino-1-phenylethyl)-2-benzyl-7-oxo-4,5,6,7-tetrahydro-2*H*-pyrazolo[3,4-*c*]pyridine-3-carboxamide hydrochloride (50 mg, 0.12 mmol), thiazole-5-carboxylic acid (16 mg, 0.12 mmol, 1 equiv), HOBt hydrate (19 mg, 0.14 mmol, 1.1 equiv), EDC·HCl (31 mg, 0.16 mmol, 1.3 equiv) and DIPEA (66 μL, 0.38 mmol, 2.4 equiv). Purified by reverse-phase column chromatography (9:1 5 mM (NH₄)HCO₃ in water/MeCN to 0:1 5 mM (NH₄)HCO₃ in water/MeCN over 30 min) to give *N*-(2-(2-benzyl-3-carbamoyl-7-oxo-2,4,5,7-tetrahydro-6*H*-pyrazolo[3,4-*c*]pyridin-6-yl)-2-phenylethyl)thiazole-5-carboxamide (**72**, 27 mg, 0.05 mmol, 42% yield) as an off-white solid. m.p.: 143–145 °C. ¹H NMR (500 MHz, DMSO-*d*₆) δ 9.20 (d, *J* = 0.7 Hz, 1H), 8.89 (t, *J* = 5.9 Hz, 1H), 8.36 (d, *J* = 0.7 Hz, 1H), 7.74 (s, 1H), 7.61 (s, 1H), 7.35–7.41 (m, 4H), 7.29–7.33 (m, 3H), 7.25–7.28 (m, 1H), 7.17–7.20 (m, 2H), 6.05 (t, *J* = 7.6 Hz, 1H), 5.65 (d, *J* = 14.6 Hz, 1H), 5.57 (d, *J* = 14.7 Hz, 1H), 3.91 (dd, *J* = 7.7, 5.9 Hz, 2H), 3.61 (ddd, *J* = 13.0, 8.4, 5.1 Hz, 1H), 3.09 (ddd, *J* = 12.5, 7.3, 5.3 Hz, 1H), 2.84 (ddd, *J* = 15.9, 7.3, 5.1 Hz), 2.70 (ddd, *J* = 15.8, 8.4, 5.2 Hz, 1H). ¹³C{¹H} NMR (126 MHz, DMSO-*d*₆) δ 161.0 (Cq), 160.3 (Cq), 160.0 (Cq), 157.9 (CH), 143.6 (CH), 141.5 (Cq), 138.2 (Cq), 137.1 (Cq), 135.3 (Cq), 132.8 (Cq), 128.6 (CH), 128.5 (CH), 127.69 (CH), 127.67 (CH), 127.5 (CH), 120.6 (Cq), 54.1 (CH₂), 53.7 (CH), 42.0 (CH₂), 38.8 (CH₂), 20.1 (CH₂). ACQUITY UPLC BEH C₁₈ 1.7 μm: Rt = 1.50 min; *m/z* 501.3 [M + H]⁺. HRMS calculated for C₂₆H₂₅N₆O₃S: 501.1709, found: 501.1708 [M + H]⁺. ELSD/UV/¹H NMR purity: 100/88/96%.

2,6-Dibenzyl-7-oxo-4,5,6,7-tetrahydro-2*H*-pyrazolo[3,4-*c*]pyridine-3-carboxylic Acid (81**).** Synthesized according to General Procedure B using methyl 2,6-dibenzyl-7-oxo-4,5,6,7-tetrahydro-2*H*-pyrazolo[3,4-*c*]pyridine-3-carboxylate (0.80 g, 2.13 mmol, **55**) and LiOH·H₂O (0.27 g, 6.39 mmol, 3 equiv). The reaction mixture was concentrated under reduced pressure, diluted with water (10 mL) and acidified with 1 M HCl. The aqueous layer was extracted with EtOAc (2 × 20 mL). The organic layers were combined, dried over NaSO₄ and concentrated under reduced pressure. The crude mixture was purified by reverse-phase column chromatography (9:1 0.1% TFA in water/MeCN to 0:1 0.1% TFA in water/MeCN over 30 min) to afford 2,6-dibenzyl-7-oxo-4,5,6,7-tetrahydro-2*H*-pyrazolo[3,4-*c*]pyridine-3-carboxylic acid (**81**, 130 mg, 0.36 mmol, 17% yield) as an off-white solid. m.p.: 86–88 °C (dec). ¹H NMR (500 MHz, DMSO-*d*₆) δ 13.72 (br s, 1H), 7.37–7.16 (m, 10H), 5.78 (s, 2H), 4.66 (s, 2H), 2.97 (t, *J* = 6.7 Hz, 2H). CH₂ not observed as overlapping with HDO peak. ¹³C{¹H} NMR (126 MHz, DMSO-*d*₆) δ 160.5 (Cq), 159.7 (Cq), 141.8 (Cq),

137.6 (Cq), 137.1 (Cq), 129.0 (Cq), 128.6 (CH), 127.64 (CH), 127.60 (CH), 127.3 (CH), 127.2 (CH), 125.6 (Cq), 54.8 (CH₂), 48.9 (CH₂), 46.7 (CH₂), 20.7 (CH₂). ACQUITY UPLC BEH C₁₈ 1.7 μm: Rt = 1.61 min; *m/z* 362.2 [M + H]⁺. HRMS calculated for C₂₁H₂₀N₂O₃, 362.1505, found 362.1520 [M + H]⁺. ELSD/UV/¹H NMR purity: 100/91/95%.

2,6-Dibenzyl-*N*-methyl-7-oxo-4,5,6,7-tetrahydro-2*H*-pyrazolo[3,4-*c*]pyridine-3-carboxamide (82**).** To a solution of 2,6-dibenzyl-7-oxo-4,5,6,7-tetrahydro-2*H*-pyrazolo[3,4-*c*]pyridine-3-carboxylic acid (100 mg, 0.27 mmol) in THF (1 mL) were added DIPEA (0.12 mL, 0.69 mmol) and T3P (50% in EtOAc, 0.53 g, 0.83 mmol). The reaction mixture was stirred at room temperature for 10 min, followed by addition of CH₃NH₂ (2 M in THF, 0.2 mL, 0.41 mmol) and further stirred at room temperature overnight. The reaction mixture was diluted with water (25 mL) and extracted with EtOAc (2 × 25 mL). The organic layers were combined, dried over NaSO₄, filtered and concentrated under reduced pressure. The crude mixture was purified by reverse-phase column chromatography (9:1 0.1% TFA in water/MeCN to 0:1 0.1% TFA in water/MeCN over 30 min). Fractions containing product were combined and concentrated under reduced pressure to afford 2,6-dibenzyl-*N*-methyl-7-oxo-4,5,6,7-tetrahydro-2*H*-pyrazolo[3,4-*c*]pyridine-3-carboxamide (**82**, 5 mg, 0.01 mmol, 5% yield) as an off-white solid. ¹H NMR (500 MHz, DMSO-*d*₆) δ 8.16 (q, *J* = 4.5 Hz, 1H), 7.37–7.21 (m, 10H), 5.61 (s, 2H), 4.65 (s, 2H), 3.48 (t, *J* = 6.7 Hz, 2H), 2.86 (t, *J* = 6.7 Hz, 2H), 2.74 (d, *J* = 4.6 Hz, 3H). ACQUITY UPLC BEH C₁₈ 1.7 μm: Rt = 1.59 min; *m/z* 375.3 [M + H]⁺. ELSD/UV/¹H NMR purity: 100/43/92%.

2,6-Dibenzyl-*N*-cyclopropyl-7-oxo-4,5,6,7-tetrahydro-2*H*-pyrazolo[3,4-*c*]pyridine-3-carboxamide (83**).** Synthesized according to General Procedure C using 2,6-dibenzyl-7-oxo-4,5,6,7-tetrahydro-2*H*-pyrazolo[3,4-*c*]pyridine-3-carboxylic acid (100 mg, 0.27 mmol), HOBt hydrate (10 mg, 0.30 mmol, 1.1 equiv), EDC·HCl (69 mg, 0.36 mmol, 1.3 equiv), DIPEA (0.12 mL, 0.69 mmol, 2.4 equiv) and cyclopropylamine (24 μL, 0.36 mmol, 1.3 equiv). Purified by reverse-phase column chromatography (9:1 0.1% TFA in water/MeCN to 0:1 0.1% TFA in water/MeCN over 30 min) to give 2,6-dibenzyl-*N*-cyclopropyl-7-oxo-4,5,6,7-tetrahydro-2*H*-pyrazolo[3,4-*c*]pyridine-3-carboxamide (**83**, 20 mg, 0.05 mmol, 18% yield) as an off-white solid. m.p.: 138–140 °C. ¹H NMR (500 MHz, CDCl₃) δ 8.31 (d, *J* = 4.1 Hz, 1H), 7.38–7.20 (m, 10H), 5.58 (s, 2H), 4.64 (s, 2H), 3.46 (t, *J* = 6.7 Hz, 2H), 2.83–2.72 (m, 3H), 0.73–0.65 (m, 2H), 0.51–0.41 (m, 2H). ¹³C{¹H} NMR (126 MHz, DMSO-*d*₆) δ 160.6 (Cq), 160.0 (Cq), 141.3 (Cq), 137.8 (Cq), 136.9 (Cq), 133.1 (Cq), 128.5 (CH), 127.83 (CH), 127.80 (CH), 127.5 (CH), 127.2 (CH), 120.5 (Cq), 54.1 (CH₂), 48.7 (CH₂), 46.8 (CH₂), 22.6 (CH), 19.8 (CH), 5.8 (CH₂). ACQUITY UPLC BEH C₁₈ 1.7 μm: Rt = 1.66 min; *m/z* 401.3 [M + H]⁺. HRMS calculated for C₂₄H₂₅N₄O₂: 401.1978, found: 401.1980 [M + H]⁺. ELSD/UV/¹H NMR purity: 100/100/100%.

2,6-Dibenzyl-7-oxo-*N*-phenyl-4,5,6,7-tetrahydro-2*H*-pyrazolo[3,4-*c*]pyridine-3-carboxamide (84**).** Synthesized according to General Procedure C using 2,6-dibenzyl-7-oxo-4,5,6,7-tetrahydro-2*H*-pyrazolo[3,4-*c*]pyridine-3-carboxylic acid (100 mg, 0.27 mmol), HOBt hydrate (40 mg, 0.30 mmol, 1.1 equiv), EDC·HCl (69 mg, 0.36 mmol, 1.3 equiv), DIPEA (0.12 mL, 0.69 mmol, 2.4 equiv) and aniline (37 μL, 0.41 mmol, 1.5 equiv). Purified by flash column chromatography (silica, 4 g, 1:0 DCM/MeOH to 9:1 DCM/MeOH over 25 CV's) to give 2,6-dibenzyl-7-oxo-*N*-phenyl-4,5,6,7-tetrahydro-2*H*-pyrazolo[3,4-*c*]pyridine-3-carboxamide (**84**, 18 mg, 0.04 mmol, 15% yield) as an off-white solid. m.p.: 174–175 °C. ¹H NMR (500 MHz, DMSO-*d*₆) δ 10.32–10.10 (m, 1H), 7.71–7.53 (m, 2H), 7.44–7.02 (m, 13H), 5.68–5.53 (m, 2H), 4.75–4.56 (m, 2H), 3.63–3.40 (m, 2H), 3.00–2.81 (m, 2H). ¹³C{¹H} NMR (126 MHz, DMSO-*d*₆) δ 159.9 (Cq), 157.9 (Cq), 141.5 (Cq), 138.2 (Cq), 137.8 (Cq), 136.8 (Cq), 133.3 (Cq), 128.9 (CH), 128.60 (CH), 128.55 (CH), 127.9 (CH), 127.8 (CH), 127.6 (CH), 127.2 (CH), 124.4 (CH), 121.2 (Cq), 120.1 (CH), 54.2 (CH₂), 48.8 (CH₂), 46.8 (CH₂), 19.9 (CH₂). ACQUITY UPLC BEH C₁₈ 1.7 μm: Rt = 1.80 min; *m/z* 437.3 [M + H]⁺. HRMS calculated for C₂₇H₂₅N₄O₂: 437.1978, found: 437.1980 [M + H]⁺. ELSD/UV/¹H NMR purity: 100/97/98%.

2,6-Dibenzyl-N-(2-methoxyethyl)-7-oxo-4,5,6,7-tetrahydro-2H-pyrazolo[3,4-c]pyridine-3-carboxamide (85). To a solution of 2,6-dibenzyl-7-oxo-4,5,6,7-tetrahydro-2H-pyrazolo[3,4-c]pyridine-3-carboxylic acid (100 mg, 0.27 mmol) in DCM (2 mL) were added DIPEA (0.12 mL, 0.69 mmol) and T3P (50% in EtOAc, 0.53 g, 0.83 mmol). The reaction mixture was stirred at room temperature for 10 min, followed by addition of 2-methoxyethylamine (36 μ L, 0.41 mmol) and further stirred at room temperature overnight. The reaction mixture was diluted with water (2 mL) and extracted with DCM (2 \times 5 mL). The organic layers were combined, dried over NaSO₄, filtered and concentrated under reduced pressure. The crude mixture was purified by reverse-phase column chromatography (9:1 0.1% TFA in water/MeCN to 0:1 0.1% TFA in water/MeCN over 30 min). Fractions containing product were combined and concentrated under reduced pressure to afford 2,6-dibenzyl-N-(2-methoxyethyl)-7-oxo-4,5,6,7-tetrahydro-2H-pyrazolo[3,4-c]pyridine-3-carboxamide (**85**, 40 mg, 0.10 mmol, 35% yield) as an off-white solid. m.p.: 92–94 °C. ¹H NMR (500 MHz, DMSO-*d*₆) δ 8.33 (t, *J* = 5.1 Hz, 1H), 7.36–7.22 (m, 10H), 5.59 (s, 2H), 4.65 (s, 2H), 3.48 (t, *J* = 6.7 Hz, 2H), 3.39–3.37 (m, 2H), 3.23 (s, 3H), 2.84 (t, *J* = 6.7 Hz, 2H). CH₂ not observed as overlapping with HDO peak. ¹³C{¹H} NMR (126 MHz, DMSO-*d*₆) δ 160.0 (Cq), 159.5 (Cq), 141.4 (Cq), 137.8 (Cq), 137.0 (Cq), 133.2 (Cq), 128.54 (CH), 128.52 (CH), 127.9 (CH), 127.8 (CH), 127.6 (CH), 127.2 (CH), 120.5 (Cq), 70.2 (CH₂), 57.9 (CH₃), 54.1 (CH₂), 48.8 (CH₂), 46.8 (CH₂), 38.7 (CH₂), 19.8 (CH₂). ACQUITY UPLC BEH C₁₈ 1.7 μ m: Rt = 1.63 min; *m/z* 419.3 [M + H]⁺. HRMS calculated for C₂₄H₂₇N₄O₃: 419.2085, found: 419.2083 [M + H]⁺. ELSD/UV/¹H NMR purity: 98/92/94%.

2,6-Dibenzyl-N-(2-(dimethylamino)ethyl)-7-oxo-4,5,6,7-tetrahydro-2H-pyrazolo[3,4-c]pyridine-3-carboxamide (86). To a solution of 2,6-dibenzyl-7-oxo-4,5,6,7-tetrahydro-2H-pyrazolo[3,4-c]pyridine-3-carboxylic acid (0.15 g, 0.41 mmol) in DCM (1 mL) were added DIPEA (0.18 mL, 1.03 mmol) and T3P (50% in EtOAc, 0.40 g, 1.24 mmol). The reaction mixture was stirred at room temperature for 10 min, followed by addition of *N,N*-dimethylethylenediamine (67 μ L, 0.62 mmol) and further stirred at room temperature overnight. The reaction mixture was diluted with water (2 mL) and extracted with DCM (2 \times 5 mL). The organic layers were combined, dried over NaSO₄, filtered and concentrated under reduced pressure. The crude mixture was purified by reverse-phase column chromatography (9:1 5 mM (NH₄)HCO₃ in water/MeCN to 0:1 5 mM (NH₄)HCO₃ in water/MeCN over 30 min). Fractions containing product were combined and concentrated under reduced pressure to afford 2,6-dibenzyl-N-(2-(dimethylamino)ethyl)-7-oxo-4,5,6,7-tetrahydro-2H-pyrazolo[3,4-c]pyridine-3-carboxamide (**86**, 15 mg, 0.03 mmol, 8% yield) as an off-white solid. ¹H NMR (500 MHz, DMSO-*d*₆) δ 8.17 (t, *J* = 5.8 Hz, 1H), 7.37–7.22 (m, 10H), 5.59 (s, 2H), 4.65 (s, 2H), 3.48 (t, *J* = 6.6 Hz, 2H), 2.85 (t, *J* = 6.7 Hz, 2H), 2.31 (t, *J* = 6.6 Hz, 2H), 2.13 (s, 6H). CH₂ not observed as overlapping with HDO peak. ¹³C{¹H} NMR (126 MHz, DMSO-*d*₆) δ 160.0 (Cq), 159.3 (Cq), 141.4 (Cq), 137.8 (Cq), 137.0 (Cq), 133.2 (Cq), 128.54 (CH), 128.51 (CH), 127.9 (CH), 127.8 (CH), 127.6 (CH), 127.2 (CH), 120.4 (Cq), 57.8 (CH₂), 54.1 (CH₂), 48.8 (CH₂), 46.8 (CH₂), 45.1 (CH₃), 37.0 (CH₂), 19.8 (CH₂). ACQUITY UPLC BEH C₁₈ 1.7 μ m: Rt = 1.31 min; *m/z* 432.3 [M + H]⁺. HRMS calculated for C₂₅H₃₀N₅O₂: 432.2400, found: 432.2406 [M + H]⁺. ELSD/UV/¹H NMR purity: 100/91/97%. ELSD/UV/¹H NMR purity: 96/96/97%.

2,6-Dibenzyl-7-oxo-4,5,6,7-tetrahydro-2H-pyrazolo[3,4-c]pyridine-3-carbohydrazide (87). To a solution of methyl 2,6-dibenzyl-7-oxo-4,5,6,7-tetrahydro-2H-pyrazolo[3,4-c]pyridine-3-carboxylate (250 mg, 0.66 mmol) in EtOH (5 mL) was added NH₂NH₂ (50% in H₂O, 1 mL). The reaction mixture was heated to 90 °C and stirred for 6 h. The reaction mixture was cooled to room temperature and concentrated under reduced pressure to afford 2,6-dibenzyl-7-oxo-4,5,6,7-tetrahydro-2H-pyrazolo[3,4-c]pyridine-3-carbohydrazide (**87**, 300 mg, 0.80 mmol) as a crude yellow gum, which was taken forward as crude to the next step.

2,6-Dibenzyl-3-(1,3,4-oxadiazol-2-yl)-2,4,5,6-tetrahydro-7H-pyrazolo[3,4-c]pyridin-7-one (89). 2,6-dibenzyl-7-oxo-4,5,6,7-tetrahydro-2H-pyrazolo[3,4-c]pyridine-3-carbohydrazide (300 mg, 0.80

mmol) was added to triethyl orthoformate (5 mL) and the reaction mixture heated to 100 °C and stirred overnight. The reaction mixture was cooled to room temperature and concentrated under reduced pressure. The crude mixture was purified by reverse-phase column chromatography (9:1 5 mM (NH₄)HCO₃ in water/MeCN to 0:1 5 mM (NH₄)HCO₃ in water/MeCN over 30 min). Fractions containing product were combined and concentrated under reduced pressure to afford 2,6-dibenzyl-3-(1,3,4-oxadiazol-2-yl)-2,4,5,6-tetrahydro-7H-pyrazolo[3,4-c]pyridin-7-one (**89**, 42 mg, 0.11 mmol, 7% yield) as an off-white solid. m.p.: 150–152 °C. ¹H NMR (500 MHz, CDCl₃) δ 8.45 (s, 1H), 7.44–7.41 (m, 2H), 7.35–7.33 (m, 4H), 7.32–7.23 (m, 4H), 5.98 (s, 2H), 4.81 (s, 2H), 3.55 (t, *J* = 6.7 Hz, 2H), 3.05 (t, *J* = 6.7 Hz, 2H). ¹³C{¹H} NMR (126 MHz, CDCl₃) δ 160.6 (Cq), 157.0 (Cq), 152.1 (CH), 143.4 (Cq), 137.2 (Cq), 135.6 (Cq), 128.9 (CH), 128.8 (CH), 128.34 (CH), 128.33 (CH), 127.8 (CH), 123.7 (Cq), 123.1 (Cq), 56.2 (CH₂), 49.8 (CH₂), 46.7 (CH₂), 20.8 (CH₂). ACQUITY UPLC BEH C₁₈ 1.7 μ m: Rt = 1.68 min; *m/z* 386.3 [M + H]⁺. HRMS calculated for C₂₂H₂₀N₅O₂: 386.1617, found: 386.1619 [M + H]⁺. ELSD/UV/¹H NMR purity: 100/91/97%.

2,6-Dibenzyl-N-(2-hydroxyethyl)-7-oxo-4,5,6,7-tetrahydro-2H-pyrazolo[3,4-c]pyridine-3-carboxamide (88). To a solution of methyl 2,6-dibenzyl-7-oxo-4,5,6,7-tetrahydro-2H-pyrazolo[3,4-c]pyridine-3-carboxylate (200 mg, 0.52 mmol) and ethanolamine (0.16 mL, 2.66 mmol) in MeOH (10 mL) was added DIPEA (0.28 mL, 1.58 mmol). The reaction mixture was heated to 130 °C and stirred overnight in a sealed tube. The reaction mixture was cooled, concentrated under reduced pressure, diluted with water (5 mL) and extracted with EtOAc (2 \times 10 mL). The organic layers were combined, dried over NaSO₄, filtered and concentrated under reduced pressure. The crude mixture was purified by flash column chromatography (silica, 12 g, 1:0 heptane/EtOAc to 7:3 heptane/EtOAc over 25 CV's). Fractions containing product were combined and concentrated under reduced pressure to afford 2,6-dibenzyl-N-(2-hydroxyethyl)-7-oxo-4,5,6,7-tetrahydro-2H-pyrazolo[3,4-c]pyridine-3-carboxamide (**88**, 160 mg, 0.40 mmol, 86% yield) as a pale yellow solid. m.p.: 140–142 °C. ¹H NMR (500 MHz, DMSO-*d*₆) δ 8.21 (t, *J* = 5.7 Hz, 1H), 7.39–7.22 (m, 10H), 5.59 (s, 2H), 4.73–4.70 (m, 1H), 4.65 (s, 2H), 3.51–3.42 (m, 4H), 3.28 (q, *J* = 6.0 Hz, 2H), 2.86 (t, *J* = 6.6 Hz, 2H). ¹³C{¹H} NMR (126 MHz, DMSO-*d*₆) δ 160.0 (Cq), 159.5 (Cq), 141.4 (Cq), 137.8 (Cq), 137.0 (Cq), 133.2 (Cq), 128.54 (CH), 128.51 (CH), 127.9 (CH), 127.8 (CH), 127.6 (CH), 127.2 (CH), 120.4 (Cq), 59.4 (CH₂), 54.1 (CH₂), 48.8 (CH₂), 46.8 (CH₂), 41.8 (CH₂), 19.9 (CH₂). ACQUITY UPLC BEH C₁₈ 1.7 μ m: Rt = 1.50 min; *m/z* 405.3 [M + H]⁺. HRMS calculated for C₂₃H₂₅N₄O₃: 405.1927, found: 405.1929 [M + H]⁺. ELSD/UV/¹H NMR purity: 100/88/99%.

2,6-Dibenzyl-3-(4,5-dihydrooxazol-2-yl)-2,4,5,6-tetrahydro-7H-pyrazolo[3,4-c]pyridin-7-one (90). To a stirred solution of 2,6-dibenzyl-N-(2-hydroxyethyl)-7-oxo-4,5,6,7-tetrahydro-2H-pyrazolo[3,4-c]pyridine-3-carboxamide (150 mg, 0.37 mmol) in toluene (2 mL) was added PPh₃ (146 mg, 0.55 mmol) and DEAD (97 mg, 0.55 mmol). The reaction mixture was stirred at room temperature overnight. The reaction mixture was concentrated under reduced pressure. The crude mixture was diluted with ice-cold water (2 mL) and extracted with EtOAc (2 \times 5 mL). The organic layers were combined, dried over NaSO₄, filtered and concentrated under reduced pressure. The crude mixture was purified by reverse-phase column chromatography (9:1 5 mM (NH₄)HCO₃ in water/MeCN to 0:1 5 mM (NH₄)HCO₃ in water/MeCN over 30 min). Fractions containing product were combined and concentrated under reduced pressure to afford 2,6-dibenzyl-3-(4,5-dihydrooxazol-2-yl)-2,4,5,6-tetrahydro-7H-pyrazolo[3,4-c]pyridin-7-one (**90**, 7 mg, 0.02 mmol, 4%) as an off-white solid. ¹H NMR (500 MHz, DMSO-*d*₆) δ 7.37–7.23 (m, 8H), 7.22–7.18 (m, 2H), 5.87 (s, 2H), 4.65 (s, 2H), 4.36 (t, *J* = 9.6 Hz, 2H), 3.98 (t, *J* = 9.6 Hz, 2H), 3.50 (t, *J* = 6.7 Hz, 2H), 2.95 (t, *J* = 6.7 Hz, 2H). ACQUITY UPLC BEH C₁₈ 1.7 μ m: Rt = 1.77 min; *m/z* 387.3 [M + H]⁺. ELSD/UV/¹H NMR purity: 100/100/96%.

2,6-Dibenzyl-7-oxo-4,5,6,7-tetrahydro-2H-pyrazolo[3,4-c]pyridine-3-carbonitrile (91). To a stirred solution of 2,6-dibenzyl-7-oxo-4,5,6,7-tetrahydro-2H-pyrazolo[3,4-c]pyridine-3-carboxamide (50 mg, 0.13 mmol) in DCM (3 mL) was added Et₃N (1.35 mL, 0.97

mmol) and trifluoroacetic anhydride (96 μ L, 0.69 mmol). The reaction mixture was stirred at room temperature overnight. The reaction mixture was concentrated under reduced pressure. The crude mixture was diluted with water (1 mL) and extracted with DCM (2 \times 2 mL). The organic layers were combined, dried over NaSO₄, filtered and concentrated under reduced pressure. The crude mixture was purified by reverse-phase column chromatography (9:1 5 mM (NH₄)HCO₃ in water/MeCN to 0:1 5 mM (NH₄)HCO₃ in water/MeCN over 30 min). Fractions containing product were combined and concentrated under reduced pressure to afford 2,6-dibenzyl-7-oxo-4,5,6,7-tetrahydro-2H-pyrazolo[3,4-c]pyridine-3-carbonitrile (**91**, 19 mg, 0.01 mmol, 40%) as an off-white solid. m.p.: 105–106 °C. ¹H NMR (500 MHz, CDCl₃) δ 7.44–7.41 (m, 2H), 7.39–7.27 (m, 8H), 5.52 (s, 2H), 4.76 (s, 2H), 3.51 (dd, J = 7.0, 6.4 Hz, 2H), 2.86 (t, J = 6.7 Hz, 2H). ¹³C{¹H} NMR (126 MHz, CDCl₃) δ 159.8 (Cq), 143.2 (Cq), 136.9 (Cq), 134.2 (Cq), 129.2 (CH), 129.1 (CH), 128.9 (CH), 128.6 (CH), 128.3 (CH), 127.9 (CH), 111.8 (Cq), 109.8 (Cq), 56.8 (CH₂), 49.8 (CH₂), 46.4 (CH₂), 19.8 (CH₂). Cq not observed. ACQUITY UPLC BEH C₁₈ 1.7 μ m: Rt = 1.77 min; m/z 343.2 [M + H]⁺. HRMS calculated for C₂₁H₁₉N₄O: 343.1559, found: 343.1564 [M + H]⁺. ELSD/UV/¹H NMR purity: 100/92/100%.

Molecular Docking. The predicted binding mode of MDI-117740 (**69**) was derived using a truncated version of chain A from protein structure 7ATU using Schrodinger software (Schrodinger, Inc., NY 10036). Although docking took a core constraint based on reference ligand LIJTFS00025 (**7**) into consideration, no fixed constraints, features or voids were imposed. The system was then minimized to give the final pose.

Cell Lines and Growth Conditions. HEK293 and SH-SY5Y cells used in this study were purchased from Sigma/Merck (Dorset, U.K.) and were cultured in Dulbecco's Modified Eagle's Medium (DMEM)/F12 (#11320033, Thermofisher Scientific, U.K.), supplemented with 10% fetal calf serum, 1% penicillin/streptomycin (Sigma-Aldrich, Dorset U.K.). MDA-MB-231 (human breast adenocarcinoma TNBC) cells were purchased from the American Type Culture Collection (ATCC, Virginia) and were cultured in DMEM containing sodium pyruvate (#11574446, Gibco, Fisher Scientific, U.K.). Cells were cultured in a standard T75 tissue-culture treated flask at 37 °C, 5% CO₂ in a humidified sterile incubator. HEK293, SH-SY5Y and MDA-MB-231 cell lines used in this study were not obtained from animal or human participants and did not require ethical approval or informed consent.

RapidFire Mass Spectrometry (RF-MS) Kinase Assays. A 50 μ L reaction was prepared in 384-well polypropylene plates. First, compounds were transferred in duplicate in a 16-point 2-fold serial dilution in DMSO (maximum inhibitor concentration of 40 μ M in the LIMK1/2 assay) using an ECHO 550 acoustic dispenser (Labcyte). To these plates, 25 μ L of 80 nM LIMK1_{330–637} (for a final concentration of 40 nM) or 30 nM LIMK2_{347–659} (final concentration of 15 nM) in assay buffer was dispensed into each well using a COMBI multidrop dispenser and the plates were incubated for 45 min at room temperature. Then, 25 μ L of 8 μ M CFL1 (for a final concentration of 4 μ M) and 4 mM ATP (final concentration 2 mM) in assay buffer was added to each well and incubated for 105 and 180 min for LIMK1 and LIMK2, respectively. The composition of the assay buffer used for LIMK1 was 50 mM tris pH 7.5, 0.1 mM EDTA, 0.1 mM EGTA, 1 mM MgCl₂, while that of the assay buffer used for LIMK2 was 50 mM HEPES pH 7.5, 0.1 mM EGTA, 1 mM EDTA, and 1 mM MnCl₂.

The LIMK phosphorylation reactions were halted by the addition of 5 μ L of 10% formic acid (final concentration of 1%), and the assay plates were transferred onto a RapidFire RF360 instrument (Agilent). Once loaded, the samples were aspirated under vacuum and the salts and the nonvolatile buffer components were removed by loading onto a C4 solid-phase extraction (SPE) cartridge (Agilent Technologies) in 0.1% formic acid in water at a flow rate of 1.5 mL/min. Elution using 85% acetonitrile and 0.1% formic acid was then used to elute analytes into the mass spectrometer (Agilent 6530 QTOF) at a flow rate of 1.2 mL/min. The resulting data were analyzed using RapidFire integrator software (Agilent), and GraphPad Prism 7 was used to calculate IC₅₀ values.

Transient Transfection of HEK293 Cells. The transfection reagent mix of 1.25 mL Opti-MEM without phenol red (Fisher Life Technologies, U.K.) and 1.25 μ g NanoLuc LIMK1 or LIMK2 kinase fusion vector, 11.25 μ g transfection carrier DNA and 37.5 μ L FuGENE HD transfection reagent (all Promega, Hampshire, U.K.) was prepared according to manufacturer's protocol. HEK293 cells were resuspended in 5 mL growth media following trypsinization, neutralization and sedimentation. Cell density was calculated and adjusted to 1×10^5 cells/mL for each transfection of either LIMK1 or LIMK2 in 25 mL growth media. The transfection mix was added directly to cells and mixed gently *via* inversion. Cells were then plated into T75 tissue culture flasks and incubated for 20 h at 37 °C, 5% CO₂.

Cellular NanoBRET LIMK1/2 Assay. The NanoBRET cellular target engagement assay was performed as previously described.²⁹ Briefly, white 96-well plates containing LIMK1/2 transfected HEK293 cells and extracellular NanoLuc inhibitor was added either positive control (NanoBRET Tracer #10), negative control (DMSO) or test compound (8-point dose–response curve in DMSO in duplicate, final concentration of 0.5% for control wells). Following incubation of plates under standard conditions (37 °C, 5% CO₂) for 2 h, plates were removed and allowed to reach RT for 15 min. Freshly prepared Nano-Glo substrate was then added to each well and luminescence measured using dual emission for the donor at 450 nm and the acceptor 610 nm on a BMG Pherastar plate reader. Kit components were purchased from Promega (Hampshire, U.K.).

AlphaLISA SureFire Assay. The AlphaLISA assay for detection of p-cofilin Ser3 levels was followed as previously described.²⁹ Briefly, 96-well plates containing SH-SY5Y cells was added either positive control (LIMKi3, 10 μ M), negative control (0.5% DMSO) or test compound (8-point, 3-fold serial dilution in DMSO from 10 μ M to 30 nM in duplicate). Cells were placed in the incubator for 2 h, after which the media was removed and the cells were lysed using 50 μ L AlphaLISA 1 \times lysis buffer (PerkinElmer) containing protease inhibitor cocktail (Sigma/Merck, Dorset, U.K.) and Pierce phosphatase inhibitor cocktail (ThermoFisher Scientific, U.K.). The cell lysate was then transferred to a clean, flat-bottom, white 384-well plate, to which 5 μ L/well of acceptor bead solution consisting of Reaction buffer 1, Reaction buffer 2, Activation Buffer and Acceptor Beads from pCofilin SureFire Ultra assay kit (PerkinElmer, Cat# ALSU-PCOF-A500) was added under dim light. After plate shaking for 2 min at 450 rpm, centrifuged briefly and incubation at RT for 1 h, 5 μ L/well of donor solution consisting of Dilution Buffer and Donor beads was added. The plate was read on a Pherastar reader (BMD Labtech Ltd., Aylesbury, U.K.) using an AlphaLISA cartridge and AlphaLISA plate settings. The AlphaLISA assay was robust and reproducible (Z' = 0.7).

Binding Affinity (K_d) Assay. Apparent binding dissociation constants (K_d) were determined using K_d ELECT platform provided by Eurofins/DiscoverX (San Diego). Briefly, LIMK1/2 transfected HEK293 cells were tagged with DNA and incubated until lysis. Streptavidin-coated magnetic beads were treated with biotinylated small molecule ligands for 30 min at RT to generate affinity resins. Liganded beads were blocked with excess biotin and washed with blocking buffer (SeaBlock (Pierce), 1% BSA, 0.05% Tween 20, 1 mM DTT) to remove unbound ligand and reduce nonspecific binding. Test compound (11-point, 3-fold serial dilution from 100 μ M to 1 nM in duplicate, final DMSO concentration of 0.9%) were transferred to 384-well plates containing beads and DNA-tagged LIMK1/2 by acoustic transfer (noncontact dispensing). The assay plates were incubated at RT with shaking for 1 h and the affinity beads washed with wash buffer (1 \times PBS, 0.05% Tween20). The beads were then resuspended in elution buffer (1 \times PBS, 0.05% Tween20, 0.5 μ M nonbiotinylated affinity ligand) and incubated at RT with shaking for 30 min. The kinase concentration in the eluates was measured by qPCR. Binding constants K_d were calculated from the dose–response curve using the Hill equation

$$\text{response} = \text{background} - \frac{\text{signal} - \text{background}}{1 + \left(\frac{K_d^{\text{hillslope}}}{\text{dose}^{\text{hillslope}}} \right)}$$

Microsomal Stability. Five microliter microsomes (20 mg/mL, Corning BV) diluted into 95 μ L PBS (pH 7.4 with 0.6% MeCN) containing 0.04% DMSO and 4 μ M compound were incubated with 100 μ L of prewarmed 4 mM NADPH in PBS (final concentrations: 0.5 mg/mL microsomes, 2 μ M compound, 0.02% DMSO, 0.3% MeCN and 2 mM NADPH). After mixing thoroughly the $T = 0$ sample (40 μ L) was immediately quenched into 80 μ L ice cold MeOH containing 4 μ M internal standard (Carbamazepine). Three further samples were quenched in the same way at $T = 3, 9,$ and 30 min. Samples were incubated on ice for 30 min before centrifugation at 4700 rpm for 20 min. The supernatant was analyzed via LC-MS/MS and compound/Carbamazepine peak area ratios calculated to determine the rate of substrate depletion.

Thermodynamic Solubility. 1–2 mg of accurately weighed compound was suspended in 1 mL PBS (pH 7.0) and incubated (rotating end over end) at room temperature for 24 h. The samples were then centrifuged at >10,000 rpm for 10 min to pellet any remaining solid. The supernatant was then diluted sequentially (1:5, 1:50, 1:500, and 1:5000) in MeCN and mixed 1:1 with MeCN containing 4 μ M of carbamazepine. To prepare the standard, an 8-point, 1:3 dilution curve was prepared in DMSO with a top concentration of 1 mM, which was then diluted to 1:100 in MeCN containing 2 μ M carbamazepine. Standards and samples were analyzed via LCMS/MS. The compound carbamazepine peak area ratios were calculated, and the test article solubility was determined by interpolation from the standard curve.

Caco-2-Permeability and Efflux. Bidirectional permeabilities and drug efflux were performed at Cyprotex (Alderley Park, U.K.). Caco-2 cells (derived from ATCC) were seeded onto Transwell plates at 1×10^5 cells/cm² and cultured in DMEM. The monolayers are prepared by rinsing both apical and basolateral surfaces twice with HBSS at pH 7.4 and incubating both compartments for 40 min to stabilize physiological parameters. For assessment of A \rightarrow B permeability, HBSS was removed from the apical compartment and replaced with either positive control (antipyrine, atenolol, talinolol, estrone 3-sulfate) or test compound dosing solution (10 μ M in assay buffer in duplicate, final DMSO concentration of $\leq 1\%$). For assessment of B \rightarrow A permeability, HBSS was removed from the basolateral compartment and replaced with positive control or test compound dosing solution as above. After 2 h, apical compartment inserts and companion plates are separated and apical and basolateral samples diluted for analysis. Test and control compounds are quantified by LCMS/MS cassette analysis using a 7-point calibration with appropriate dilution of the samples. Permeability coefficient (P_{app}) for each compound is calculated from the following equation

$$P_{app} = \frac{dQ/dT}{C_0 \times A}$$

where dQ/dT is the rate of permeation of compound across the cells, C_0 is the donor compartment concentration at time zero, and A is the area of the cell monolayer. Only $P_{app} A \rightarrow B$ is reported for clarity. Efflux ratio (ER) is derived from $P_{app(B \rightarrow A)}/P_{app(A \rightarrow B)}$.

In Vivo DMPK. *In vivo* studies were carried out under appropriate licenses at Sai Life (India) or internally using male Sprague–Dawley rats. MDI-117740 (**69**) was either dosed: (i) i.v. in a formulation of 10% DMSO, 20% Cremophor EL, 70% saline (v/v/v) at a concentration of 0.04 mg/mL with dose volume of 5 mL/kg for final dose of 0.2 mg/kg, (ii) p.o. in a formulation of 20% hydroxypropyl- β -cyclodextrin in dH₂O (w/v) at a concentration of 0.3 mg/mL with dose volume of 10 mL/kg for final dose of 3 mg/kg, or, (iii) i.p. in a formulation of 20% hydroxypropyl- β -cyclodextrin in dH₂O (w/v) at a concentration of 2 mg/mL with dose volume 5 mL/kg for final dose of 10 mg/kg. Serial plasma samples were obtained at predetermined time points and then stored at -20 °C. Brain samples from a CNS satellite group were isolated at 1 h, homogenized and stored at -20 °C. Samples were then thawed, protein precipitated with MeCN followed by LC-MS/MS quantification. No adverse effects were noted for the duration of the *in vivo* experiments.

Wound Healing Assay. The wound healing or scratch assay used for monitoring adherent cell migration over time following the induction of a “scratched” area in the monolayer with a 200 μ L pipet tip. The MDA-MB-231 breast cancer cell line was seeded in a clear, 12-well plate, approximately 24 h prior to the experiment to form a complete monolayer. Following wound induction, the disrupted cells were gently removed from the wells and fresh medium supplemented with or without compound was added. The cells were incubated for 48 h and images were taken using the ZOE cell imager (BIO-RAD) to monitor the wounded gap. The initial width of the wound was measured, followed by measurements after 48 h. The images were measured using ImageJ software and the wound closure rate, indicative of cellular motility and migration, was calculated using GraphPad Prism 10.5.0.

Statistical Analysis. Statistical analysis was performed using GraphPad Prism (v10.5.0). For wound healing assays, percentage wound closure at 48 h was compared across treatment groups using an ordinary one-way ANOVA followed by Dunnett’s post hoc test to determine significance ($p < 0.05$) of differences between control sample and test samples. Data are presented as mean \pm SEM from $n = 4$ independent experiments. Statistical significance was set at $p < 0.05$. Details about the multiple comparisons test can be found in Table S2.

X-ray Crystallography. X-ray diffraction structures of MDI-117740 (**69**) and intermediates **39** and **49** are deposited with Cambridge Crystallographic Data Centre (CCDC) under deposition numbers 2467213, 2440761 and 2440762, respectively. Thermal ellipsoids for compound **69** and intermediates **39** and **49** can be found in Figures S1–S3.

■ ASSOCIATED CONTENT

Supporting Information

The Supporting Information is available free of charge at <https://pubs.acs.org/doi/10.1021/acs.jmedchem.5c00974>.

DiscoverX scanMAX panel for compound **69**; thermal ellipsoids for compound **69** and intermediates **39** and **49**; statistical data used to compare effect of LIMK inhibitors on cell migration in the wound healing assay; ¹H, ¹³C NMR, and UPLC-MS characterization data and details of chemical synthesis of all final compounds (PDF)

Formula Strings containing SMILES string and associated biochemical and biological data (CSV)

■ AUTHOR INFORMATION

Corresponding Author

Simon E. Ward – Medicines Discovery Institute, School of Biosciences, Cardiff University, Cardiff CF10 3AT, United Kingdom; orcid.org/0000-0002-8745-8377; Phone: (+44)2920 876984; Email: WardS10@cardiff.ac.uk

Authors

Alex G. Baldwin – Medicines Discovery Institute, School of Biosciences, Cardiff University, Cardiff CF10 3AT, United Kingdom; orcid.org/0000-0002-7126-5220

David W. Foley – Medicines Discovery Institute, School of Biosciences, Cardiff University, Cardiff CF10 3AT, United Kingdom; Present Address: Tay Therapeutics Limited, Dundee University Incubator, 3 James Lindsay Place, Dundee DD1 5JJ, United Kingdom

D. Heulyn Jones – Medicines Discovery Institute, School of Biosciences, Cardiff University, Cardiff CF10 3AT, United Kingdom

Hyunah Lee – Centre for Medicines Discovery, University of Oxford, Oxford OX3 7FZ, United Kingdom; Present Address: Division of Structural Biology, The Institute of

Cancer Research (ICR), London SW3 6JB, United Kingdom

Ross Collins – Medicines Discovery Institute, School of Biosciences, Cardiff University, Cardiff CF10 3AT, United Kingdom; Present Address: Recursion plc, 155 Brook Drive, Milton Park, Abingdon OX14 4SD, United Kingdom

Ben Wahab – Medicines Discovery Institute, School of Biosciences, Cardiff University, Cardiff CF10 3AT, United Kingdom

Josephine H. Pedder – Medicines Discovery Institute, School of Biosciences, Cardiff University, Cardiff CF10 3AT, United Kingdom; Present Address: Institute of Systems, Molecular and Integrative Biology, University of Liverpool, Biosciences Building, Crown Street, Liverpool L69 7BE, United Kingdom

Loren Waters – Medicines Discovery Institute, School of Biosciences, Cardiff University, Cardiff CF10 3AT, United Kingdom

Marie Paine – Medicines Discovery Institute, School of Biosciences, Cardiff University, Cardiff CF10 3AT, United Kingdom

Lauramariú Schino – Medicines Discovery Institute, School of Biosciences, Cardiff University, Cardiff CF10 3AT, United Kingdom

Gui Jie Feng – Medicines Discovery Institute, School of Biosciences, Cardiff University, Cardiff CF10 3AT, United Kingdom; Present Address: European Cancer Stem Cell Research Institute, School of Biosciences, Cardiff University, Haydn Ellis Building, Maindy Road, Cardiff CF24 4HQ, United Kingdom; orcid.org/0000-0002-6145-8504

Benson M. Kariuki – School of Chemistry, Cardiff University, Cardiff CF10 3AT, United Kingdom; orcid.org/0000-0002-8658-3897

Jonathan M. Elkins – Centre for Medicines Discovery, University of Oxford, Oxford OX3 7FZ, United Kingdom; orcid.org/0000-0003-2858-8929

John R. Attack – Medicines Discovery Institute, School of Biosciences, Cardiff University, Cardiff CF10 3AT, United Kingdom

Complete contact information is available at:

<https://pubs.acs.org/10.1021/acs.jmedchem.5c00974>

Author Contributions

Conceptualization: A.G.B., D.W.F., D.H.J., J.M.E., J.R.A., S.E.W.; Methodology: A.G.B., D.W.F., D.H.J., J.M.E., J.R.A., S.E.W.; Investigation: A.G.B., D.W.F., D.H.J., H.L., R.C., B.W., J.P., L.W., M.P., L.S., G.F., B.K.; Writing—original draft: A.G.B.; Writing—editing: D.W.F., D.H.J.; Writing—review: all authors; Funding Acquisition: J.M.E., J.R.A., S.E.W.; Supervision: D.W.F., J.M.E., J.R.A., S.E.W. All authors have given approval to the final version of the manuscript.

Funding

This project was funded through the UK's Medical Research Council's Developmental Pathway Funding Scheme, grant reference MR/S005331/1.

Notes

The authors declare no competing financial interest.

ACKNOWLEDGMENTS

The DMPK and chemistry teams at Sai Life are acknowledged for their contribution to the *in vivo* PK data and synthesis of

selected compounds presented in this manuscript. We thank Simon Waller from Analytical Services, School of Chemistry, Cardiff University for running HRMS analyses.

ABBREVIATIONS USED

ADF, actin-depolymerizing factor; ASD, autism spectrum disorder; AUC_{inf}, area under the curve (to infinity); B/P, brain-to-plasma ratio; BMPR2, bone morphogenetic protein receptor type 2; CaMKIV, calcium/calmodulin-dependent protein kinase IV; CL_{int}, intrinsic clearance; C_{max}, maximum plasma concentration; DMPK, drug metabolism and pharmacokinetics; ER, efflux ratio; F%, % oral bioavailability; FMRP, fragile X mental retardation protein; FXS, fragile X syndrome; i.p., intraperitoneal; i.v., intravenous; LIMK, LIM domain kinase; MRCK α , myotonic dystrophy kinase-related Cdc42-binding kinase α ; PAK, p21-activated kinase; P_{app}, apparent permeability; p.o., oral administration; RIPK1, receptor-interacting protein 1 kinase; ROCK, Rho-associated protein kinase; T_{1/2}, half-life; TESK, testis specific protein kinase; TKL, tyrosine kinase-like kinase; T_{max}, time taken to reach maximum plasma concentration; V_D, volume of distribution

REFERENCES

- (1) Scott, R. W.; Olson, M. F. LIM kinases: function, regulation and association with human disease. *J. Mol. Med.* **2007**, *85* (6), 555–568.
- (2) Casanova-Sepúlveda, G.; Sexton, J. A.; Turk, B. E.; Boggon, T. J. Autoregulation of the LIM kinases by their PDZ domain. *Nat. Commun.* **2023**, *14* (1), No. 8441.
- (3) Casanova-Sepúlveda, G.; Boggon, T. J. Regulation and signaling of the LIM domain kinases. *BioEssays* **2025**, *47* (1), No. 2400184.
- (4) Edwards, D. C.; Sanders, L. C.; Bokoch, G. M.; Gill, G. N. Activation of LIM-kinase by Pak1 couples Rac/Cdc42 GTPase signalling to actin cytoskeletal dynamics. *Nat. Cell Biol.* **1999**, *1* (5), 253–259.
- (5) Ohashi, K.; Nagata, K.; Maekawa, M.; Ishizaki, T.; Narumiya, S.; Mizuno, K. Rho-associated kinase ROCK activates LIM-kinase 1 by phosphorylation at threonine 508 within the activation loop. *J. Biol. Chem.* **2000**, *275* (5), 3577–3582.
- (6) Sumi, T.; Matsumoto, K.; Shibuya, A.; Nakamura, T. Activation of LIM kinases by myotonic dystrophy kinase-related Cdc42-binding kinase α . *J. Biol. Chem.* **2001**, *276* (25), 23092–23096.
- (7) Dan, C.; Kelly, A.; Bernard, O.; Minden, A. Cytoskeletal changes regulated by the PAK4 serine/threonine kinase are mediated by LIM kinase 1 and cofilin. *J. Biol. Chem.* **2001**, *276* (34), 32115–32121.
- (8) Takemura, M.; Mishima, T.; Wang, Y.; Kasahara, J.; Fukunaga, K.; Ohashi, K.; Mizuno, K. Ca²⁺/calmodulin-dependent protein kinase IV-mediated LIM kinase activation is critical for calcium signal-induced neurite outgrowth. *J. Biol. Chem.* **2009**, *284* (42), 28554–28562.
- (9) Prunier, C.; Prudent, R.; Kapur, R.; Sadoul, K.; Lafanechere, L. LIM kinases: cofilin and beyond. *Oncotarget* **2017**, *8* (25), 41749–41763.
- (10) Gorovoy, M.; Niu, J.; Bernard, O.; Profirovic, J.; Minshall, R.; Neamu, R.; Voyno-Yasenetskaya, T. LIM kinase 1 coordinates microtubule stability and actin polymerization in human endothelial cells. *J. Biol. Chem.* **2005**, *280* (28), 26533–26542.
- (11) Yoshioka, K.; Foletta, V.; Bernard, O.; Itoh, K. A role for LIM kinase in cancer invasion. *Proc. Natl. Acad. Sci. U.S.A.* **2003**, *100* (12), 7247–7252.
- (12) McConnell, B. V.; Koto, K.; Gutierrez-Hartmann, A. Nuclear and cytoplasmic LIMK1 enhances human breast cancer progression. *Mol. Cancer* **2011**, *10*, No. 75.
- (13) Malvi, P.; Janostiak, R.; Chava, S.; Manrai, P.; Yoon, E.; Singh, K.; Harigopal, M.; Gupta, R.; Wajapeyee, N. LIMK2 promotes the metastatic progression of triple-negative breast cancer by activating SRPK1. *Oncogenesis* **2020**, *9* (8), No. 77.

- (14) You, T.; Gao, W.; Wei, J.; Jin, X.; Zhao, Z.; Wang, C.; Li, Y. Overexpression of LIMK1 promotes tumor growth and metastasis in gastric cancer. *Biomed. Pharmacother.* **2015**, *69*, 96–101.
- (15) Mardilovich, K.; Gabrielsen, M.; McGarry, L.; Orange, C.; Patel, R.; Shanks, E.; Edwards, J.; Olson, M. F. Elevated LIM kinase 1 in nonmetastatic prostate cancer reflects its role in facilitating androgen receptor nuclear translocation. *Mol. Cancer Ther.* **2015**, *14* (1), 246–258.
- (16) Nikhil, K.; Chang, L.; Viccaro, K.; Jacobsen, M.; McGuire, C.; Satapathy, S. R.; Tandiyar, M.; Broman, M. M.; Cresswell, G.; He, Y. J.; et al. Identification of LIMK2 as a therapeutic target in castration resistant prostate cancer. *Cancer Lett.* **2019**, *448*, 182–196.
- (17) Aggelou, H.; Chadla, P.; Nikou, S.; Karteri, S.; Maroulis, I.; Kalofonos, H. P.; Papadaki, H.; Bravou, V. LIMK/cofilin pathway and Slingshot are implicated in human colorectal cancer progression and chemoresistance. *Virchows Arch.* **2018**, *472* (5), 727–737.
- (18) Hagerman, R. J.; Berry-Kravis, E.; Hazlett, H. C.; Bailey, D. B., Jr.; Moine, H.; Kooy, R. F.; Tassone, F.; Gantois, I.; Sonenberg, N.; Mandel, J. L.; Hagerman, P. J. Fragile X syndrome. *Nat. Rev. Dis. Primers* **2017**, *3*, No. 17065.
- (19) Kashima, R.; Roy, S.; Ascano, M.; Martinez-Cerdeno, V.; Ariza-Torres, J.; Kim, S.; Louie, J.; Lu, Y.; Leyton, P.; Bloch, K. D.; et al. Augmented noncanonical BMP type II receptor signaling mediates the synaptic abnormality of fragile X syndrome. *Sci. Signaling* **2016**, *9* (431), No. ra58.
- (20) Pyronneau, A.; He, Q.; Hwang, J. Y.; Porch, M.; Contractor, A.; Zukin, R. S. Aberrant Rac1-cofilin signaling mediates defects in dendritic spines, synaptic function, and sensory perception in fragile X syndrome. *Sci. Signaling* **2017**, *10* (504), No. eaan0852, DOI: 10.1126/scisignal.aan0852.
- (21) Santini, E.; Huynh, T. N.; Longo, F.; Koo, S. Y.; Mojica, E.; D'Andrea, L.; Bagni, C.; Klann, E. Reducing eIF4E-eIF4G interactions restores the balance between protein synthesis and actin dynamics in fragile X syndrome model mice. *Sci. Signaling* **2017**, *10* (504), No. eaan0665, DOI: 10.1126/scisignal.aan0665.
- (22) Kashima, R.; Redmond, P. L.; Ghatpande, P.; Roy, S.; Kornberg, T. B.; Hanke, T.; Knapp, S.; Lagna, G.; Hata, A. Hyperactive locomotion in a Drosophila model is a functional readout for the synaptic abnormalities underlying fragile X syndrome. *Sci. Signaling* **2017**, *10* (477), No. eaai8133, DOI: 10.1126/scisignal.aai8133.
- (23) Irwin, S. A.; Patel, B.; Idupulapati, M.; Harris, J. B.; Crisostomo, R. A.; Larsen, B. P.; Kooy, F.; Willems, P. J.; Cras, P.; Kozlowski, P. B.; et al. Abnormal dendritic spine characteristics in the temporal and visual cortices of patients with fragile-X syndrome: a quantitative examination. *Am. J. Med. Genet.* **2001**, *98* (2), 161–167.
- (24) He, C. X.; Portera-Cailliau, C. The trouble with spines in fragile X syndrome: density, maturity and plasticity. *Neuroscience* **2013**, *251*, 120–128.
- (25) Henderson, B. W.; Greathouse, K. M.; Ramdas, R.; Walker, C. K.; Rao, T. C.; Bach, S. V.; Curtis, K. A.; Day, J. J.; Mattheyses, A. L.; Herskowitz, J. H. Pharmacologic inhibition of LIMK1 provides dendritic spine resilience against beta-amyloid. *Sci. Signaling* **2019**, *12* (587), No. eaaw9318, DOI: 10.1126/scisignal.aaw9318.
- (26) Sivadasan, R.; Hornburg, D.; Drepper, C.; Frank, N.; Jablonka, S.; Hansel, A.; Lojewski, X.; Sterneckert, J.; Hermann, A.; Shaw, P. J.; et al. C9ORF72 interaction with cofilin modulates actin dynamics in motor neurons. *Nat. Neurosci.* **2016**, *19* (12), 1610–1618.
- (27) Datta, D.; Arion, D.; Corradi, J. P.; Lewis, D. A. Altered expression of CDC42 signaling pathway components in cortical layer 3 pyramidal cells in schizophrenia. *Biol. Psychiatry* **2015**, *78* (11), 775–785.
- (28) Gory-Fauré, S.; Powell, R.; Jonckheere, J.; Lante, F.; Denarier, E.; Peris, L.; Nguyen, C. H.; Buisson, A.; Lafanechere, L.; Andrieux, A. Pyr1-Mediated Pharmacological Inhibition of LIM Kinase Restores Synaptic Plasticity and Normal Behavior in a Mouse Model of Schizophrenia. *Front. Pharmacol.* **2021**, *12*, No. 627995.
- (29) Collins, R.; Lee, H.; Jones, D. H.; Elkins, J. M.; Gillespie, J. A.; Thomas, C.; Baldwin, A. G.; Jones, K.; Waters, L.; Paine, M.; et al. Comparative Analysis of Small-Molecule LIMK1/2 Inhibitors: Chemical Synthesis, Biochemistry, and Cellular Activity. *J. Med. Chem.* **2022**, *65* (20), 13705–13713.
- (30) Ross-Macdonald, P.; de Silva, H.; Guo, Q.; Xiao, H.; Hung, C. Y.; Penhallow, B.; Markwalder, J.; He, L.; Attar, R. M.; Lin, T. A.; et al. Identification of a nonkinase target mediating cytotoxicity of novel kinase inhibitors. *Mol. Cancer Ther.* **2008**, *7* (11), 3490–3498.
- (31) Li, R.; Doherty, J.; Antonipillai, J.; Chen, S.; Devlin, M.; Visser, K.; Baell, J.; Street, I.; Anderson, R. L.; Bernard, O. LIM kinase inhibition reduces breast cancer growth and invasiveness but systemic inhibition does not reduce metastasis in mice. *Clin. Exp. Metastasis* **2013**, *30* (4), 483–495.
- (32) Park, J. B.; Agnihotri, S.; Golbourn, B.; Bertrand, K. C.; Luck, A.; Sabha, N.; Smith, C. A.; Byron, S.; Zadeh, G.; Croul, S.; et al. Transcriptional profiling of GBM invasion genes identifies effective inhibitors of the LIM kinase-Cofilin pathway. *Oncotarget* **2014**, *5* (19), 9382–9395.
- (33) Hanke, T.; Mathea, S.; Woortman, J.; Salah, E.; Berger, B. T.; Tumber, A.; Kashima, R.; Hata, A.; Kuster, B.; Muller, S.; Knapp, S. Development and Characterization of Type I, Type II, and Type III LIM-Kinase Chemical Probes. *J. Med. Chem.* **2022**, *65* (19), 13264–13287.
- (34) Dolan, B. M.; Duron, S. G.; Campbell, D. A.; Vollrath, B.; Shankaranarayana Rao, B. S.; Ko, H. Y.; Lin, G. G.; Govindarajan, A.; Choi, S. Y.; Tonegawa, S. Rescue of fragile X syndrome phenotypes in Fmr1 KO mice by the small-molecule PAK inhibitor FRAX486. *Proc. Natl. Acad. Sci. U.S.A.* **2013**, *110* (14), 5671–5676.
- (35) Harrison, B. A.; Whitlock, N. A.; Voronkov, M. V.; Almstead, Z. Y.; Gu, K. J.; Mabon, R.; Gardyan, M.; Hamman, B. D.; Allen, J.; Gopinathan, S.; et al. Novel class of LIM-kinase 2 inhibitors for the treatment of ocular hypertension and associated glaucoma. *J. Med. Chem.* **2009**, *52* (21), 6515–6518.
- (36) Harrison, B. A.; Almstead, Z. Y.; Burgoon, H.; Gardyan, M.; Goodwin, N. C.; Healy, J.; Liu, Y.; Mabon, R.; Marinelli, B.; Samala, L.; et al. Discovery and Development of LX7101, a Dual LIM-Kinase and ROCK Inhibitor for the Treatment of Glaucoma. *ACS Med. Chem. Lett.* **2015**, *6* (1), 84–88.
- (37) Yin, Y.; Zheng, K.; Eid, N.; Howard, S.; Jeong, J. H.; Yi, F.; Guo, J.; Park, C. M.; Bibian, M.; Wu, W.; et al. Bis-aryl urea derivatives as potent and selective LIM kinase (Limk) inhibitors. *J. Med. Chem.* **2015**, *58* (4), 1846–1861.
- (38) <https://clinicaltrials.gov/study/NCT01528111>.
- (39) Baldwin, A. G.; Foley, D. W.; Collins, R.; Lee, H.; Jones, D. H.; Wahab, B.; Waters, L.; Pedder, J.; Paine, M.; Feng, G. J.; et al. Discovery of MDI-114215: A potent and selective LIMK inhibitor to treat Fragile X syndrome. *J. Med. Chem.* **2025**, *68* (1), 719–752.
- (40) Boland, S.; Bourin, A.; Alen, J.; Geraets, J.; Schroeders, P.; Castermans, K.; Kindt, N.; Boumans, N.; Panitti, L.; Vanormelingen, J.; et al. Design, synthesis and biological characterization of selective LIMK inhibitors. *Bioorg. Med. Chem. Lett.* **2015**, *25* (18), 4005–4010.
- (41) Goodwin, N. C.; Cianchetta, G.; Burgoon, H. A.; Healy, J.; Mabon, R.; Strobel, E. D.; Allen, J.; Wang, S.; Hamman, B. D.; Rawlins, D. B. Discovery of a Type III Inhibitor of LIM Kinase 2 That Binds in a DFG-Out Conformation. *ACS Med. Chem. Lett.* **2015**, *6* (1), 53–57.
- (42) Mandel, S.; Hanke, T.; Mathea, S.; Chatterjee, D.; Saraswati, H.; Berger, B. T.; Schwalm, M. P.; Yamamoto, S.; Tawada, M.; Takagi, T.; et al. Repurposing of the RIPK1-Selective Benzo[1,4]oxazepin-4-one Scaffold for the Development of a Type III LIMK1/2 Inhibitor. *ACS Chem. Biol.* **2025**, *20*, 1087–1098, DOI: 10.1021/acscchembio.5c00097.
- (43) Yoshikawa, M.; Saitoh, M.; Katoh, T.; Seki, T.; Bigi, S. V.; Shimizu, Y.; Ishii, T.; Okai, T.; Kuno, M.; Hattori, H.; et al. Discovery of 7-Oxo-2,4,5,7-tetrahydro-6 H-pyrazolo[3,4- c]pyridine Derivatives as Potent, Orally Available, and Brain-Penetrating Receptor Interacting Protein 1 (RIP1) Kinase Inhibitors: Analysis of Structure-Kinetic Relationships. *J. Med. Chem.* **2018**, *61* (6), 2384–2409.
- (44) Harris, P. A.; Berger, S. B.; Jeong, J. U.; Nagilla, R.; Bandyopadhyay, D.; Campobasso, N.; Capriotti, C. A.; Cox, J. A.; Dare, L.; Dong, X.; et al. Discovery of a First-in-Class Receptor Interacting Protein 1 (RIP1) Kinase Specific Clinical Candidate

(GSK2982772) for the Treatment of Inflammatory Diseases. *J. Med. Chem.* **2017**, 60 (4), 1247–1261.

(45) Weisel, K.; Berger, S.; Papp, K.; Maari, C.; Krueger, J. G.; Scott, N.; Tompson, D.; Wang, S.; Simeoni, M.; Bertin, J.; Tak, P. P. Response to Inhibition of Receptor-Interacting Protein Kinase 1 (RIPK1) in Active Plaque Psoriasis: A Randomized Placebo-Controlled Study. *Clin. Pharmacol. Ther.* **2020**, 108 (4), 808–816.

(46) Weisel, K.; Scott, N.; Berger, S.; Wang, S.; Brown, K.; Powell, M.; Broer, M.; Watts, C.; Tompson, D. J.; Burriss, S. W.; et al. A randomised, placebo-controlled study of RIPK1 inhibitor GSK2982772 in patients with active ulcerative colitis. *BMJ Open Gastroenterol.* **2021**, 8 (1), No. e000680, DOI: 10.1136/bmjgast-2021-000680.

(47) Weisel, K.; Berger, S.; Thorn, K.; Taylor, P. C.; Peterfy, C.; Siddall, H.; Tompson, D.; Wang, S.; Quattrocchi, E.; Burriss, S. W.; et al. A randomized, placebo-controlled experimental medicine study of RIPK1 inhibitor GSK2982772 in patients with moderate to severe rheumatoid arthritis. *Arthritis Res. Ther.* **2021**, 23 (1), No. 85.

(48) Harris, P. A.; King, B. W.; Bandyopadhyay, D.; Berger, S. B.; Campobasso, N.; Capriotti, C. A.; Cox, J. A.; Dare, L.; Dong, X.; Finger, J. N.; et al. DNA-Encoded Library Screening Identifies Benzo[b][1,4]-oxazepin-4-ones as Highly Potent and Monoselective Receptor Interacting Protein 1 Kinase Inhibitors. *J. Med. Chem.* **2016**, 59 (5), 2163–2178.

(49) Harris, P. A.; Marinis, J. M.; Lich, J. D.; Berger, S. B.; Chirala, A.; Cox, J. A.; Eidam, P. M.; Finger, J. N.; Gough, P. J.; Jeong, J. U.; et al. Identification of a RIP1 Kinase Inhibitor Clinical Candidate (GSK3145095) for the Treatment of Pancreatic Cancer. *ACS Med. Chem. Lett.* **2019**, 10 (6), 857–862.

(50) Cohen, D. T.; Buchwald, S. L. Mild palladium-catalyzed cyanation of (hetero)aryl halides and triflates in aqueous media. *Org. Lett.* **2015**, 17 (2), 202–205.

(51) Schunk, S.; Reich, M.; Koenigs, R. M. Pyrazolyl Substituted Tetrahydropyranylsulfones. U.S. Patent, US10,100,041, 2018.

(52) Atkinson, S. J.; Demont, E. H.; Harrison, L. A.; Liwicki, G. M.; Lucas, S. C. C.; Preston, A. G.; Seal, J. T.; Wall, I. D.; Watson, R. J. Pyrazole Derivatives As Bromodomain Inhibitors. U.S. Patent, US10,966,961, 2021.

(53) Salah, E.; Chatterjee, D.; Beltrami, A.; Tumber, A.; Preuss, F.; Canning, P.; Chaikuad, A.; Knaus, P.; Knapp, S.; Bullock, A. N.; Mathea, S. Lessons from LIMK1 enzymology and their impact on inhibitor design. *Biochem. J.* **2019**, 476 (21), 3197–3209.

(54) Lyu, L.; Li, H.; Lu, K.; Jiang, S.; Li, H. PAK inhibitor FRAX486 decreases the metastatic potential of triple-negative breast cancer cells by blocking autophagy. *Br. J. Cancer* **2024**, 130 (3), 394–405.

The advertisement features a vertical image on the left showing a blue, translucent, spherical object with a yellow, textured, tube-like structure extending from its base, which is surrounded by a cluster of green and pink spheres. The background of the advertisement is dark blue. Text on the right side includes 'CAS BIOFINDER DISCOVERY PLATFORM™' in yellow, 'PRECISION DATA FOR FASTER DRUG DISCOVERY' in large white letters, 'CAS BioFinder helps you identify targets, biomarkers, and pathways' in white, and 'Unlock insights' in white text inside a yellow rectangular box. At the bottom right is the CAS logo, consisting of the letters 'CAS' in white and a blue and yellow dot matrix graphic, with the text 'A division of the American Chemical Society' below it.

CAS BIOFINDER DISCOVERY PLATFORM™

**PRECISION DATA
FOR FASTER
DRUG
DISCOVERY**

CAS BioFinder helps you identify
targets, biomarkers, and pathways

Unlock insights

CAS
A division of the
American Chemical Society